STRUCTURAL AND THERMAL CHARACTERISATION OF NSAIDS AND CYCLODEXTRIN-NSAID COMPLEXES

BY: PAMELA MARY DEAN
B.Sc. (Hons.) University of Cape Town

Dissertation presented to the University of Cape Town
for the degree of Master of Science

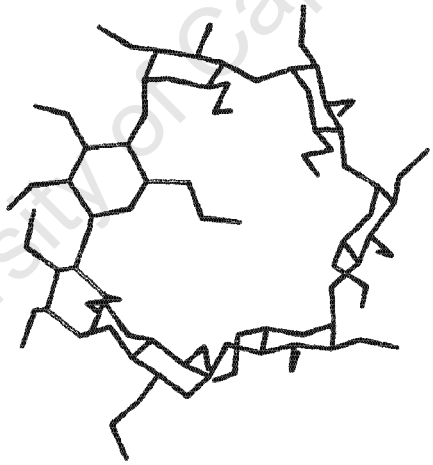

October 2004

"And He will judge among the nations, and will rebuke many people; and they shall beat their swords into plow-shares, and their spears into pruning-hooks; nation shall not lift up sword against nation, neither shall they learn war any more."
Isaiah 2:4

Acknowledgements

I would like to express my sincere gratitude towards:

- Professor M. R. Caira for his wisdom, patience and humility.
- Associate Professor S. A. Bourne for her jovial manner and support.
- Professor P. van der Bijl for his invaluable help and comments.
- Dr. H. Su for data collection on the Kappa CCD diffractometer.
- Emeritus Professor P. W. Linder for his guidance with the Huber Guinier powder diffractometer.
- Professor L. R. Nassimbeni and Ms. K. Badenhorst for the efficient running of the laboratory.
- 'Dr'. C. Oliver for his excellent instruction involving crystallographic software.
- The members of the Crystallography Research Group for their assistance and espousing of various philosophies of life.
- The National Research Foundation and the University of Cape Town for financial support.
- My various friends and family for bringing me back to earth from the 'scientific ivory tower'.
- My Father God, without whom nothing is possible.

Publications and Conferences

- Parts of this dissertation that have been published:

Caira, M.R; Bourne, S.A; Mhlongo, W.T; Dean, P.M. *New Crystalline Forms of Permethylated-β-cyclodextrin, Chemical Communications,* **2004,** DOI:10.1039/B408660K, Article in press.

- Parts of this dissertation have been presented at the following conferences:

A poster entitled : Inclusion of the Non- steroidal Anti- inflammatory Suprofen in permethylated β-cyclodextrin" was presented at SACI – 37, 4-9 July 2004, CSIR Conference Center, Pretoria, South Africa.

A poster entitled : Inclusion of the Non- steroidal Anti- inflammatory Suprofen in permethylated β-cyclodextrin" was presented at the 25th Annual Academy of Pharmaceutical Sciences, 12-15 September 2004, Rhodes University, Grahamstown, South Africa.

Abstract

Non- steroidal anti-inflammatory drugs (NSAIDs) are used for the prevention of pain and inflammation. These symptoms are brought about by the action of biochemicals such as prostaglandins, which result from the conversion of a fatty acid, known as arachidonic acid, by the enzyme cyclooxygenase (COX) in the presence of oxygen. NSAIDs act on this biochemical pathway by inhibiting the COX enzyme, thereby exerting their analgesic effect. Since, however, the solubility and bioavailability of NSAIDs are generally poor, encapsulation of these drugs in cyclodextrins was attempted in order to alter their dissolution properties.

Cyclodextrins are cyclic oligosaccharides consisting of α-D-glucopyranose units; their cone-like molecular structures comprise a hydrophilic exterior and a hydrophobic interior. This molecular property results in cyclodextrins (hosts) being able to include certain organic pharmaceuticals (guests) and thereby increase their aqueous solubility and stability, amongst other things.

Under different thermodynamic and kinetic conditions a chemical substance may crystallise into different crystalline forms (polymorphs), i.e. it is able to arrange in more than one three-dimensional arrangement. Crystalline drug solvates and amorphous (non-crystalline) forms also exist. These different species, due to their different crystal structures have different physical properties such as solubility and dissolution rate and therefore the most appropriate polymorph needs to be identified for optimum bioavailability of the drug.

In the work reported here six NSAIDs, namely Bucetin, Lornoxicam, Diflunisal, Suprofen, Celecoxib and Rofecoxib were studied for possible inclusion in cyclodextrins or novel crystalline phase isolation. Several cyclodextrins were used for possible inclusion; these were the native species β- and γ-CD and six methylated cyclodextrins, namely Heptakis(2,6-di-O-methyl)-β-cyclodextrin (DIMEB), Heptakis(2,3,6-tri-O-methyl)-β-cyclodextrin (TRIMEB), Octakis(2,3,6-tri-O-methyl)-γ-cyclodextrin (TRIMEG),

Hexakis(2,3,6-tri-O-methyl)-α-cyclodextrin (TRIMEA), Randomly-methylated β-Cyclodextrin (RAMEB) and Hydroxypropyl-β-cyclodextrin (HPβCD).

The techniques used to attempt inclusion were co-precipitation, kneading and co-grinding. The techniques used to attempt production of novel crystalline phases were recrystallisation, sublimation, co-grinding, vapour diffusion and recrystallisation from the melt. Physicochemical characterisation techniques were then used to assess the products. The methods used were hot stage microscopy, differential scanning calorimetry and thermogravimetric analysis to determine the thermal behaviour of the compounds. Ultra-violet spectrophotometry, elemental analysis and high performance liquid chromatography were used to determine the chemical compositions. Finally to determine the structures, nuclear magnetic resonance spectroscopy, X-ray powder diffraction and single crystal X-ray structure determination were used.

Three new solid forms involving Celecoxib, Rofecoxib and permethylated β-cyclodextrin were obtained and characterised. The experimental results showed that an amorphous form of celecoxib and a decomposition product of rofecoxib had been prepared. A novel crystalline form of permethylated β-cyclodextrin was also prepared; this form containing methylglucose residues exclusively in the $^4C_1$ conformation was in contrast to the known monohydrate in which one methylglucose residue adopts the $^1C_4$ conformation.

Five inclusion complexes involving β- and γ-CD were identified using powder X-ray diffraction. The crystal structures of the β-CD and TRIMEB inclusion complexes of Suprofen were fully elucidated. In both cases the (S)-enantiomer of Suprofen was preferentially included in the characterised crystal. The guest was disordered in both crystal structures and both hosts adopt the usual conformation seen in analogous inclusion complexes.

Abbreviations and Symbols

Compounds

NSAID	Non-Steroidal Anti-Inflammatory Drug
COX	Cyclooxygenase
CD	Cyclodextrin
β-CD	Beta cyclodextrin
γ-CD	Gamma Cyclodextrin
DIMEB	Heptakis(2,6-di-O-methyl)-β-cyclodextrin
TRIMEB	Heptakis(2,3,6-tri-O-methyl)-β-cyclodextrin
TRIMEG	Octakis(2,3,6-tri-O-methyl)-γ-cyclodextrin
TRIMEA	Hexakis(2,3,6-tri-O-methyl)-α-cyclodextrin
RAMEB	Randomly-methylated β-Cyclodextrin
HPβCD	Hydroxypropyl-β-cyclodextrin
RFMcele	Recrystallisation from the melt form of Celecoxib
TRIB	New crystalline form of TRIMEB
BCDSUP	β-cyclodextrin-suprofen inclusion complex
TRIBSUP	TRIMEB-suprofen inclusion complex

Techniques

DSC	Differential Scanning Calorimetry
HSM	Hot Stage Microscopy
TGA	Thermogravimetric Analysis
UV	Ultraviolet Spectrophotometry
FTIR	Fourier Transform Infrared Spectroscopy
XRPD	X-Ray Powder Diffraction
NMR	Nuclear Magnetic Resonance Spectroscopy
HPLC	High Performance Liquid Chromatography

Symbols

α	The angle between b and c unit cell axes
β	The angle between a and c unit cell axes
γ	The angle between a and b unit cell axes
CSD	Cambridge Structural Database
CCD	Charge Coupled Device
$\Delta\delta$	Change in chemical shift
E	Normalised structure factor
e.s.d.	Estimated standard deviation
F	Structure factor
F(000)	Number of electrons in the unit cell
I	Intensity
μ	Linear absorption coefficient
S	Goodness of fit (F^2)
s.o.f.	Site-occupancy factor
τ / ω	Torsion angle
W	Water
Z	Number of molecules or complex units in the unit cell
G	Glucopyranose residue

Table of Contents

Chapter One

Chapter One: Introduction

1.1 General Overview

This project is entitled: *Structural and thermal characterization of NSAIDs and cyclodextrin-NSAID complexes.* As the title implies the scientific investigation that shall be pursued in this study is the production of novel solid forms of non-steroidal anti-inflammatory drugs. This shall be researched using two methods, firstly the inclusion of the drugs within cyclic oligosaccharides named *Cyclodextrins* and secondly through exploration of the possible different crystalline phases of the drugs, commonly referred to as *Polymorphism.* The following sections discuss these entities and how these methods could improve the effectiveness of Non-steroidal anti-inflammatory drugs.

1.2 Non-Steroidal Anti-Inflammatory Drugs (NSAIDs)

1.2.1 Background

Since antiquity the therapeutic properties of willow bark were known, with the Egyptians and Assyrians using a decoction of myrtle and willow leaves as analgesics. Even Hippocrates, regarded as the father of medicine, recommended the chewing of willow leaves for this purpose. The active compound within willow bark was subsequently characterised and synthetically modified to form acetylsalicylic acid, commonly known as Aspirin, by Felix Hoffman from the Bayer Company in 1875 (Figure 1.1).[1] Subsequently in the 20th century Aspirin was discovered to exert in addition antipyretic and anti-inflammatory effects, thereby becoming the first known anti-inflammatory. Thereafter a plethora of anti-inflammatory drugs were synthesized, notably phenylbutazone, which was classed the first non-steroidal anti-inflammatory in 1949.[2]

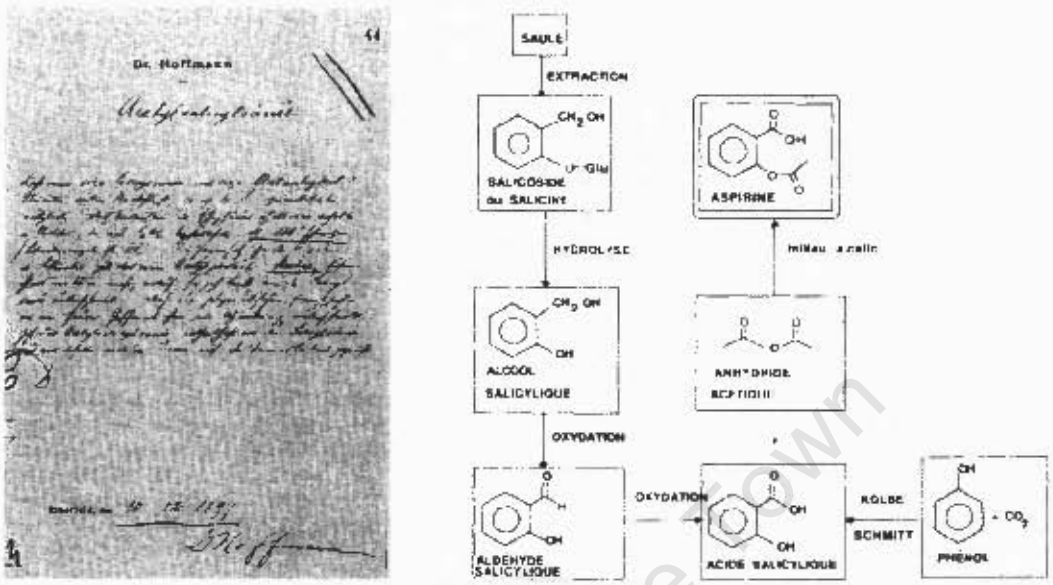

Figure 1.1: A report and synthetic route for Acetylsalicylic acid by Hoffmann in 1897.[1]

1.2.2 Mechanism

Non-steroidal anti-inflammatory drugs (NSAIDs) are used for the prevention of pain and inflammation. Pain was initially prevented by analgesics, which had reduced anti-inflammatory action and had undesirable side effects such as nausea; therefore, to counteract the pain, the correct mechanism of action needed to be targeted, and the correct drugs used. Pharmacologically, inflammation and pain symptoms are brought about by the action of biochemicals such as prostaglandins, prostacyclins and thromboxanes, which result from the conversion of a fatty acid, known as arachidonic acid, by the enzyme cyclooxygenase (COX) in the presence of oxygen (Figure 1.2).[3] It was discovered that NSAIDs act on this biochemical pathway by inhibiting the COX enzyme, thereby exerting their analgesic effect. However, these drugs have been shown to have very poor aqueous solubility, which may possibly impede their pharmaceutical profile. Since this problem may be addressed by different approaches, such as cyclodextrin inclusion and the use of alternative solid forms (polymorphs, solvates) of the NSAIDs, these topics are highlighted below.

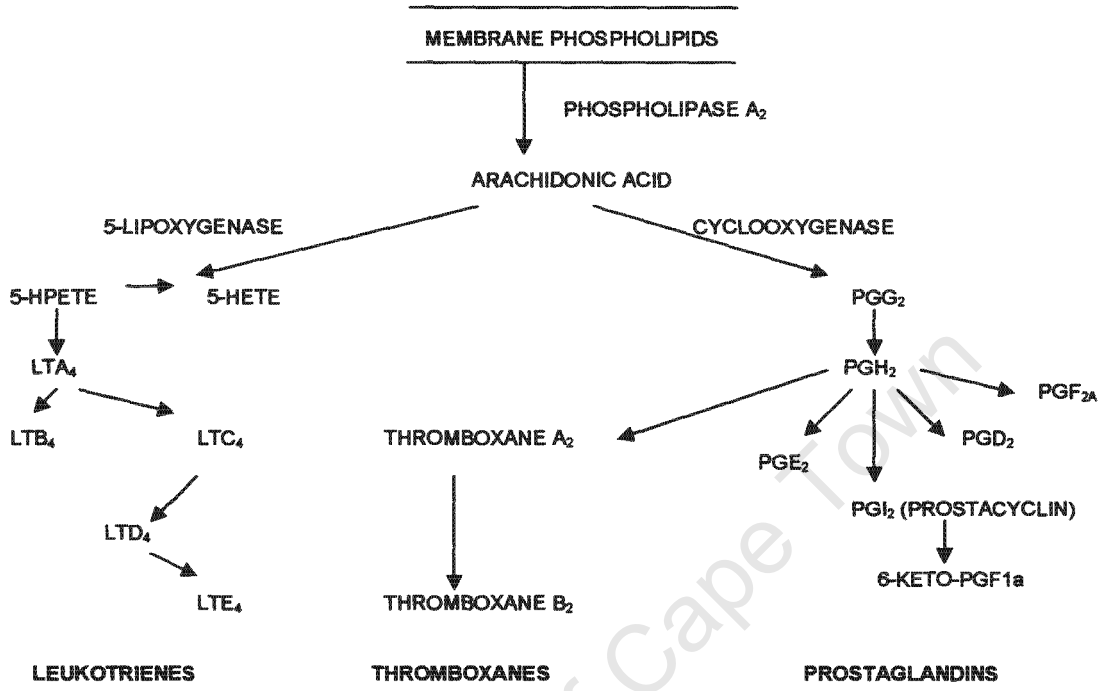

Figure 1.2: The Arichidonic Acid Cascade.[2]

1.3 Cyclodextrins

1.3.1 Background

Villiers first discovered cyclodextrins in 1891 by digesting starch with *Bacillus amylobacter*, which he originally named cellulosine, but Schardinger achieved most of the groundwork in 1903 by using the microbe *Bacillus macerans* in digesting the starch.[4] However, only the chemical composition of the cyclodextrins, and no knowledge of the scientific process of the digestion, was known by Schardinger. Subsequently it has been discovered that the above-mentioned microorganisms produce an enzyme named glucosyl transferase, which is currently used in industry to produce large amounts of cyclodextrin by acting on hydrolysed starch at optimum temperature.[4] Furthermore, allegations of cyclodextrins being toxic by French *et al* were refuted by toxicological studies in the 1970's, [5] motivating increased interest in creating cyclodextrin-containing

products and technologies. Presently, numerous articles pertaining to cyclodextrin research are published annually, international symposia are organized and several companies are producing cyclodextrins by the ton per year, indicating that cyclodextrins have become a useful product for human consumption and other purposes.

1.3.2 Structure

Cyclodextrins (CDs) are cyclic oligosaccharides consisting of α-D-glucopyranose units, which are linked via rigid α-1,4 bonds and which usually adopt the $^4C_1$ chair conformation. All secondary hydroxyl groups are positioned on one side (wider side) of the cyclodextrin and the primary hydroxyl groups on the other (narrow side), imparting a cone-like shape to the molecule (Figure 1.3). The primary O(6) hydroxy groups may rotate around the C(5)-C(6) bond (Figure 1.4) resulting in either the O(6) hydroxyls pointing away from the cavity forming a (-) *gauche* [ω = -60°] O(5)-C(5)-C(6)-O(6) torsion angle (ω), or pointing towards the ring forming the less preferred (+) *gauche* conformation [ω = +60°]. The *trans* orientation [ω = +180°] has not been observed as yet. Glycosidic oxygen bridges line both rims and non-bonding electrons face the centre of the cone resulting in a high electron density within, thereby creating the characteristic hydrophobic interior and hydrophilic exterior.[6] In most cyclodextrins intramolecular hydrogen bonding occurs between the hydroxyl groups of adjacent glucose rings creating a rigid structure, thereby imparting crystalline properties.

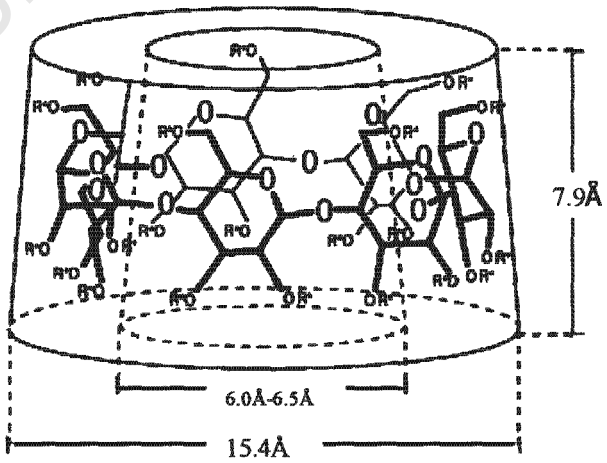

Figure 1.3: Schematic representation of β-cyclodextrin (R=R'=R''=H).

Owing to steric demands a CD molecule usually does not form rings with fewer than six units, the most common numbers represented being six, seven and eight units (α-, β- and γ-cyclodextrin). Larger rings do occur containing nine (δ) and twelve (η) units but the rings are collapsed and their thermodynamic properties dissuade their use.[6,7] As mentioned previously there are several types of unmodified (parent) cyclodextrins and there are numerous modified cyclodextrins. Modification of the cyclodextrin via hydroxyl group H-atom substitution, results in classes accommodating these modified CDs, such as methylated CDs, hydroxyalkylated CDs and acetylated CDs. [7,8]

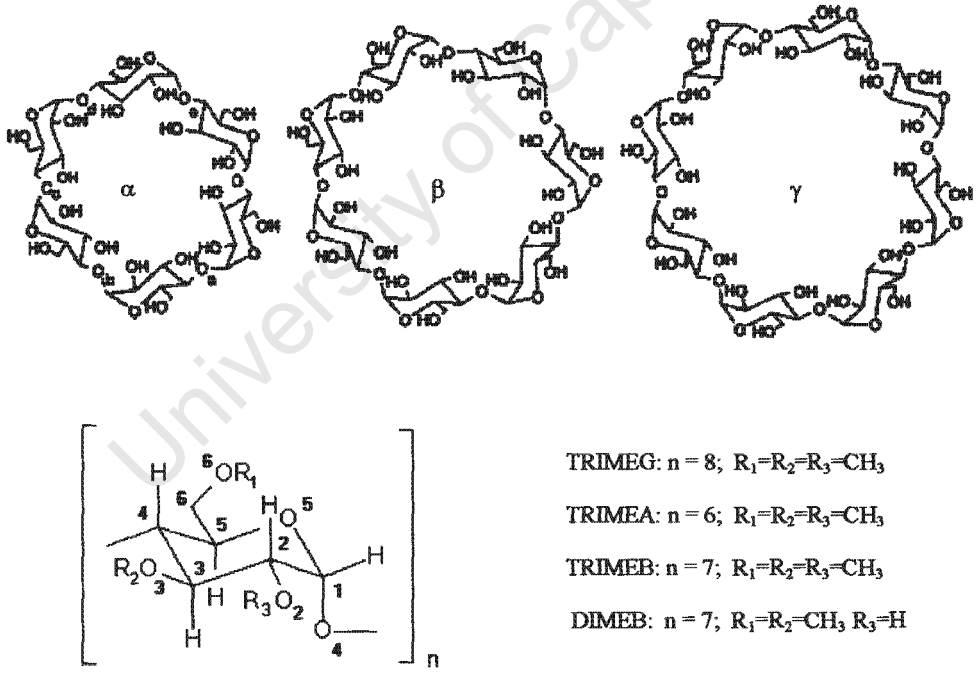

Figure 1.4: Structures of Parent and Modified CDs.

1.3.3 Conformation

The macrocyclic *n*-fold symmetrical conformation is described by certain parameters, ultimately indicating whether deviation from the symmetry has occurred.[9] These include the distances between the linking glycosidic oxygen atoms O(4)···O(4') (*l*), the radius of the polygon (*r*) which is the distance measured from the centroid to each O(4) atom, the O(4)···O(4')···O(4'') angle (*a*), the torsion angle O(4)···O(4')···O(4'')···O(4''') (*t*), the O(2)···O(3) distance, the intersaccharide bond angle (φ) which is defined as φ = C(1')-O(4)-C(4) (Figure 1.5) and the tilt angle (τ). The latter is the measure of the relative inclination of each glucose unit from the ideal *n*-fold symmetry. This tilt angle is defined as the angle made by the mean O(4) plane and the mean plane through the atoms O(4'), C(1), C(4) and O(4) of each glucose unit. A positive tilt angle is obtained if the glucose unit O(6) side is inclined towards the centre of the cavity; a negative tilt angle is obtained if the glucose unit O(6) side is inclined towards the outside of the cavity.[9]

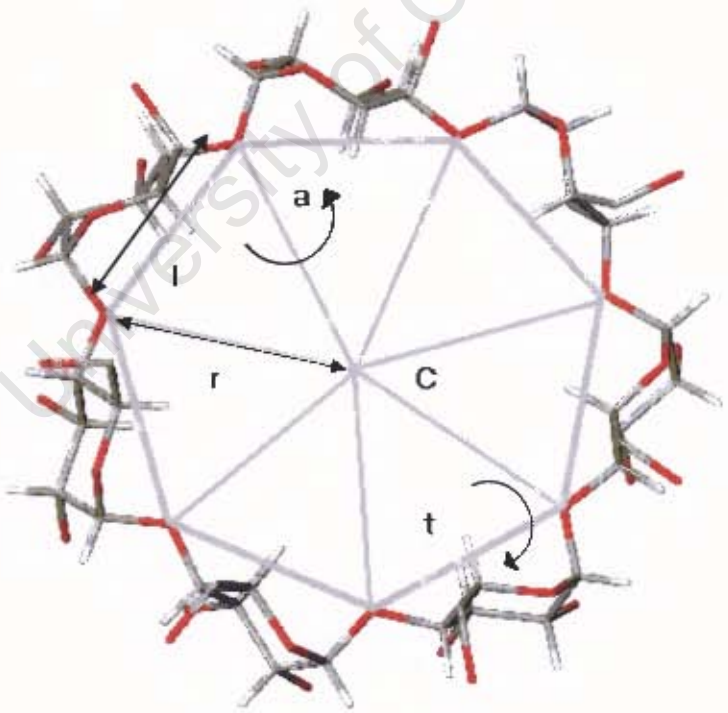

Figure 1.5 Principal geometrical parameters of the O(4) polygon.

1.3.4 Properties

Certain properties are ascribed to cyclodextrins owing to their structure, one of which is the afore-mentioned hydrophilic exterior and a hydrophobic interior. Other intrinsic physico-chemical properties of the parent cyclodextrins such as solubility, diffusion coefficient and dielectric constant and water content are listed in Table 1.1.

Table 1.1: Properties of cyclodextrins.[5]

Parameter	α-CD	β-CD	γ-CD
Number of glucose units	6	7	8
MW (Da)	972	1135	1297
Solubility in water at RT (g per 100mL)	14.5	1.85	23.2
$[\alpha]_D$ at 25 °C (°)	150 ± 0.5	162.5 ± 0.5	177.4±0.5
Cavity diameter (pm)	470-530	600-650	750-830
Height of Torus (pm)	790 ± 10	790 ± 10	790 ±10
Diameter of outer periphery (pm)	1460± 40	1540± 40	1750± 40
Approximate volume of cavity (10^8 pm^3)	174	262	427
Crystal form (from water)	Hexagonal plates	Monoclinic prisms	Tetragonal prisms
Crystallographic parameters			
C4-O4-C4' angle (°)	119.0	117.7	112.6
ϕ/ψ	166/-169	169/-172	165/-169
O-4···O-4' distance (pm)	423	439	448
O-2···O-3' distance (pm)	300	286	281
Crystal water (wt.%)	10.2	13.2-14.5	8.13-17.7
Diffusion coefficient at 40°C (cm^2s^{-1})	3.443	3.224	3.260
Dielectric constant on incorporating the toluidinyl group of 6-*p*-toluidinyl-naphthalene-2-sulphonate at pH 5.3 and 25°C	47.5	52.0	70.0
p*K*a (by potentiometry) at 25°C	12.332	12.202	12.081
Partial molar volume in solution ($mLmol^{-1}$)	611.4	703.8	801.2
Adiabatic compressibility in aqueous solution (10^4 $mLmol^{-1}bar^{-1}$)	7.2	0.4	-5.0

The aqueous solubility of parent CDs is relatively lower than that of modified CDs, due to high crystal lattice energies, intramolecular hydrogen bonding resulting in unfavourable enthalpies of solution, and lack of mobility.[7] Temperature also plays an important role in CD solubility; the solubility of parent CDs increases with increasing temperature but the modified CDs display an inverse solubility coefficient whereby the solubility decreases

with increasing temperature.[5] Although CDs are not hygroscopic they do form stable hydrates where the water may either be included within the cavity of the CDs or in interstitial sites.[8] Different amounts of water may be involved with each CD resulting in different crystal parameters. Another area of importance apart from physico-chemical properties relates to the biological properties of CDs. Questions regarding how the cyclodextrin interacts with the biochemical and physiological system of humans arise and need to be answered thoroughly to appease the public; therefore, a complete toxicological investigation of each CD compound is necessary. Studies have indicated that consumed CDs are metabolised in the colon by microflora, yielding acyclic maltodextrins, maltose and glucose and that negligible amounts are absorbed into the bloodstream.[5] However, chemically modified CDs are resistant to enzymatic degradation and may end up in the circulatory system and complexation of crucial membrane components such as cholesterol and phospholipids also occurs. Complexation is dependent on the cavity size and solubility. Therefore β-cyclodextrin and DIMEB are the most damaging.[5] In summary, chemically modified CDs and CDs that have an affinity for cholesterol are the most toxic and should not be consumed.

1.3.5 Crystal Packing

Packing arrangements are described using β-cyclodextrin as a model, where all forms of packing are observed for cyclodextrin complexes. Packing is observed where the CDs interact with each other forming dimers via O(3)···O'(3) hydrogen bonds along the secondary rim.[10] Once crystallized monomeric and dimeric CDs may pack in two ways, cage or channel structure; channel-type structures are recognized by the CDs being stacked directly on top of one another thereby forming a continuous cavity. Conversely, in cage type structures, the cavities are isolated due to blockage by adjacent CDs. Two cage type models exist, namely the herringbone and the brick-type.[11] Both classes may be subdivided even further; monomeric structures are arranged in five packing arrangements: herringbone, zigzag, brickwork, layer and helical channel; dimeric structures are arranged in four types: channel, screw channel, intermediate and chessboard. These packing schemes are illustrated in Figures 1.6 and 1.7.

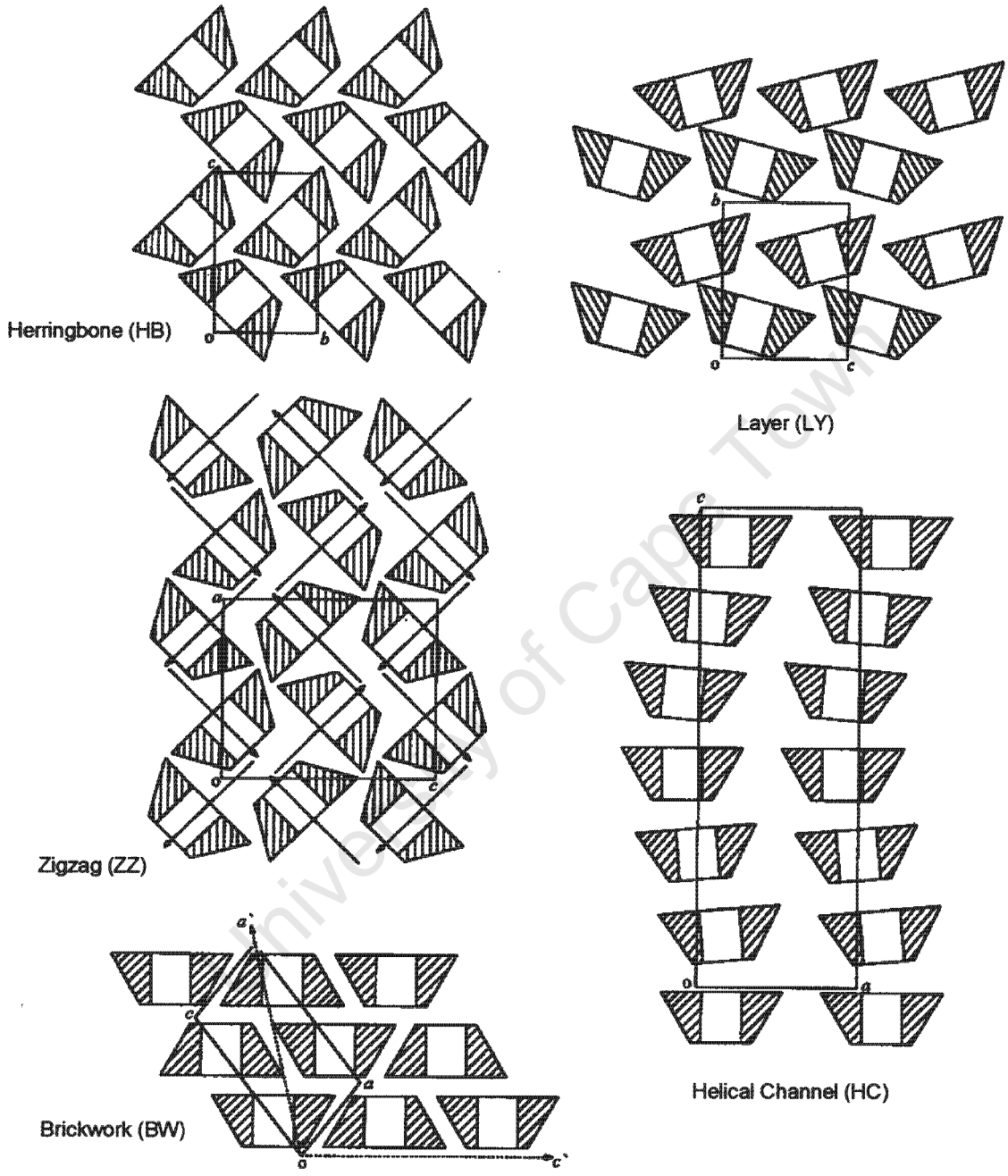

Figure 1.6 Packing arrangements of β-CD monomers.

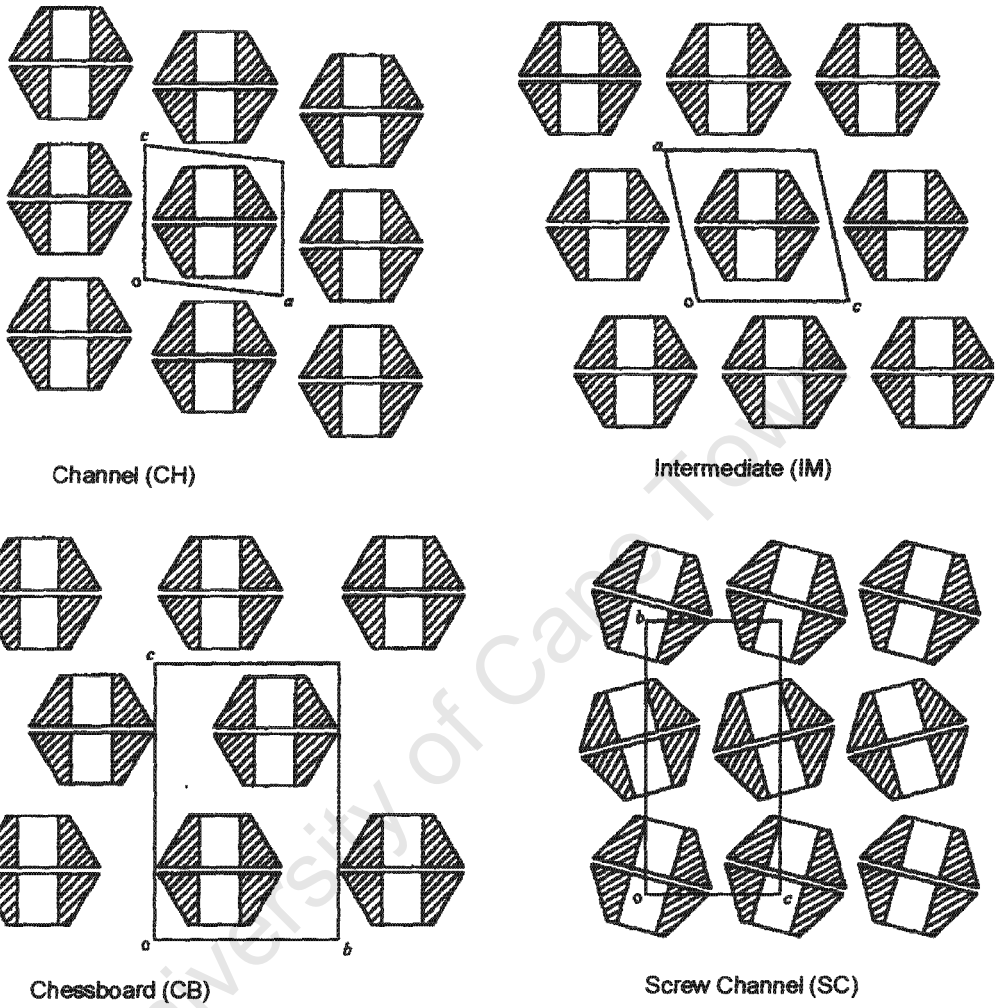

Figure 1.7 Packing arrangements of β-CD dimers.

1.3.6 Applications

Owing to the amphiphilic character of CDs, these molecules are excellent hosts for complexing apolar guests (Figure 1.8).[7,8,12] The driving forces behind this feat include the electrostatic interaction, van der Waals interaction, hydrophobic interaction, hydrogen bonding and charge-transfer interaction, ultimately yielding a more stable lower energy state of the CD with an accompanying decrease in ring strain.[13,14] Although no covalent bonds are broken or formed during complexation the guest is 'locked' within the cavity via so-called supramolecular forces,[15] thereby modifying the guest's physicochemical

properties. Experimentally, some of the properties that are modified are: solubility enhancement, stabilisation against oxidation, visible or UV light and heat damage and control of volatility and sublimation.[13]

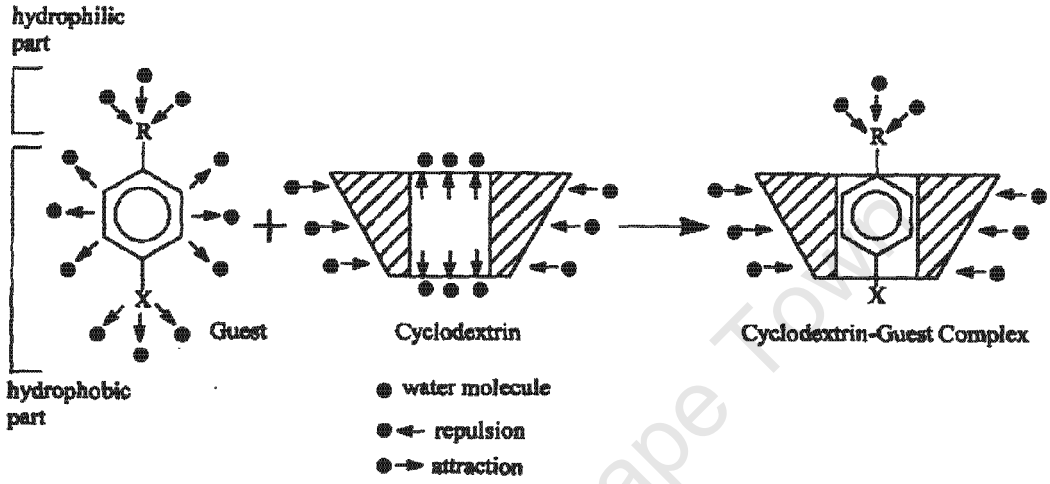

Figure 1.8 Illustration of cyclodextrin Inclusion.

With the full contingent of these remarkable inclusion properties, scientists have capitalized on CDs and used them for an array of scientific endeavours such as chromatographic separations, modification of food flavourants, masking unpleasant odours and controlled release of pharmaceuticals.[13] Consistent with the theme of this project there are numerous examples of CDs used in the pharmaceutical industry to enhance drug delivery through biological membranes.[7,8] Drugs are required to have an adequate level of water solubility in order to be delivered to the human body. This is efficiently achieved via CD complexation. Externally the CDs are hydrophilic and carry the drug within solution to the surface of the membrane whereby the hydrophobic drug partitions into the membrane leaving the CD in the aqueous membrane exterior. Furthermore, unlike other penetration enhancers such as fatty acids, the CD does not disrupt the lipid layers of the membrane.[13] This increased solubility and stability may improve the bioavailability of the drug thereby possibly increasing its pharmacological effect.

1.4 Polymorphism

The study of polymorphism has flourished in the last three decades, with improved technology and scientific techniques. More and more scientists have become aware of the intrinsic importance of polymorphism in structural crystallographic studies.[16] Under different thermodynamic and kinetic conditions a chemical substance may crystallize in different phases, i.e. it is able to arrange in more than one three-dimensional arrangement or conformation in a crystal. These new forms are referred to as polymorphs.[17] With the resultant differing unit cell content the polymorphs inherently have different physical properties such as density, melting point, solubility and heat of fusion. Figure 1.9 is a schematic of the different polymorphs obtainable. (A) and (B) are polymorphs that have molecules in the same conformation but different crystal structures. When the molecule changes conformation as seen with (C) this is viewed as a conformational polymorph. Crystal solvates, whereby solvent molecules become incorporated into the crystal structure also exist, as seen with (D) and (E). In addition amorphous (non-crystalline) forms also exist; these are thermodynamically unstable and eventually crystallize to a stable polymorph. [17]

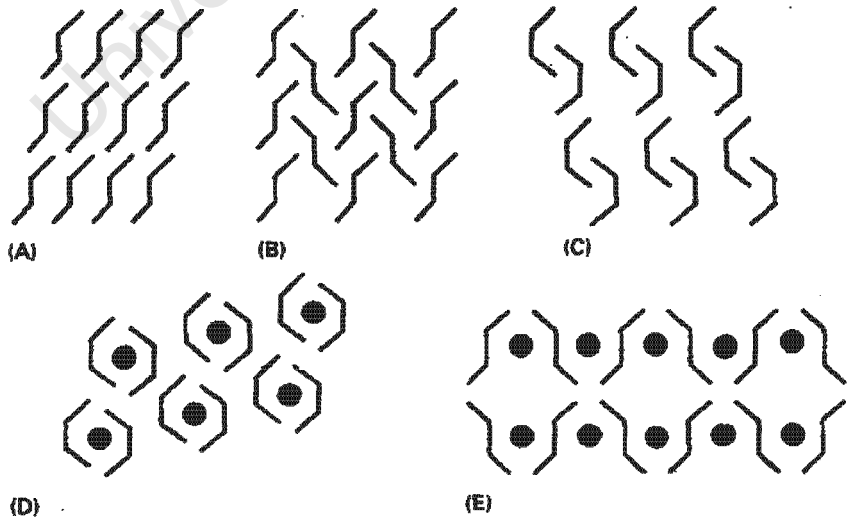

Figure 1.9 Illustration depicting polymorphs (A-C) and solvates (D-E)

As polymorphs essentially display different physical properties such as solubility, bioavailability and dissolution rate,[18] the most appropriate polymorph needs to be identified. This is particularly important in the pharmaceutical industry where different polymorphs can result from processes such as milling, desolvation and storage (Figure 1.10). A thorough examination of the polymorphic properties of a drug accompanied by its isolation and characterization are necessary in this industry for patents and characterization regulations. This information may also be subsequently used to 'engineer' an optimum polymorphic type of the pharmaceutical under study.[19]

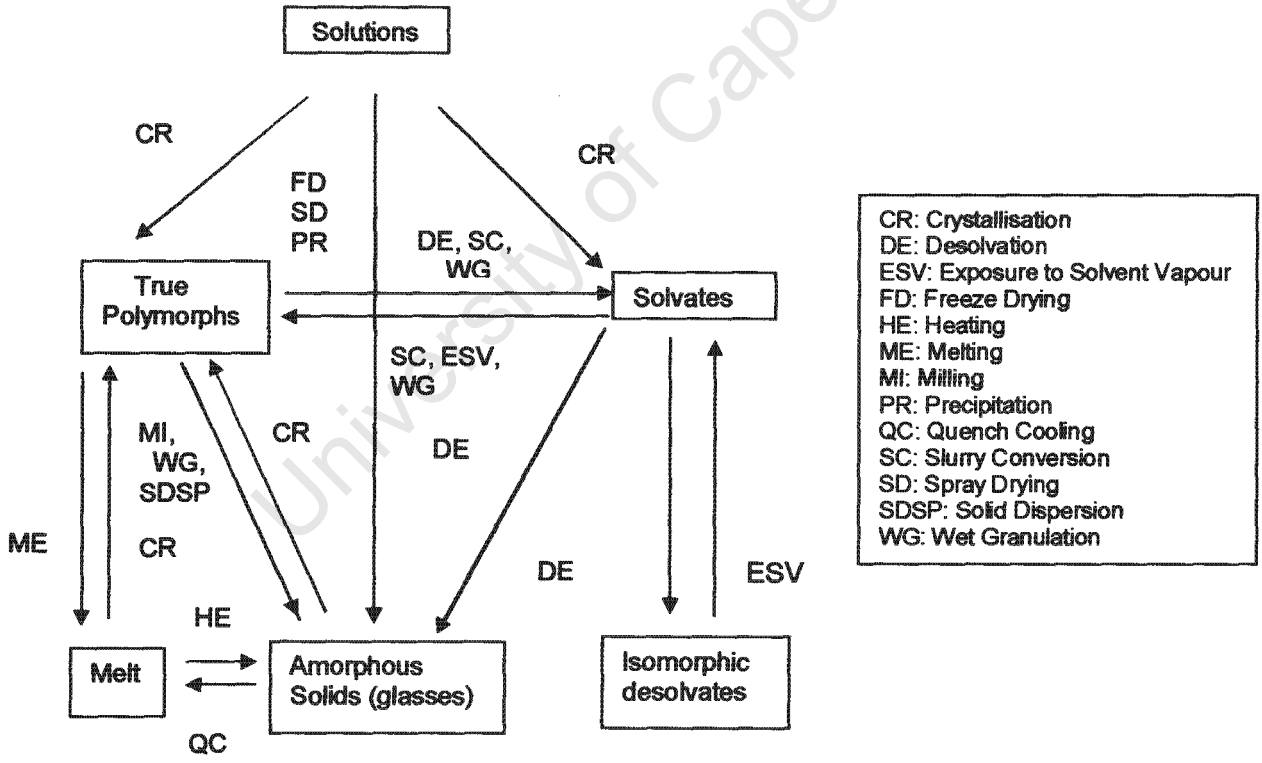

Figure 1:10 Polymorphs that may be produced by standard pharmaceutical processes.[19]

1.5 Aim of Study

1.5.1 Non-Steroidal Anti-Inflammatory Drugs

The NSAIDs were selected for study in this project due to their low aqueous solubility. These may be utilised as anti-inflammatories and analgesics. Six drugs were chosen and are depicted in Table 1.2 below.

Table 1.2 The NSAIDs used for investigation.

NSAID	Structure and IUPAC name	Chemical Class
Rofecoxib[20]	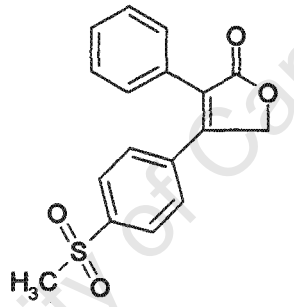 4-(4-methyl-sulphonylphenyl)-3 -phenyl-2,5-dihydro-2-furanone	Di-aryl-substituted furanones
Celecoxib[21]	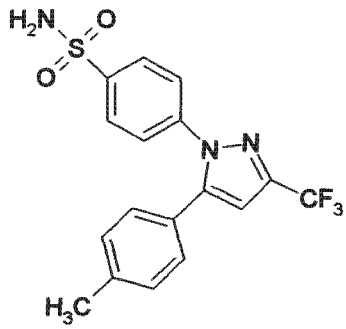 4-(5-(4-methylphenyl)-3-trifluoromethyl-1*H*- pyrazol-1-yl) benzenesulphonamide	Di-aryl-substituted pyrazoles

Bucetin	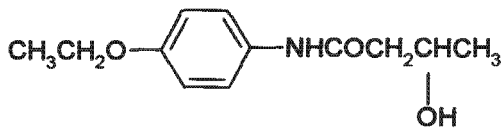	Phenetidine derivative

N-(4-ethoxyphenyl)-3-hydroxybutanamide

Lornoxicam	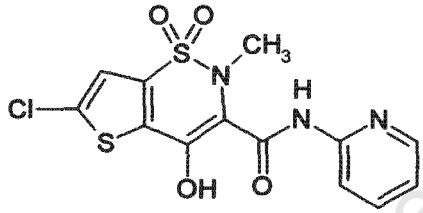	Thiazinecarboxamides

6-chloro-4-hydroxy-2-methyl-N-2-pyridinyl-2H-thieno[2,3-e]-1,2-thiazine-3-carboxamide 1,1-dioxide

Suprofen[22]	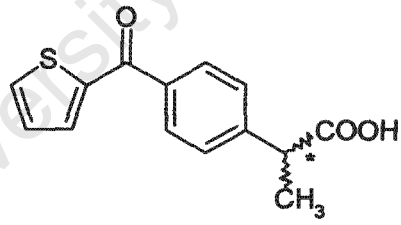	Arylpropionic acid derivatives

α-methyl-4-(2-thienylcarbonyl)benzeneacetic acid

Diflunisal[23]	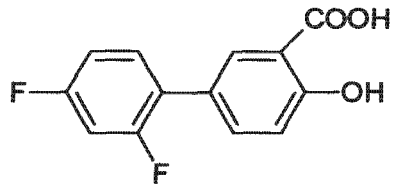	Salicylic acid derivatives

2',4'-difluoro-4-hydroxy-[1,1'-biphenyl]-3-carboxylic acid

As mentioned previously NSAIDs generally have very poor aqueous solubility (section 1.2.2). Described below are recent selected articles reporting cyclodextrin inclusion (section 1.5.2) and polymorphism (section 1.5.3) of NSAIDs. These articles clearly indicate how these two methods improve dissolution and enhance absorption of NSAIDs, thereby improving the pharmaceutical performance. This was the basis for the approach adopted in this study.

1.5.2 Cyclodextrin Inclusion

Within the published literature, recent work performed on inclusion of non-steroidal anti-inflammatory drugs with CDs was reported by Mavridis *et al* [24] and Rawat *et al.*[25] The former used ^{1}H NMR and HPLC to examine inclusion of the NSAID *Acemetacin sodium* in order to study sustained release of the drug and for the practical purpose of patent application. The latter research group used phase solubility experiments to study the interaction between *Rofecoxib* and CDs, finding a significant increase in the solubility of the drug in the presence of the macromolecules. Similar aims attended this project, whereby in order to modify the chosen therapeutic performance of the NSAIDs, encapsulation by CDs was considered. Using several characterization techniques, notably X-ray structure elucidation, the prepared inclusion complexes were characterised to illuminate their properties.

1.5.3 Polymorphism

In a recent article describing NSAIDs and crystal polymorphism, Chawla *et al* [26] reported the characterization of different solid state forms of the drug *Celecoxib*. By finding alternative solid forms the aim was to improve the poor aqueous solubility and non-ideal physicochemical properties of this drug. Similarly, in this project, a comprehensive study of the chosen NSAIDs was pursued, where the drugs were subjected to numerous tests analogous to pharmaceutical procedures. Whether a new polymorph resulted or not was elucidated using diverse chemical characterization techniques such as thermoanalytical, crystallographic, microscopic, spectroscopic and elemental analyses.

1.5.4 Final Remarks

This project focused on the i) preparation, ii) determination of chemical composition, iii) analysis of thermal behaviour and iv) investigation of the molecular structures of the obtained inclusion complexes and polymorphs. Thereby, information about their i) thermal stability and ii) structural features, such as spatial distribution and role of water in the crystal structure, could be elucidated.

1.6 References

1. Lévesque, H; Lafont, O. *Rev. Méd. Interne,* **2000**, *21,* 8-17.
2. Celotti, F; Laufer, S. *Pharmacol. Res.,* **2001**, *43*, 429-436.
3. Van der Bijl, P; Van der Bijl, P. *SADJ,* **2002**, *57,* 328-331.
4. D'Souza, V.T; Lipkowitz, K.B. *Chem. Rev.,* **1998**, *5*, 1741-2076.
5. Szejtli, J. *Comprehensive Supramolecular Chemistry, Cyclodextrins,* Atwood, J.L., Davies, J.E.D., MacNicol, D.D, Vogtle, F., (eds.), Pergamon: Oxford, **1996**, *3*, 1-5.
6. Szejtli, J. *Chem. Rev.,* **1998**, *98*, 1743-1753.
7. Loftsson, T; Brewster, M.E. *J. Pharm. Sci.,* **1996**, *85,* 1017-1025.
8. Fromming, K; Szejtli, J. *Cyclodextrins in Pharmacy,* Kluwer Academic Publishers, **1994.**
9. Saenger, W. *Inclusion Compounds,* (Vol. 2), Atwood, J; Davies, J.E.D; MacNicol, D. (eds.), Oxford University Press, London, **1984**, Ch 8.
10. Mentzafos, D; Mavridis, I.M. *Acta Crystallogr.,* **1991**, *B47*, 746-757.
11. Saenger, W; Jacob, J; Gessler, K; Steiner, T; Hoffmann, D; Sanbe, H; Koizuma, K; Smith, S; Takaha, T. *Chem. Rev.,* **1998**, *98*, 1787-1803.
12. Dodds, D. R. *PhD Thesis, Physicochemical Study of Inclusion of Drug Molecules in Cyclodextrins,* University of Cape Town, South Africa, **1999.**
13. Martin Del Valle, E.M. *Process Biochem.,* **2004**, *39,* 1033-1046.
14. Liu, L; Guo, Q. *J. Incl. Phenom. Macrocycl. Chem.,* **2002**, *42*, 1-14.
15. Chapman, R; Sherman, J. *Tetrahedron No. 434,* **1997**, *53,* 15911-15945.
16. Bernstein, J. *Polymorphism in Molecular Crystals,* Oxford University Press, **2002.**
17. Grant, D.J.W. *Polymorphism in Pharmaceutical Solids,* Marcel Dekker, Inc. **1999.**
18. Caira, M.R; Pienaar, E.W; Lötter, A.P. *Mol. Cryst. Liq. Cryst.,* **1996**, *279,* 241-264.
19. Lian, Y; Reutzel, S.M; Stephenson, G.A. *Pharm. Sci. Technol. To.,* **1998**, *1*, 118-127.
20. Shashi Rekha, K; Vyas, K; Raju, C.M; Chandrashekar, B; Reddy, G. *Acta Crystallogr. ,* **2000**, *C56,* e68.
21. Vasu Dev, R; Shashi Rekha, K; Vyas, K; Mohanti, S.B; Rajender, P; Reddy, G. *Acta Crystallogr.,* **1999**, *C55,* e161.
22. Peeters, O; Blaton, N; de Ranter, C. *Bull. Soc. Chim. Belg.,* **1983**, *92,* 191-192.
23. Hansen, L; Perlovich, G; Bauer-Brandl, A. *Acta Crystallogr.,* **2001**, *E57,* 477-478.
24. Mavridis, I.M; Zouvelakis, D; Yannakapoulou, K; Vyza, E. *Carbohyd. Res.,* **2002**, *337,* 1387-1395.

25. Rawat, S; Jain, S.K. *Pharmazie,* **2003**, *58,* 639-641.

26. Chawla, G; Gupta, P; Thilagavathi, R; Chakraborti, A.K; Bansal, A.K. *Eur. J. Pharm. Sci.,* **2003**, *20,* 305-317.

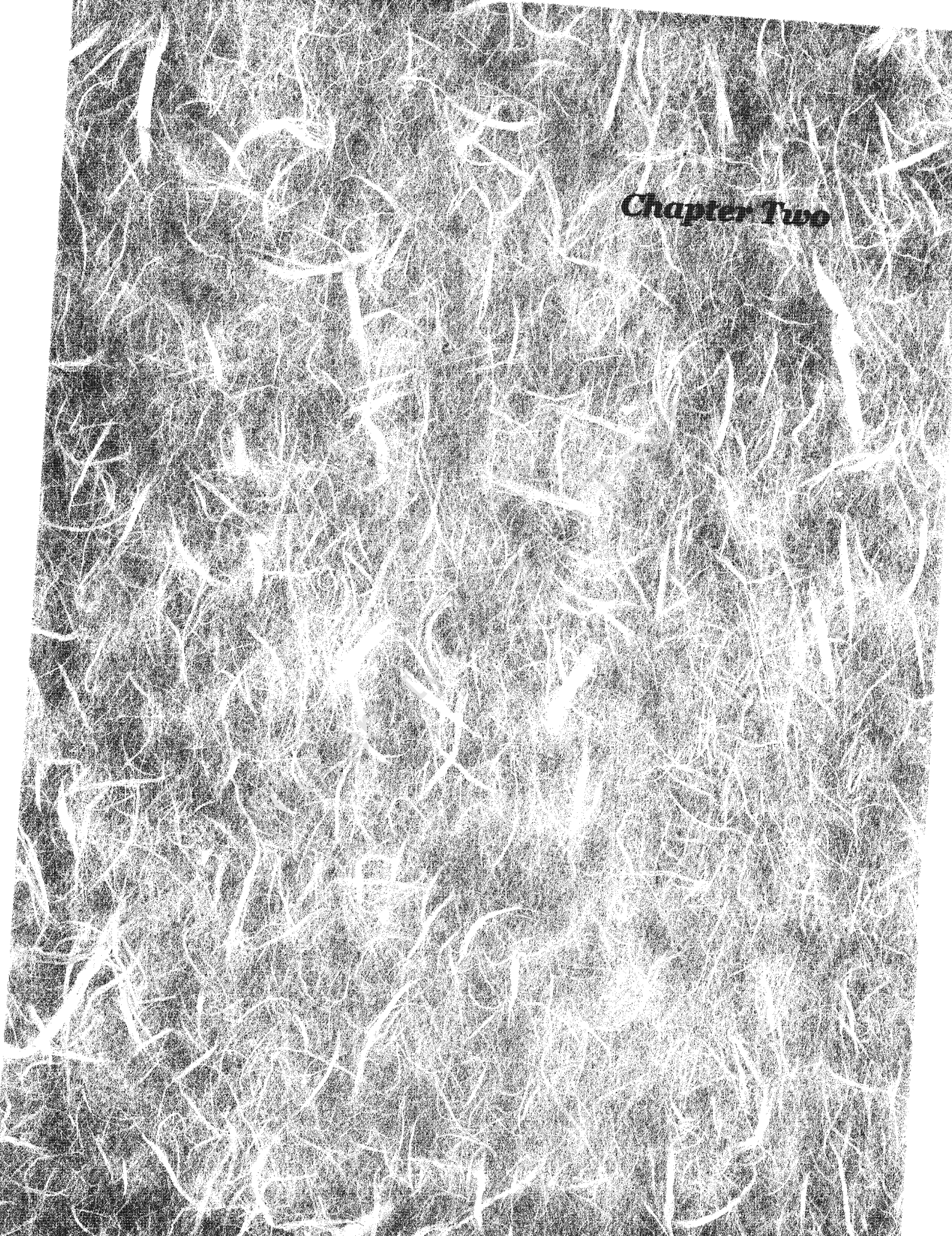
Chapter Two

Chapter Two: Experimental

2.1 Materials

The host compounds β-cyclodextrin, γ-cyclodextrin, Heptakis(2,6-di-O-methyl)-β-cyclodextrin (DIMEB), Heptakis(2,3,6-tri-O-methyl)-β-cyclodextrin (TRIMEB), Octakis(2,3,6-tri-O-methyl)-γ-cyclodextrin (TRIMEG), Hexakis(2,3,6-tri-O-methyl)-α-cyclodextrin (TRIMEA), Randomly-methylated β-cyclodextrin (RAMEB) and Hydroxypropyl-β-cyclodextrin (HPβCD) were purchased from Cyclolab (Budapest, Hungary) and used without further purification. The NSAIDs Bucetin, Lornoxicam, Suprofen and Diflunisal were purchased from Sigma Chemical Company [St. Louis, Missouri, USA], Rofecoxib from Merck & Co Inc. [Rahway, NJ, USA] and Celecoxib from Pharmacia [Morpeth, Northumberland, UK]. All these were used without pre-treatment.

2.2 Methods of preparation

Several methods were attempted to produce complexes and/ or polymorphs during the course of this project. Tables 2.1 and 2.2 below contain a summary of the techniques used.

Table 2.1: Polymorph production techniques used.

Technique:	Conditions:
Recrystallisation	A saturated solution consisting of 10 mg drug in 2 ml of a particular solvent was prepared and filtered with microfilters (pore size 0.45 μm). The filtrate was then left to evaporate at various temperatures. Different conditions attempted: 1.Single solvents: • 1-Butanol • Acetonitrile • Methanol • Ethanol • Toluene • 1,4-dioxane • Carbon tetrachloride • Benzene • 2-Butanone • Ethyl Acetate • Water • Dimethylformamide • Hexane • Cyclohexane • Diethyl Ether • Cyclohexanol • 1-Propanol • Acetone • Dichloromethane 2.Binary mixtures • Water: methanol (1:10 v/v) • Water: acetonitrile (1:10 v/v) • Water: ethanol (1:10 v/v) 3.Varied temperatures of evaporation (25 °C, 60 °C and 0 °C)
Sublimation	40 mg of drug was placed in a sublimation apparatus under vacuum at 100 °C and left for seven days. The recrystallised drug deposited on the cold finger.
Co-grinding	25 mg of the drug was mechanically agitated in a 'Wig-L-Bug amalgamator (model: 3110-3A)' device for 25 minutes
Vapour diffusion	25 mg of drug was dissolved in 2 ml of a good solvent (ethyl acetate) and the vessel placed in a larger vessel containing a miscible 'bad' solvent in which the drug was insoluble (diethyl ether). This set-up was placed within a desiccator under vacuum and was allowed to stand for 1 week.
Recrystallisation from the melt	Small quantities of the drug were melted in the DSC machine. The drug was then taken out of the machine and allowed to cool at room temperature for 0, 10, 30 minutes and 3 and 7 days respectively.

Table 2.2: Cyclodextrin complexation techniques used.

Technique:	Conditions:
Co-precipitation	RAMEB, HPβCD, β- and γ-CD: the drug was added to a hot saturated aqueous solution of CD, in a 1:1 stoichiometric ratio. DIMEB, TRIMEB, TRIMEG, TRIMEA: the drug was added to a cold saturated aqueous solution of CD (inverse solubility coefficient), in a 1:1 stoichiometric ratio. The solutions were stirred until clear and the resultant filtered with microfilters, pore size 0.45 μm. The methylated CD:drug filtrates were placed in the oven at 60 °C, the others exposed to 25 °C to induce crystallisation. Different conditions attempted: 1. Different molar ratios (CD:drug) 2. Surfactant (Tween 80) 3. Co-solvent (ethanol, methanol and acetone) 4. Rate of addition of drug to CD solution 5. Refluxing (100 °C, 24 hr) 6. Ultra-sonification (22 kHz, 25 °C, 30 min) 7. Suspension 8. Different volumes of aqueous solvent 9. Different temperatures during stirring and evaporation: 25 °C, 60 °C, 0 °C 10. Recrystallising pre-kneaded material
Kneading	The parent CDs were initially kneaded into a paste with a mortar and pestle and distilled water. The drug was then subsequently added and kneaded for various times. Different conditions attempted: 1. Different molar ratios 2. Different times of kneading 3. Co-solvent
Co-grinding	1:1 molar ratio mixture of drug:CD with no water was placed within a 'Wig-L-Bug amalgamator (model: 3110-3A)' co-grinding apparatus and ground for 25 minutes.

2.3 Thermal Analysis

Any variation in physical properties resulting from a change in temperature is monitored and analysed by the following techniques.

2.3.1 Hot Stage Microscopy (HSM)

This technique is used for preliminary identification of a new polymorph or complex via morphology and visual thermal event differences. Occurrences such as melting, decomposition and loss of solvent are observed and the nature of polymorphic transition, or whether a hydrate has formed may be deduced.[1] Suitable crystals were placed on a slide and submerged in inert silicone oil; the slide was duly placed on a heating block and the temperature was raised at a rate of 10 °C/min. The hot stage used was a Linkam TH600, which is connected to a Linkam CO600 temperature controller. A NIKON SMZ-10 microscope fitted with a polarizing trans-illuminator and overhead light was linked to the hot stage. The photomicrographs were recorded using a Sony real time Digital Hyper HAD video camera, and analysed using the software analySIS.[2]

2.3.2 Thermogravimetric Analysis (TGA)

This technique measures mass loss as a function of applied temperature. Monitoring mass loss, decomposition and desolvation are readily identified. Hence a clear distinction may be made between anhydrous, hydrated or specifically solvated crystal forms.[1] Mass loss from a cyclodextrin inclusion complex indicated the number of water molecules of crystallisation.[3] Measurements were performed on a Mettler Toledo TGA ISDTA851. Sample masses of 0.5-6.5 mg were placed in a platinum open pan and put in a furnace with a 10 ml/min Nitrogen flow rate and run at a heating rate of 10 °C/min.

2.3.3 Differential Scanning Calorimetry (DSC)

The heat flow to maintain the temperature difference constant at 0 °C between the sample and an inert reference is measured. If there is a change in thermal energy, an endotherm or exotherm results in the DSC plot of differential rate of heating versus temperature.[1] This may signify phase changes, loss of included solvent and melting. Comparisons of the traces indicate whether a new polymorph or complex has resulted. Experiments were performed on a Perkin-Elmer PC Series 7 System. Samples of mass 1-6 mg were sealed in a vented aluminium pan and placed in a furnace with a 40 ml/min Nitrogen stream; the temperature was raised at 10 °C/min. The reference pan was an empty aluminium pan.

2.4 Ultra-Violet (UV) Spectrophotometry

UV spectrometry is used to identify new CD complexes by comparing UV absorption maxima of the uncomplexed drug chromophore to that of the complex. CDs are UV inactive; therefore the chromophore will be partly shielded and will result in a shift in the spectrum. The CD: drug molar ratio is also determined via spectrophotometry. The spectra were recorded on a Cintra 20 UV System at 285 nm.

2.5 Elemental Analysis

This procedure determined the percentage of carbon, hydrogen, nitrogen and sulphur in putative complexes and verified the host: guest ratio. Measurements using 2-3 mg of sample were performed on a Fisons EA1108 CHNS-O Elemental Analyser.

2.6 X-Ray Powder Diffraction (XRPD)

XRPD is a fundamental method whereby compound characterisation may be done quickly and efficiently. Every compound exhibits a unique powder pattern owing to its exclusive structural features; consequently identification of a new polymorph or complex may be achieved via comparison of the diffractograms of the specific test subject versus the reference polymorph and a physical mixture of the CD and drug respectively. Differences found in the succession of peaks detected at the distinctive scattering angles permit phase identification.[1,3] A microcrystalline sample of 5-10 mg was placed randomly on a Mylar® flat sample holder and intensities measured using a Huber Imaging Plate Guinier Camera 670. Nickel filtered CuKα_1 radiation (λ = 1.5405981 Å) was produced at 40 kV and 20 mA by a Philips PW1120/00 generator fitted with a Huber long fine-focus tube PW2273/20 and a Huber Guinier Monochromator Series 611/15. For high temperature XRPD, the Huber High Temperature Controller HTC 9634 unit was used with the capillary rotation device 670.2. The samples were manually ground and packed into Lindemann capillaries with an internal diameter of 1 mm and a glass thickness of 0.01 mm. The capillaries were obtained from Hilgenberg, Germany. A 2θ-range of 4 to 100.0° was used with a step size of 0.005° 2θ.

The program LAZY PULVERIX[4] generated idealised X-ray powder patterns. Refined unit cell parameters, space group symmetry, atomic co-ordinates and thermal parameters for crystal structures determined were input and the idealised XRPD pattern obtained.

2.7 Nuclear Magnetic Resonance (NMR) Spectroscopy

This is a technique used for determination and confirmation of new unknown structures. Radio-frequency pulses are applied to the sample within a magnetic field which subsequently gives rise to the observed signals. Information derived from these signals such as chemical shift, coupling constants and integration suggests the possible sample structure. The spectra were recorded on a Mercury VXR 400 Spectrometer using deuterated chloroform as the solvent and tetramethylsilane as the internal standard.

2.8 High Performance Liquid Chromatography (HPLC)

HPLC is used to identify certain compounds within a mixture, whereby a particular compound will have a characteristic peak. The concentration of the compound is calculated via the integration of the chromatographic peak. Analysis of the solutions was achieved using an Agilent 1100 Series HPLC instrument.

2.9 Crystal Structure Determination

Crystals exhibit the property of diffracting radiation of wavelength similar to the translational repeat period of the molecular pattern. This wavelength coincides with that of X-rays and it is the electron density of the crystal that is responsible for diffraction. Using this fundamental knowledge, single crystal X-ray diffraction was formulated whereby measuring the diffraction intensities, the internal structure of crystals is ultimately deduced. This technique is ideal for polymorph and complex identification. Single crystals between 0.2 and 0.5 mm in all dimensions and which were able to extinguish plane-polarised light uniformly were selected. These were coated with Paratone N oil,[5] to prevent decomposition and to secure the specimen rigidly, and mounted on a glass fibre that was placed on a goniometer head. The reflection intensity data were measured on a Nonius Kappa CCD Single Crystal X-ray Diffractometer, using graphite-monochromated MoK_α radiation (λ = 0.71069 Å) generated by a Nonius FR590

generator operated at 50 kV and 30 mA. Low temperature measurements were performed using a constant stream of N_2 gas with a flow rate of 20 cm^3/min maintained by an Oxford Cryostream cooler. Data reduction and unit cell refinement were performed using the programs DENZO and SCALEPACK[6] with accompanying correction of Lorentz-polarisation effects. The program X-PREP[7] was used for assignment of the correct space group.

2.10 Crystal Structure Analysis and Refinement

Structures were solved either by direct methods using the programs SHELXS-97[8] and SHELXD[9] or by isomorphous replacement using as trial model the published co-ordinates for non-hydrogen atoms from an isostructural structure in the program SHELXL-97.[10] For all structure refinements low-angle reflections truncated by the beam-stop were omitted. The mean $|E^2-1|$ values were determined, where E is the normalised structure factor. If this value is close to 0.968 the structure is centrosymmetric. If it is close to 0.736 the structure is acentric.

SHELXL-97 uses full-matrix least-squares refinement on F^2 and was operated through the X-SEED interface.[11] The quantity $\sum w (F_o^2 - F_c^2)^2$ was minimised. If the residual index (R_1, definition 1) involving structure factor amplitudes is small (~0.02-0.05), a satisfactory model has been obtained. Agreement between structure factors for the refinement against F^2 is expressed by the residual index (wR_2, definition 2). A default weighting scheme (w) including the parameters a and b, is represented below [expression 3]. The weighting scheme was refined at the end of each structure refinement. The Goodness-of-Fit (S) [expression 4] which is based on F^2 should be close to unity for well behaved structures, and the over-determination ratio (n/p) should be of the order 10, where n is the number of reflections and p is the total number of parameters refined.

[1] $$R_1 = [\sum | |F_o| - |F_c| |] / \sum |F_o|$$

[2] $$wR_2 = \{ [\sum w (F_o^2 - F_c^2)^2] / [\sum w (F_o^2)^2] \}^{1/2}$$

[3] $$w = 1 / [\sigma^2 (F_o^2) + (aP)^2 + bP] \text{ where } P = [\max (0, F_0^2) + 2 F_c^2] / 3$$

[4] $$S = [\sum [w (F_o^2 - F_c^2)^2] / (n - p)]^{1/2}$$

2.11 Additional Resources

Several computer software programs were used for crystal structure analysis:

- The CAMBRIDGE STRUCTURAL DATABASE (CSD)[12] was used for comparison of previously published crystal structures with the structures obtained in this study.
- LAYER[13] displays the measured intensity data as simulated precession photographs of all levels of the reciprocal lattice. Systematic absences, and hence space group symmetries were determined from this program.
- Analysis of molecular conformations and other structural parameters was performed using PLATON.[14]
- Molecular packing diagrams were created using POV-RAY.[15]
- WEBLAB ViewerPro Version 3.5[16] was used to model various bond lengths and angles thereby mimicking bond rotation, hence elucidating disorder models.
- SADABS Version 2.03[17] was used to exploit data redundancy to correct three-dimensional integrated data for errors due to X-ray absorption.
- The thermal ellipsoid plotting program ORTEP III[18] was used to produce ball and stick crystal structure illustrations including atoms drawn as ellipsoids at the 50% probability level.

2.12 References

1. Brittain, H.G. *Polymorphism in Pharmaceutical Solids*, Marcel Dekker Inc, New York, **1999**, 227-263.
2. Soft Imaging System GmbH, *Digital Solutions for Imagining and Microscopy,* Version 3.1 for Windows (Copyright **1987 – 2000**).
3. Szente, L. *In Comprehensive Supramolecular Chemistry, Cyclodextrins* , Atwood, J.L., Davies, J.E.D., MacNicol, D.D, Vogtle, F., (eds.), Pergamon: Oxford, Elsevier Science Ltd, **1996**, *8*, 253-274.
4. Yvon, K; Jeitschko, W; Parthé, E. *J. Appl. Crystallogr.,* **1977**, *10*, 73-74.
5. Paratone N oil (Exxon Chemical Co., TX, USA).
6. Otwinowski, Z; Minor, W. *Processing of X-ray Diffraction Data in Oscillation Mode in Methods in Enzymology,* (Vol. 276) Academic Press, New York, **1996**, 307.
7. *Data Preparation and Reciprocal Space Exploration,* Version 5.1, (Copyright Bruker Analytical X-ray Systems, **1997**).
8. Sheldrick, G.M. *Crystallographic Computing,* (Vol. 3) Sheldrick, G.M; Kruger, C; Goddard, R (eds.), Oxford University Press, London, **1985**, 175.
9. Schneider, T; Sheldrick, G. M. *Acta Crystallogr.,* **2002**, D*58,* 1772-1779.
10. Sheldrick, G.M. SHELXL-97, *Program for the Refinement of Crystal Structures,* University of Göttingen, Germany, **1997.**
11. Barbour, L.J. X-Seed, A Software Tool for Supramolecular Crystallography, *Supramolecular Chemistry,* **2001**, *1,* 189-190.
12. *Cambridge Structural Database and Cambridge Structural Database System,* Version 5.*23*, April **2004**, Cambridge Crystallographic Data Centre, University Chemical Laboratory, Cambridge, England.
13. Barbour, L.J. LAYER, A computer program for the graphic display of intensity data as simulated precession photographs, *J. Appl. Crystallogr.,* **1999**, *32,* 31-32.
14. Spek, A.L. PLATON, A multipurpose crystallographic tool, Version 10500, © **1980-2000.**
15. Pov-Ray for Windows, Version 3.1e.watcom.win32, The persistence of vision development Team, © **1991-1999.**
16. WebLab viewerPro Version 3.5 (Copyright **1999** by Molecular Simulations Inc., San Diego, CA).
17. Sheldrick, G.M. SADABS, Version 2.03, Bruker/Siemens area detector

absorption and other corrections, **1999**.

18. Ortep-III for Windows: Farrugia,L.J. *J. Appl. Crystallogr.*, **1997**, *30*, 565-566.

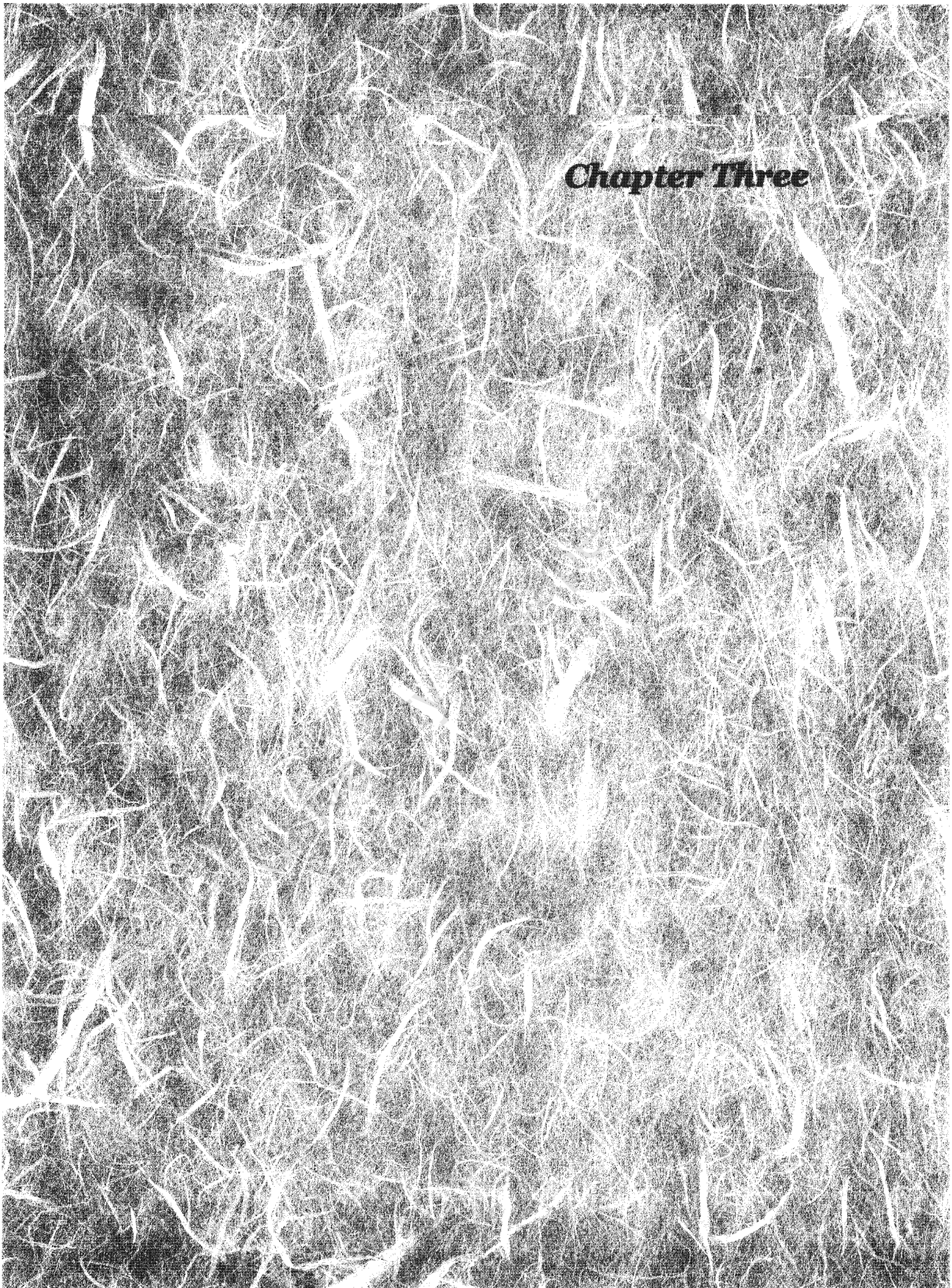

Chapter Three

Chapter Three: Characterisation of Novel Solid Forms

3.1 General Overview

In the course of this study, no new solid forms of the drugs lornoxicam, diflunisal, bucetin and suprofen were discovered. However, new solid forms derived from celecoxib, rofecoxib and permethylated β-cyclodextrin were encountered. These include an amorphous form of celecoxib, a degradation product of rofecoxib and a new crystalline modification of the host permethylated-β-CD (TRIMEB). Their characterization and significance are discussed below.

3.2 Solid state studies of Celecoxib

3.2.1 Introduction

Celecoxib, 4-(5-(4-methylphenyl)-3-trifluoromethyl-1*H*-pyrazol-1-yl) benzene sulphonamide, is a selective COX inhibitor with anti-inflammatory activity (Figure 3.1). One crystalline form of celecoxib has been reported.[1] The unit cell is triclinic, space group $P\bar{1}$. Molecules of celecoxib are linked by intermolecular hydrogen bonds (N-H···O) into chains.

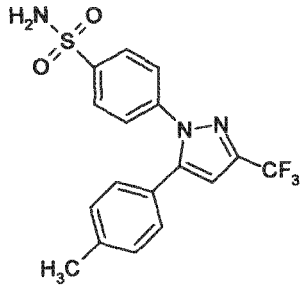

Figure 3.1: Structure of Celecoxib

Since its approval for marketing in 1998, celecoxib has been used for the treatment of osteoarthritis, rheumatoid arthritis and management of pain.[2] Pharmacologically though,

celecoxib exhibits poor flow properties, compressibility, cohesiveness and very poor aqueous solubility (~5 μg/ml at 25°C),[3, 4] thereby complicating its processing into solid forms and reducing its efficacy on its biological target. Thus, it is imperative that improvement of its overall bioavailabilty and physicochemical properties is achieved. Utilising alternate solid forms may bring this about.[2] The objective of this study is to attempt production of polymorphs, pseudopolymorphs and amorphous forms which may improve the effectiveness of celecoxib.

3.2.2 Preparation of solid forms

An amorphous form of celecoxib was prepared by melting 5 mg of the drug in the DSC apparatus (200 °C) and allowing it to cool to room temperature. This new amorphous form shall be referred to as RFMcele.

3.2.3 Elemental Analysis

This technique was used to prove that no new product was formed. The calculated values based on the given formula of celecoxib are compared to the experimental values of RFMcele.

Table 3.1: Elemental analysis results for C, H, N and S of $C_{17}H_{14}F_3N_3O_2S_1$.*

	Celecoxib (Calculated)	RFMcele (Experimental)
% C	53.6	53.1
% H	3.5	3.2
% N	11.2	10.9
% S	8.1	8.1

* The errors in experimental values are ± 0.5%.

The results indicate that the amorphous form has not altered chemically from the original celecoxib.

3.2.4 Thermal analysis

DSC and TGA analysis

Variations in the thermal events of the drug indicate that a new solid phase has formed. The DSC trace depicted below shows endotherm peaks directed upwards and exotherm peaks downwards

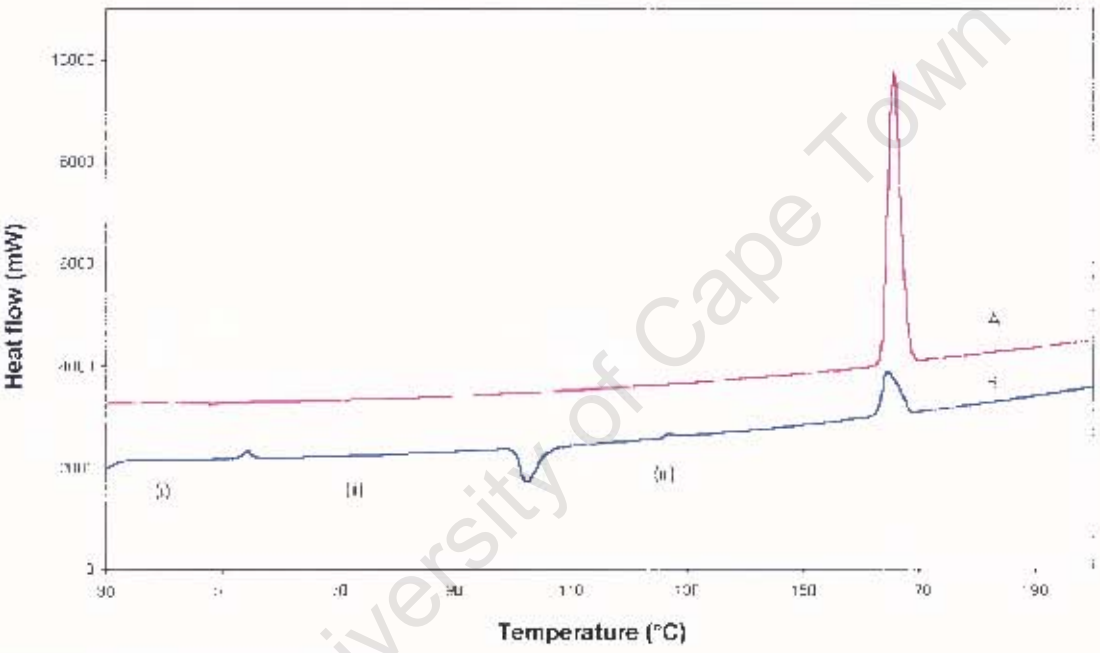

Legend. A= DSC curve of Celecoxib
B= DSC curve of RFMcele

Figure 3.2: DSC curves for Celecoxib and RFMcele.

The TG curves for both forms (not shown) indicated that no decomposition took place and that both were free of solvent, since zero mass loss was recorded in the temperature range 30°C-200 °C. In the DSC analysis (curve A) celecoxib exhibited a single endotherm corresponding to melting in the temperature range of 160.6-165.4 °C (ΔH_f = 99.3 J/g) (Figure 3.2). After cooling, the heating DSC trace of RFMcele (curve B) indicated an endotherm at the onset temperature of 52.9 °C corresponding to a glass transition. It is often found that the glass transition temperature is about two-thirds of that of the melting temperature.[5] In this case the ratio works out to be 0.74, thereby strongly

supporting the interpretation of this endotherm as a glass transition. An exotherm was observed at onset temperature 100.3 °C corresponding to a recrystallisation and finally an endotherm at onset temperature 162.8 °C which corresponds to the melt. There is a very slight endotherm at 129.6 °C, which most probably corresponds to the release of occluded air, since no water loss was shown in the TG trace. Confirmation of these assignments was obtained using the HSM and XRPD techniques.

HSM analysis

Figure 3.3 shows the photomicrographs of the transitions occurring in RFMcele examined under silicone oil. Due to the difference in the conditions and geometry that the sample is exposed to in the DSC and HSM equipment, the temperatures of the thermal events occurring differ slightly.

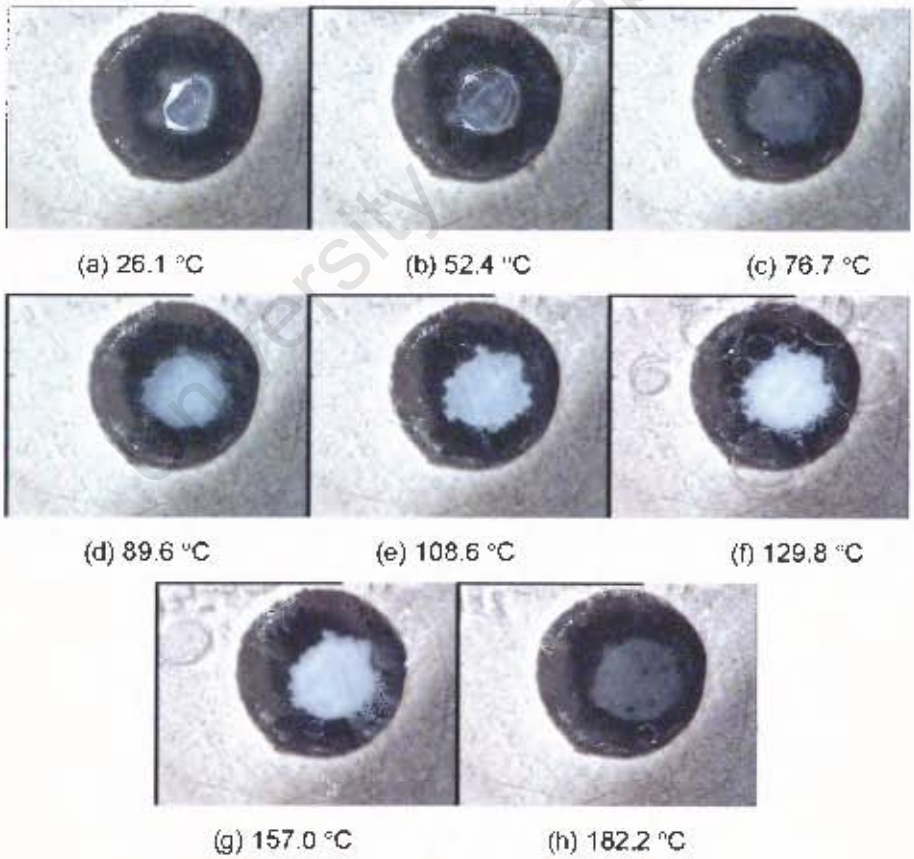

Figure 3.3: Photomicrographs of RFMcele.

The glass transition is seen beginning at 52.4 °C (Figure 3.3 (b)). The recrystallisation is seen around 89.6 °C (Figure 3.3 (d)). The melt is completed at 182.2 °C (Figure 3.3 (h)). Bubbles are emitted starting from 89.6 °C (Figure 3.3 (d-g)). Since TG calculations proved that no solvent is lost, these bubbles correspond to loss of occluded air.

3.2.5 XRD Powder Analysis

Incremental temperature XRPD recordings were performed to establish whether RFMcele was indeed amorphous in nature and whether or not new polymorphic phases of the drug appeared at various temperatures. The traces shown in Figure 3.4 correspond to temperatures in-between the endo- and exothermic events depicted in the DSC trace (Figure 3.2 (i), (ii), (iii)).

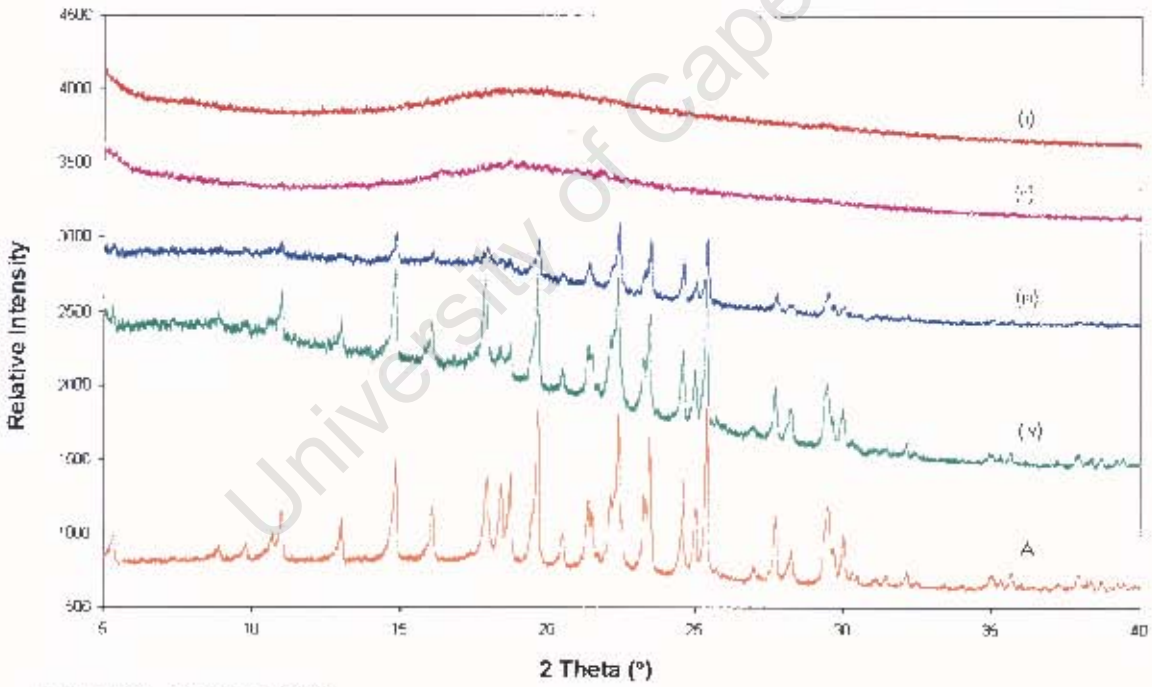

Legend: (i) = RFMcele, 28 °C
(ii) = RFMcele; 70 °C
(iii) = RFMcele, 110 °C
(iv) = RFMcele; 150 °C
A = Celecoxib; 28 °C

Figure 3.4: XRPD Traces of RFMcele and Celecoxib.

The traces (i) and (ii) confirm the amorphous nature of RFMcele; these are devoid of any diffraction peaks confirming lack of three-dimensional long-range ordered structure. These temperature readings precede the recrystallisation exotherm at 100.3 °C, whereafter the material adopts the same crystal structure as the original non-melted celecoxib as seen in (iii) and (iv). PXRD also verifies that air was evolved corresponding to the small endotherm at 129.6 °C in the DSC trace in Figure 3.2. The two XRPD patterns shown at 110 °C (iii) and 150 °C (iv) lie on either side of the slight endotherm in question. No discrepancy occurs between the two patterns proving that no change in the structure of celecoxib has occurred.

Apart from the amorph reported here, no other solid forms of celecoxib were encountered using the extensive protocol described in Chapter 2, section 2.2.

3.3 Derivative of Rofecoxib

3.3.1 Introduction

Rofecoxib, 4-(4-methyl-sulphonylphenyl)-3-phenyl-2, 5-dihydro-2-furanone (Figure 3.5), is a Cox-2 inhibitor belonging to the di-aryl-substituted furanones. The molecules within the crystal structure are held together by van der Waals interactions and the crystal is tetragonal with space group $P4_12_12$. [6]

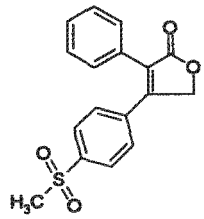

Figure 3.5: Structure of Rofecoxib.

Rofecoxib, since being introduced in 1999, has been used for the treatment of osteoarthritis, primary dysmenorrhoea and acute pain.[7] However, as with celecoxib, its effectiveness may be reduced due to its low solubility in water (~0.0086 mg/ml at 25 °C) and limited dissolution rate.[8] Therefore, to combat this problem different solid forms were pursued that might show superior solubility behaviour.

3.3.2 Experimental Conditions

In the attempt to discover a new polymorph, an unexpected product was obtained. It resulted from two methods, recrystallisation and/or co-precipitation. In the recrystallisation experiment 10 mg of rofecoxib was dissolved in 2 ml of ethyl acetate and stirred at 65 °C for 15 minutes. For the co-precipitation experiment 10 mg of rofecoxib was stirred in 2 ml 10% HPβCD solution at 60 °C for 72 hours. All solutions were exposed to room light intensity. The resultant solution was thereafter filtered and left to evaporate at room temperature. After one month crystals formed. Following unequivocal elucidation of the structure by single crystal X-ray analysis (section 3.3.7), the product was found to correspond to 6-methyl sulphonyl phenanthro [9,10-c] furan-1 (3H)-one, [9] a photodegradation product of rofecoxib (figure 3.6). Further characterisation of the product was performed using PXRD, thermal analysis, HPLC, elemental analysis

and ^{1}H-NMR spectroscopy. The last technique was used to confirm that the proton count and chemical shifts were consistent with the structure determined crystallographically.

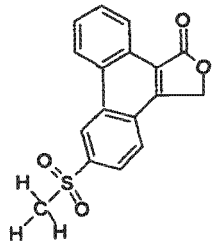

Figure 3.6: Structure of Compound A.

3.3.3 Thermal Analysis

DSC and TGA analysis

These techniques were used as preliminary tests to ascertain whether rofecoxib had indeed changed in molecular structure to compound A.

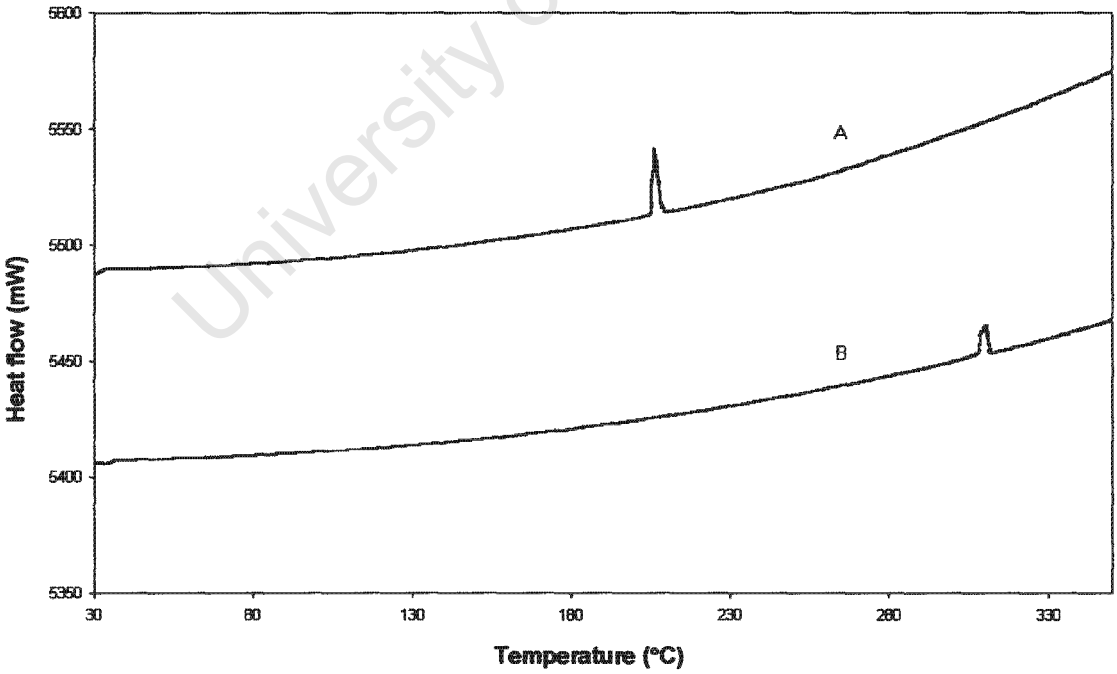

Legend: A = Rofecoxib
B = Compound A

Figure 3.7: DSC curve of Rofecoxib and Compound A.

Rofecoxib exhibited a fusion endotherm (Figure 3.7) at onset temperature 209.3 °C (ΔH_f = 125.0 J/g). Compound A also exhibited a single fusion endotherm but at the different onset temperature of 307.1 °C (ΔH_f = 48.5 J/g) thereby implying that these are two different chemical species. TGA proved that both forms were free of solvent since there was a zero mass loss in the temperature range 30°C- 350 °C.

3.3.4 High Performance Liquid Chromatography

Reverse Phase HPLC was performed with a detection wavelength of 280 nm using a variable wavelength UV detector. A 5 µg/ml, 1:1 stoichiometric ratio of rofecoxib and HPβCD solution was made and tested (Figure 3.8 and Table 3.2).

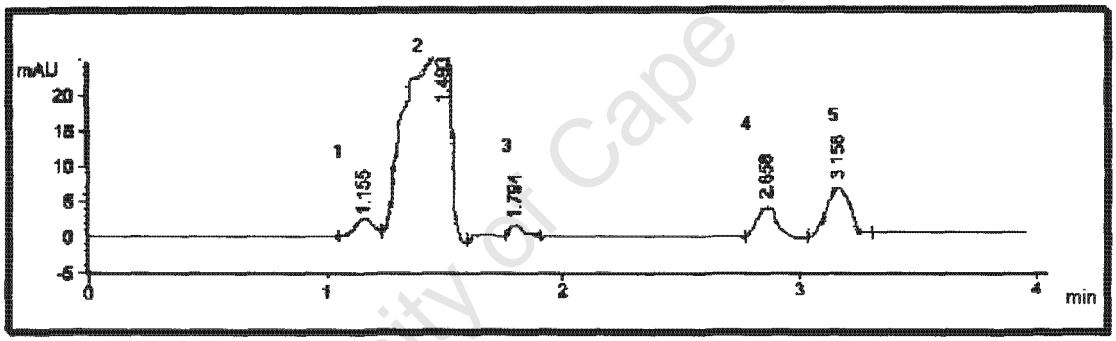

Figure 3.8: HPLC trace for Rofecoxib and HPβCD solution.

The following peaks were obtained:

Table 3.2: Results of HPLC run with Rofecoxib and HPβCD solution concentration 5 µg/ml.

Peak #	RetTime (min)	Width (min)	Height (mAU)	Area %
1	1.155	0.1023	2.7533	3.885
2	1.493	0.1216	42.8310	83.451
3	1.794	0.0665	2.0463	1.990
4	2.858	0.0680	4.0621	3.843
5	3.158	0.0730	6.7646	6.831

Peaks (1) to (3) are common retention peaks that are found in all the HPLC traces of this HPLC, and may be omitted for clarity in this discussion. A peak for pure rofecoxib

appears at 2.858 min (peak 4). Cyclodextrins are UV inactive. However, for this sample, a dual peak (4) and (5) is seen, indicating that rofecoxib and additionally another possible degradation product of rofecoxib (compound A) is present.

3.3.5 Elemental Analysis

The C, H and S elemental percentages were calculated for compound A according to the given formula. These are verified experimentally, supporting that compound A has been formed.

Table 3.3: Elemental Analysis results for Compound A ($C_{17}H_{12}O_4S_1$).*

Form A	Calculated (%)	Experimental (%)
C	65.4	65.4
H	3.9	3.9
S	10.3	9.8

* The errors in experimental values are ± 0.5%.

3.3.6 Nuclear Magnetic Resonance Spectroscopy

Figure 3.9 shows the Nuclear Magnetic Spectra obtained from the VXR 300 NMR spectrometer using TMS as an internal standard and $CDCl_3$ as the solvent.

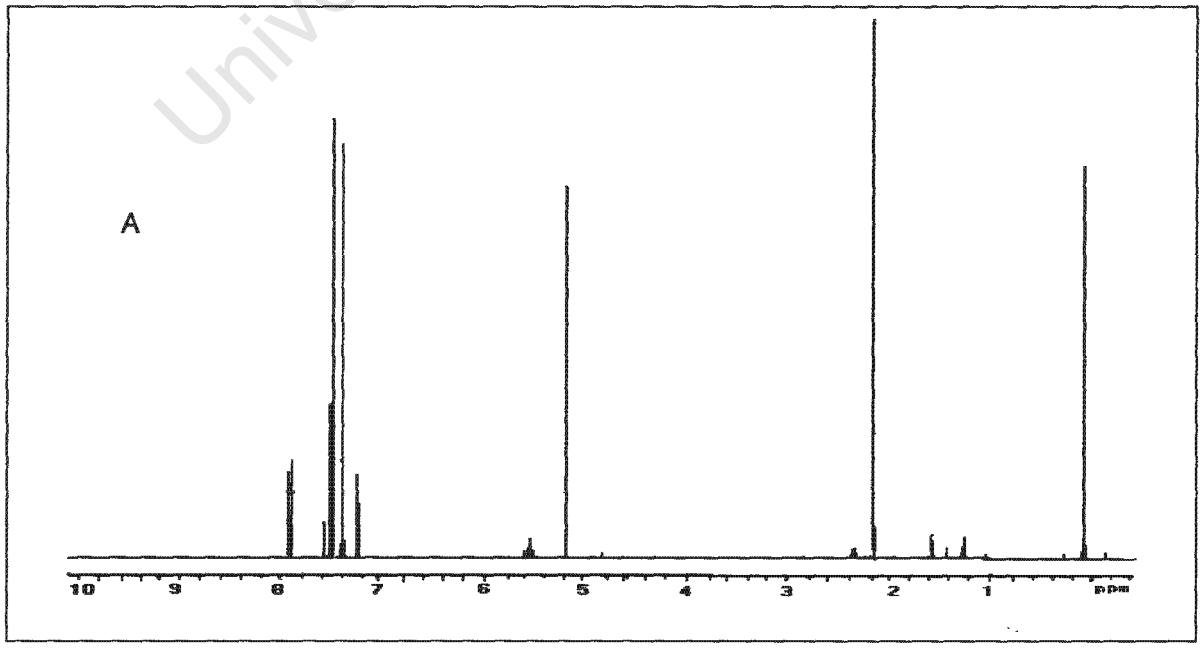

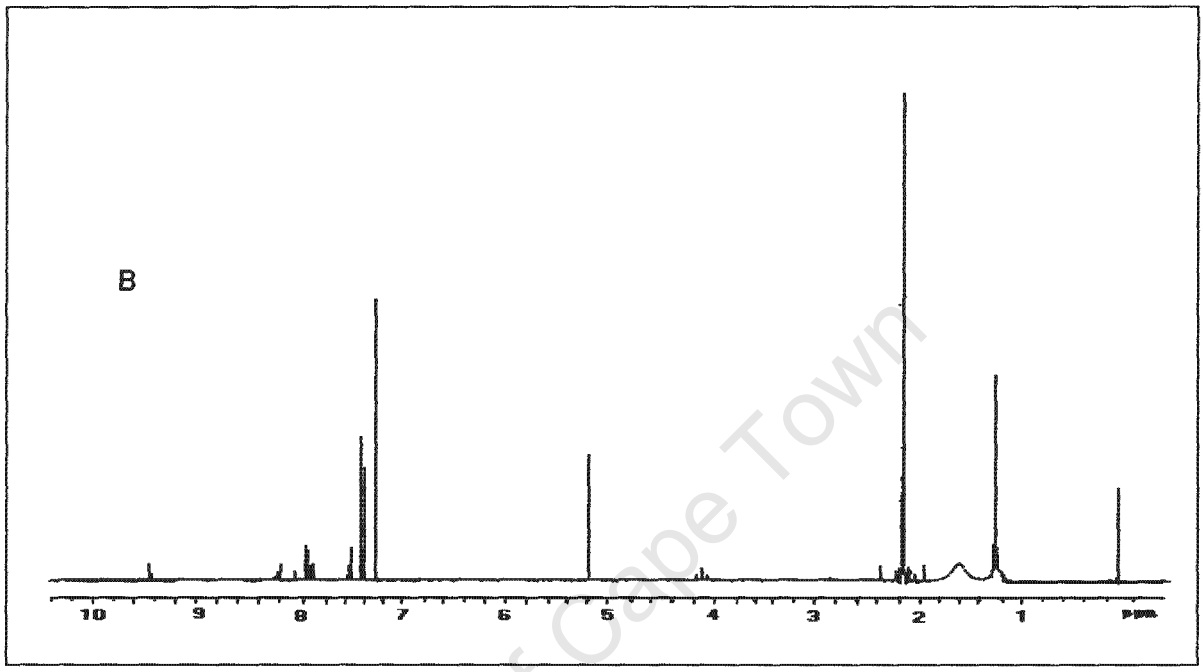

Legend: A: ^{1}H-NMR spectrum of Rofecoxib

B: ^{1}H-NMR spectrum of Compound A

Figure 3.9: NMR Spectra for Rofecoxib and Compound A.

A NMR spectrum provides information on the number of chemically equivalent protons, the electron density surrounding the proton and the integration (number of protons responsible for a certain signal). From this information the molecular structure may be deduced. [10] For this project only the proton count and chemical shifts were necessary to confirm the structure of compound A. Proton assignments are depicted in Tables 3.4 and 3.5.

The NMR results of Table 3.4 correspond to the known structure of rofecoxib, thus verifying that an unaltered form was initially used for the experiments. However, the NMR results for compound A (Table 3.5) were different from those for rofecoxib, proving that a possible degradation product of rofecoxib has formed.

Table 3.4: NMR results for Rofecoxib.

Rofecoxib			
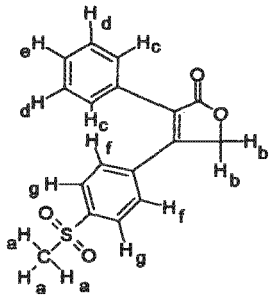			
Chemical Shift (δ)	Multiplicity	Integration	Assignment
2.162	s	3H	Ha
5.187	s	2H	Hb
7.397	d	2H	Hc
7.492	d	1H	He
7.521	t	2H	Hd
7.921	d	2H	Hf
7.985	d	2H	Hg

Table 3.5: NMR results for Compound A.

Compound A			
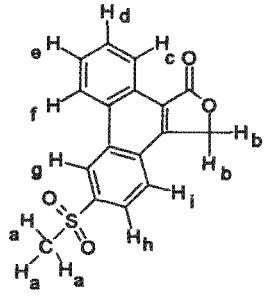			
Chemical Shift (δ)	Multiplicity	Integration	Assignment
2.153	s	3H	Ha
5.190	s	2H	Hb
7.399	t	1H	Hd
7.494	t	1H	He
7.942	d	1H	Hc
7.954	d	1H	Hf
7.985	d	1H	Hi
8.089	d	1H	Hh
9.221	d	1H	Hg

After assignment of the peaks obtained in the spectrum of compound A and comparison with the results of pure rofecoxib, it was clear that certain protons were absent and the symmetry of the aromatic systems altered with greater dispersion of aromatic proton signals with differing chemical and magnetic environments. Thus it was deduced that aryl-aryl cross-coupling had occurred. The structure of compound A was thereafter tentatively assigned from the NMR results (Table 3.5) which subsequently verified the crystallographic analysis.

3.3.7 X-Ray Crystallographic Analysis

Unit cell determination

The unit cell parameters and crystal system of the new product were determined rapidly using the Nonius Kappa CCD diffractometer. A crystal of high quality was selected and mounted using Paratone N oil and used for data-collection. Table 3.6 lists the parameters determined for compound A in comparison to rofecoxib.

Table 3.6: Unit cell parameters for Compound A and Rofecoxib.

	Compound A	Rofecoxib[8]
Space group	$P\bar{1}$	$P4_12_12$
a	8.4641 (1) Å	11.374 (2) Å
b	9.2247 (2) Å	11.374 (2) Å
c	9.4227 (2) Å	22.939 (3) Å
α	79.8987 (1) °	90 °
β	85.9977 (9) °	90°
γ	67.5502 (2) °	90°
Volume	669.41 (2) $Å^3$	2967.6 (9) $Å^3$
Z	2	8

Data-Collection

The intensity data were collected on the Nonius Kappa CCD diffractometer using graphite-monochromated MoKα radiation with the crystal cooled to 113K. No phase changes occurred during cooling. Intensity data were corrected for absorption using the

program SADABS.[11] Listed in Table 3.7 are the crystal data and data-collection parameters.

Table 3.7: Crystal data and data-collection parameters for Compound A.

Molecular Formula	$C_{17}H_{12}O_4S$
Formula Weight/g mol^{-1}	312.31
Crystal System	Triclinic
Space group	$P\bar{1}$
a / Å	8.4641 (1)
b / Å	9.2247 (2)
c / Å	9.4227 (2)
α / °	79.8987 (1)
β / °	85.9977 (9)
γ / °	67.5502 (2)
Volume / Å^3	669.41 (2)
Density$_{calc}$ / g cm^{-3}	1.5494
μ (MoKα) / mm^{-1}	0.260
F(000)	324
Crystal size / mm^3	0.15 × 0.20 × 0.20
Range scanned θ / °	$2 \leq \theta \leq 26$
Index ranges	h: -10, 10 k: -11, 11 l: -11, 11
ϕ scan angle / °	1.0
ω scan angle / °	1.5
Dx / mm	33.0
Total no. of reflections collected	18325
No. of independent reflections	2679
No. of reflections with $I > 2\sigma(I)$	2333
No. of parameters	200
R_{int}	0.0517
S	1.049
R_1 ($F_o > 4\sigma$ (F_o))	0.0475
Reflections omitted	9
wR_2	0.1055
Weighting scheme	a = 0.0497 b = 0.5942
$(\Delta / \sigma)_{mean}$	< 0.001
$\Delta\rho$ excursions / eÅ^{-3}	0.53 and –0.58

Structure determination and refinement

Direct methods yielded the positions of all the non-hydrogen atoms of the asymmetric unit. The atomic numbering scheme is shown in Figure 3.10. The space filling diagram is shown in Figure 3.11. The hydrogen atoms are numbered according to their parent atoms to which they are bonded. Refinement was carried out with all of the non-hydrogen atoms treated anisotropically. The hydrogen atoms were located in subsequent difference electron density maps and placed in geometrically constrained positions and refined with isotropic temperature factors assigned at 1.2 times the U_{isc} values of the parent atoms.

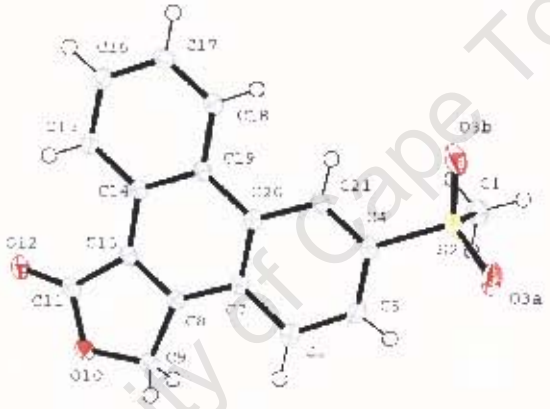

Figure 3.10: The asymmetric unit of Compound A.

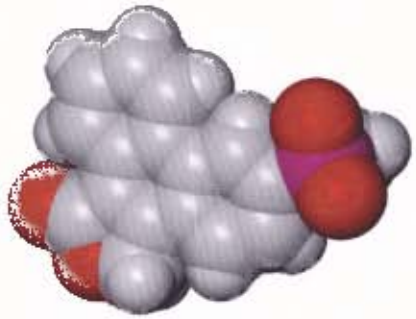

Figure 3.11: Space filling diagram of the asymmetric unit.

Geometrical analysis

The rings are planar with a significant (0.114(3) Å) deviation of C6 above the plane of the phenyl ring and an equal deviation (0.114(2) Å) of C5 below the plane of the phenyl ring. The methyl-sulphonyl substituent is directed below the plane. All hydrogen bonding is of C-H···O type. These are listed in Table 3.8.

Table 3.8: Hydrogen bond data for Compound A.

[i] Related by symmetry operation: 1-x, 1-y, 1 z

Donor —H···Acceptor	Distance (Å)			Angle (°)
	D - H	H···A	D···A	D - H···A
C(1) –H(1A) ···O(3B)[i]	0.98	2.56	3.444(3)	150
C(15) –H(15) ···O(12)[ii]	0.95	2.54	3.168(2)	124
C(21) –H(21) ···O(3B)[ii]	0.95	2.50	2.904(2)	106

[i] Intramolecular bonding

The other prominent interactions occurring are X--H···π and π-π ring contacts. These are described in Tables 3.9 and 3.10. Cg is the centre of gravity of the aromatic ring indicated by a numeral in Figure 3.12.

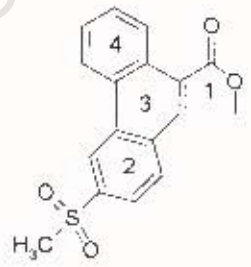

Figure 3.12: Compound A with Cg ring labels.

Table 3.9: X--H···π Ring interactions in Compound A.

X–H···Cg (Pi-Ring)	Distance (Å)		Angle (°)
	H···Cg	X···Cg	X—H···Cg
C(9) –H(9B) ···Cg(4)[i]	2.681	3.447	134.4

[i] Related by symmetry operation: -x -y,2-z

Table 3.10: π-π ring contacts in Compound A

Cg(A) ··· Cg(B)	Distance (Å) Cg···Cg
Cg(1) ··· Cg(3)[i]	3.554(1)
Cg(1) ··· Cg(4)[i]	3.724(1)
Cg(2) ··· Cg(2)[ii]	3.812(2)
Cg(2) ··· Cg(3)[ii]	3.813(1)
Cg(3) ··· Cg(3)[i]	3.596(1)
Cg(4) ··· Cg(1)[i]	3.724(1)

[i] Related by symmetry operation : -x,-y,2-z
[ii] Related by symmetry operation: 1-x,-y,2-z

The packing of Compound A is shown in Figures 3.13 and 3.14, clearly showing the π-π ring interactions and the orientation of the molecule to allow the hydrogen bonding. The torsion/dihedral angles involving the sulphone substituent are described in Table 3.11.

Table 3.11: Torsion/Dihedral angles involving Sulphur.

Atoms involved	Angle (°)
C(5)-C(4)-S(2)-O(3A)	-38.5(2)
C(21)-C(4)-S(2)-O(3A)	145.1(2)
S(2)-C(4)-C(5)-C(6)	167.9(2)
C(5) C(4) S(2) O(3B)	168.4(2)
C(21)-C(4)-S(2)-O(3B)	15.2(2)
C(5)-C(4)-S(2)-C(1)	76.2(2)
C(21)-C(4)-S(2) C(1)	-100.2(2)
S(2)-C(4)-C(21)-C(20)	177.0(1)

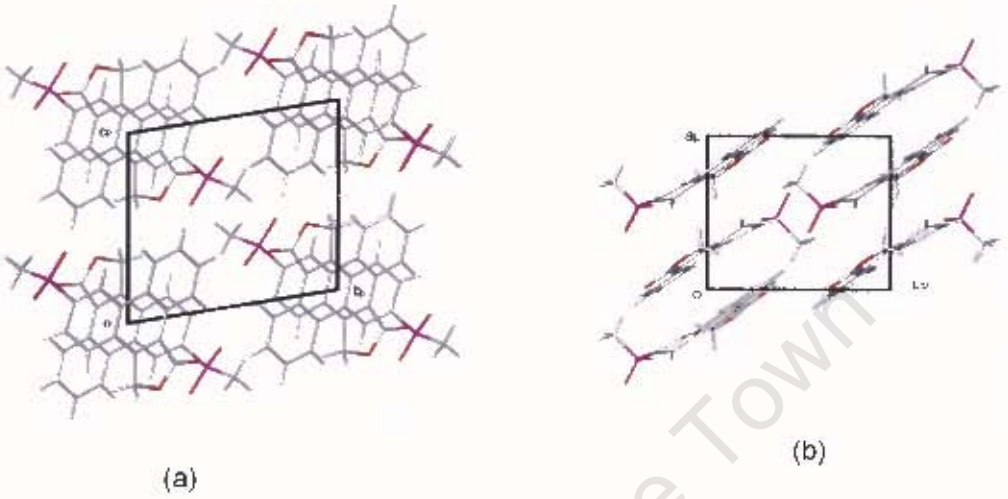

(a) (b)

Figure 3.13: Packing diagrams of the (a) *a*-axis projection and (b) *b*-axis projection of Compound A.

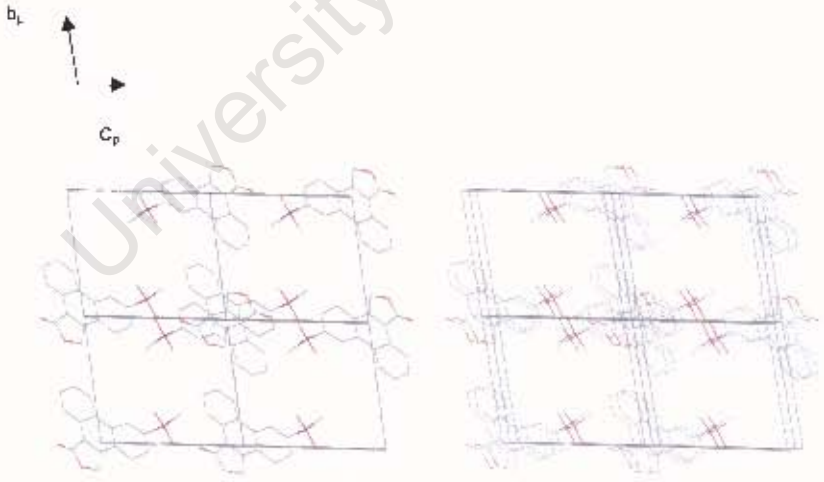

Figure 3.14: Stereo view of the crystal packing down the a-axis of Compound A.

3.3.8 XRD Powder analysis

This is the most informative technique to establish whether a new crystalline phase has been created. If the XRPD trace of the material investigated differs from that of the reference material this implies that either a new polymorph has been formed or a chemical transformation has taken place.

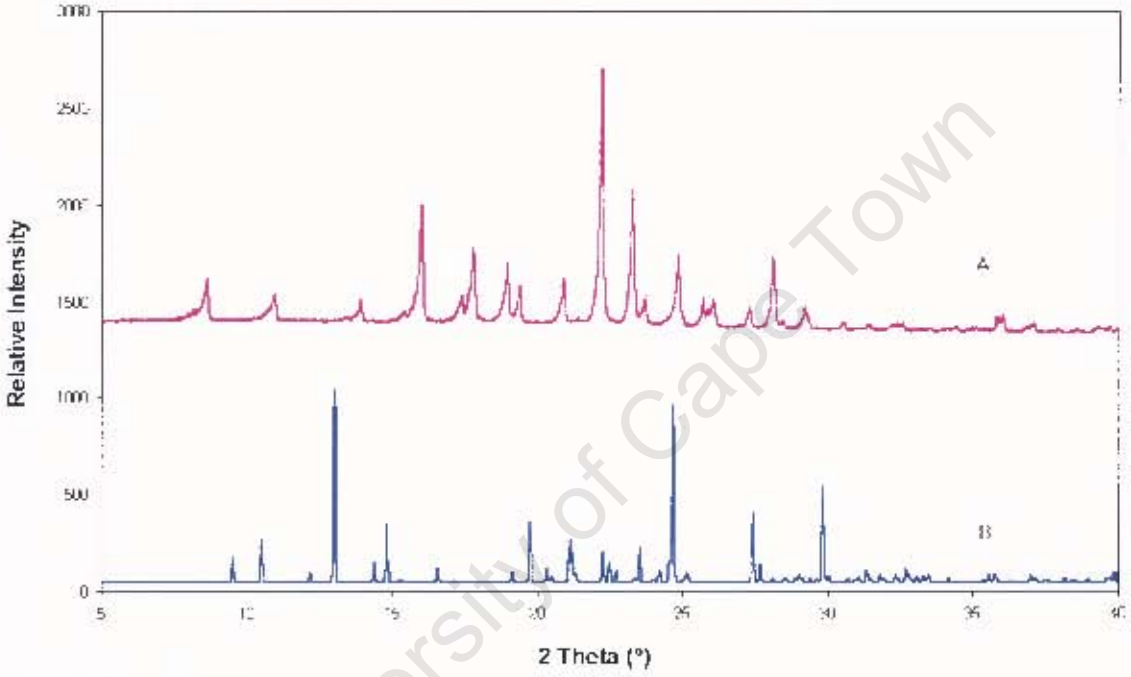

Legend. A = Rofecoxib
B = Compound A

Figure 3.15: XRPD traces for Rofecoxib and Compound A.

The XRPD trace of rofecoxib is compared with the Lazy Pulverix[12] calculated trace for compound A. The completely different traces shown in Figure 3.15 verify that a new crystal phase had indeed been created.

3.3.9 Mechanism

The starting material rofecoxib (**1**) formed the product compound A (**2**) when various solvents (ethyl acetate and HPβCD solution) were used and when it was heated (65 °C) in room light intensity. A suggested mechanism is given in Figure 3.16. The class of

pericyclic reactions that the mechanism corresponds to is electrocyclic, whereby one new σ bond forms across the ends of a single conjugated π system.[13] The stereo-outcome of this reaction is based on the Woodward and Hoffmann rules: the symmetry of the highest occupied molecular orbital (HOMO) controls the stereochemical outcome in thermal reactions and that of the lowest unoccupied molecular orbital (LUMO) controls the outcome of light induced reactions.[14] However, since the intermediate is not seen, the bond rotation of this 4n+2 π electron system (**1**) cannot be experimentally determined.

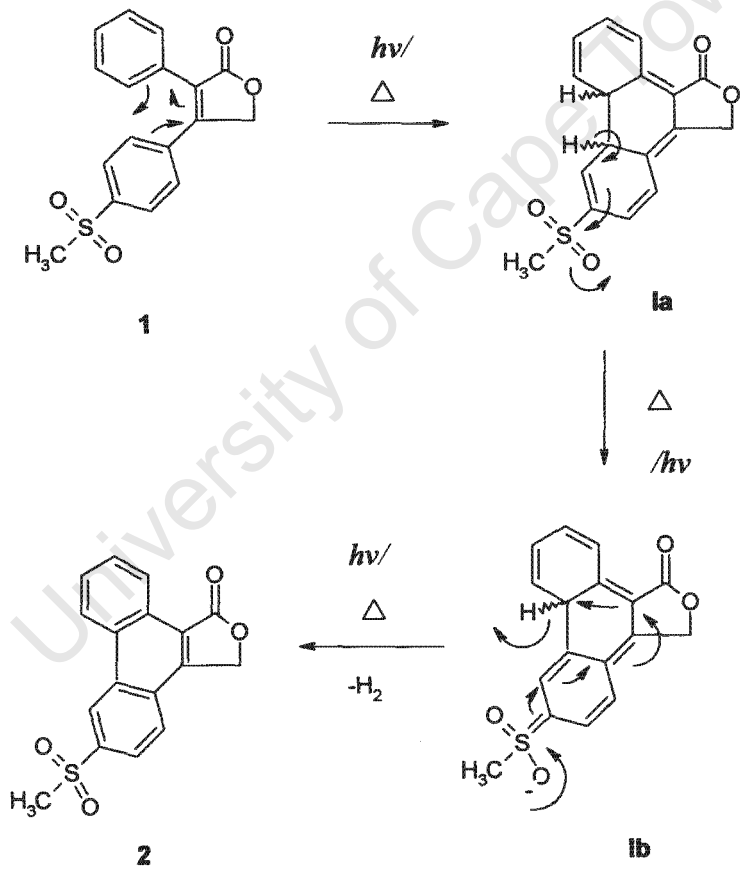

Figure 3.16: Mechanistic scheme.

In the particular experiment carried out it was not established whether it is thermally driven or light induced and this can be the subject of further study. However, the

literature suggests that this is a photo-cyclization product. This compound has been reported and was found to be formed via photocyclic processes, thus implying that this has a conrotatory bond outcome.[14,15,16] The complimentary reaction that takes place thereafter is dehydrogenation via oxidation (**Ia** and **Ib**) ultimately forming the product (**2**). The excellent anion-stabilising sulphone group provides the driving force behind aromatisation. This substituent is highly electron-withdrawing thereby promoting dehydrogenation. High temperatures favour this series of reactions as dehydogenation has a very high activation energy that is overcome by high temperatures. High temperatures also favour elimination by increasing the entropy in the free energy of the reaction. It could be tentatively hypothesized that the solvent could be acting as a poor nucleophile in aiding the primary dehydrogenation.

Only the degradation product of rofecoxib, 6-methyl sulphonyl phenanthro [9,10-C] furan-1 (3H)-one, was encountered in attempts to generate new forms of the drug. This is, however, a significant finding because it indicates that without appropriate control of the recrystallisation procedures, the structural integrity of rofecoxib may be seriously compromised.

3.4 Novel Crystalline Form of TRIMEB

3.4.1 Introduction

TRIMEB, Heptakis(2,3,6-tri-O-methyl)-β-cyclodextrin, is a permethylated cyclodextrin, in which the hydroxyl groups O(2)-H, O(3)-H and O(6)-H have been methylated (Figure 3.17). Currently there are several reported TRIMEB crystalline inclusion complexes,[17-20] and one reported crystalline phase of TRIMEB itself, which is the TRIMEB monohydrate.[21] TRIMEB monohydrate crystallises in the orthorhombic system in space group $P2_12_12_1$.

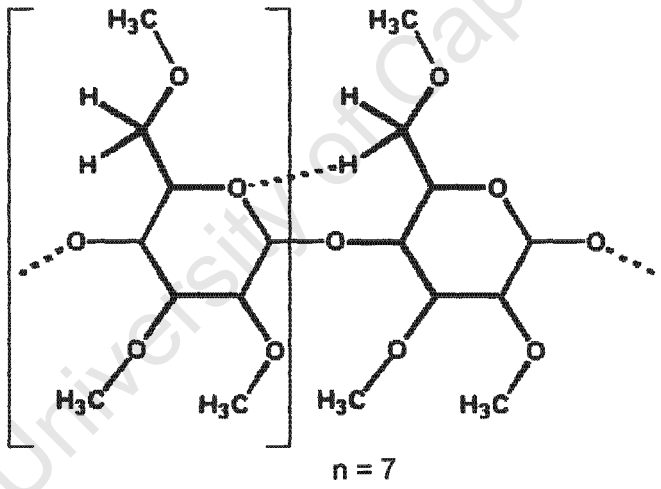

Figure 3.17: Structure of TRIMEB

Methylated β-cyclodextrins show different physical properties in comparison to the corresponding native CDs. Methylated CDs are much more soluble in aqueous milieu and exhibit a negative temperature coefficient for their aqueous solubility.[22] Additionally, it has been discovered that methylated CDs have different properties of macromolecular recognition in comparison to their native counterparts.[23] In this study a new phase of TRIMEB has been separately, and simultaneously, identified by the author and by Mr. W. Mhlongo (Supramolecular Group, UCT).

3.4.2 Crystal Preparation

In the attempt to create a new CD inclusion complex between TRIMEB and the NSAID Bucetin, a new crystalline form of the host crystallised. In a 1:1 molar ratio, a solution was prepared consisting of the monohydrate TRIMEB (0.0648 g) and the drug Bucetin (10 mg) with 1 ml of distilled water. This was stirred in ice for 24 hours then heated to 70 °C for 30 minutes and finally stirred for a further 30 minutes in ice. The solution was filtered and left at 50 °C in the oven to evaporate. Single crystals were found in the vial upon inspection one month later. These were harvested from the sides of the vial, above the level of the mother liquor. The new crystalline form of TRIMEB shall be referred to as TRIB.

3.4.3 Thermal analysis

Due to a limited supply of crystals, only the DSC and HSM thermal analyses were performed. Crystallographically though, it was proved that these crystals are dehydrated.

DSC analysis

The DSC trace depicted below shows endotherm peaks directed upwards and exotherm peaks downwards (Figure 3.18).

The melting point of TRIMEB monohydrate is 157.5 °C (ΔH_f = 3.80 J/g) and the onset temperature of TRIB is 140.4 °C (ΔH_f = 8.48 J/g), clearly indicating that these are two different phases.

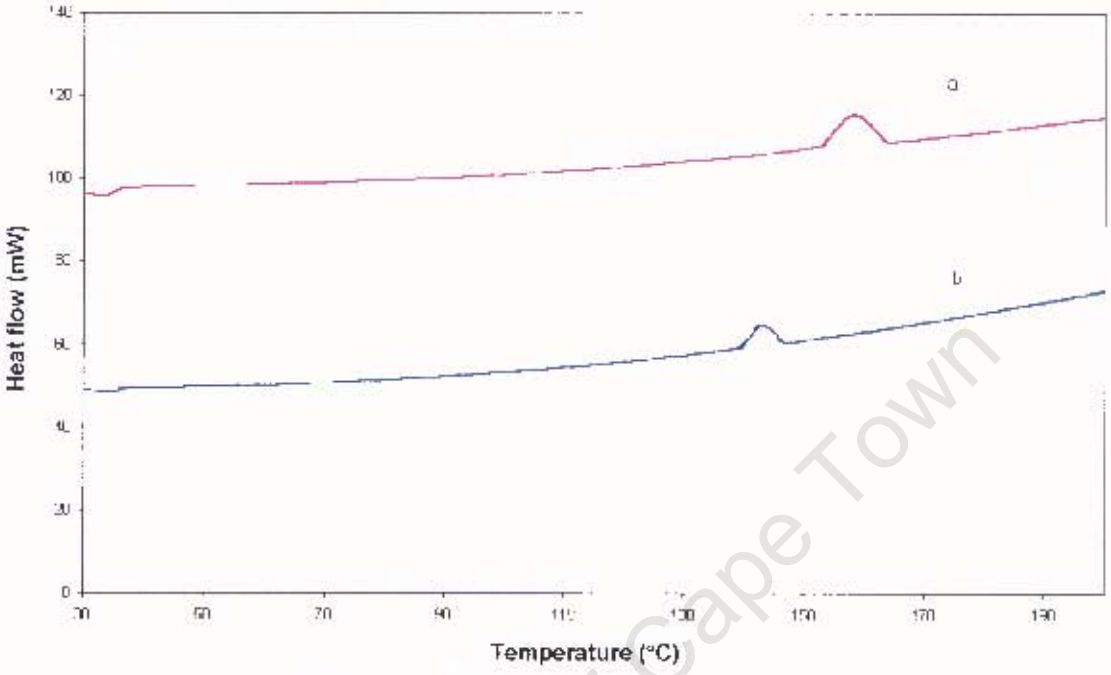

Legend: a: DSC curve of TRIMEB monohydrate
b: DSC curve of TRIB

Figure 3.18: DSC Curves for TRIB and TRIMEB monohydrate.

HSM analysis

The different thermal properties characteristic of TRIMEB monohydrate and TRIB are shown in the HSM photomicrographs below (Figure 3.19). TRIB melts over the range 146.6-148.9 °C (Figure 3.19 (iii) and (iv)). No loss of water i.e. the evolution of bubbles is seen, as it is anhydrous. TRIMEB monohydrate shows bubble formation beginning at 124.5 °C indicating water loss and the melt occurs around 157.5-160.2 °C (Figure 3.19 (d)).

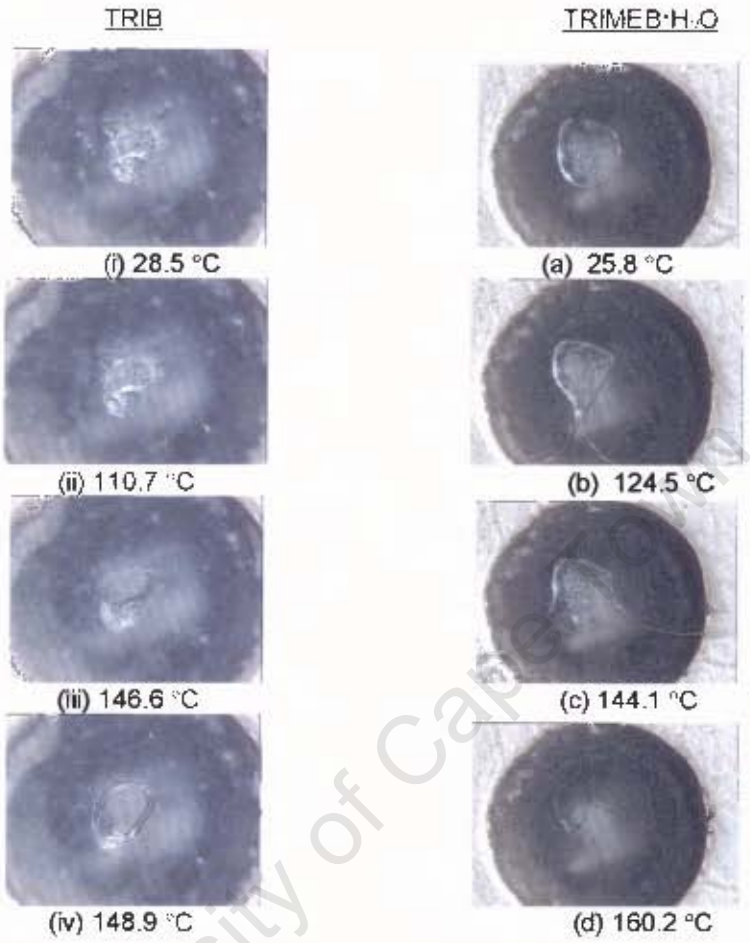

Figure 3.19: Photomicrographs of TRIB and TRIMEB monohydrate.

3.4.4 Elemental analysis

C and H analysis were performed to display the difference between the TRIMEB monohydrate and the dehydrated form. Evidently, these two values will be very similar but as shown below the experimental values of %C more closely correspond to the dehydrated form.

Table 3.12: Elemental analysis results for TRIMEB•H_2O and TRIB.*

	TRIMEB • H_2O Calculated	TRIB Calculated	Experimental
% C	52.3	52.9	52.8
% H	7.9	7.9	8.0

* The errors in experimental values are ± 0.5%.

3.4.5 X-Ray Crystallographic Analysis

Unit cell determination

A preliminary check was performed using the Nonius Kappa CCD diffractometer to determine the unit cell parameters, crystal system and space group. The measured unit cell parameters did not correspond with those of TRIMEB monohydrate nor with those of known inclusion complexes of TRIMEB.[24] It was therefore considered appropriate to pursue the study of this phase. Table 3.13 lists the parameters of TRIB in comparison to those of TRIMEB monohydrate. The crystal intensity data of TRIB were collected at 113K and those of TRIMEB monohydrate at 294K.

Table 3.13: Unit cell parameters for TRIB and TRIMEB monohydrate.

	TRIMEB • H_2O[21]	TRIB
Crystal system	Orthorhombic	Orthorhombic
Space group	$P2_12_12_1$	$P2_12_12_1$
a	14.823 (4) Å	15.951 (1) Å
b	19.382 (9) Å	16.577 (1) Å
c	26.534 (2) Å	28.941 (2) Å
Volume	7623.2 (2) $Å^3$	7652.69 (5) $Å^3$
Z	4	4

Data-Collection, structure determination and refinement

The intensity data were collected on the Nonius Kappa CCD diffractometer using graphite-monochromated MoKα radiation at 113K. Table 3.14 lists the crystal data and data-collection parameters.

Table 3.14: Crystal data and data-collection parameters for TRIB.

Molecular Formula	$C_{63}H_{112}O_{35}$
Formula Weight/g mol^{-1}	1429.66
Crystal System	Orthorhombic
Space group	$P2_12_12_1$
$Density_{calc}$ / g cm^{-3}	1.2406
μ (MoKα) / mm^{-1}	0.101
Temperature / K	113
F(000)	3080
Crystal size / mm^3	0.20 × 0.30 × 0.20
Range scanned θ / °	$3.61 \leq \theta \leq 25.70$
Index ranges	h: -19, 19 k: -20, 20 l: -35, 35
ϕ scan angle / °	1.0
ω scan angle / °	1.0
Dx / mm	52.80
Total no. of reflections collected	56677
No. of independent reflections	14499
No. of reflections with $I > 2\sigma(I)$	13091
No. of parameters	899
R_{int}	0.0602
S	1.107
R_1 ($F_o > 4\sigma$ (F_o))	0.0531
Reflections omitted	48
wR_2	0.1304
Weighting scheme	a = 0.0516 b = 6.2614
$(\Delta / \sigma)_{mean}$	< 0.001
$\Delta\rho$ excursions / e. $Å^{-3}$	0.40 and –0.49

The structure was solved using direct methods (program SHELXS-97[25]). All non-hydrogen atoms were revealed in the E-map and subsequent difference electron density maps and thus placed. The model was subsequently refined isotropically by full-matrix least-squares methods. Thereafter, the hydrogen atoms were placed with fixed geometry in a riding model and assigned common variable isotropic temperature factors. All non-hydrogen atoms [except C9G7] were assigned anisotropic temperature factors and refined. No water molecules were located.

Geometrical analysis of TRIB

The asymmetric unit consists of a single TRIMEB molecule. This structure, with numbering scheme and thermal ellipsoids, is shown in figure 3.20. The glucose units are referred to as G1, G2, G3, G4, G5, G6 and G7.

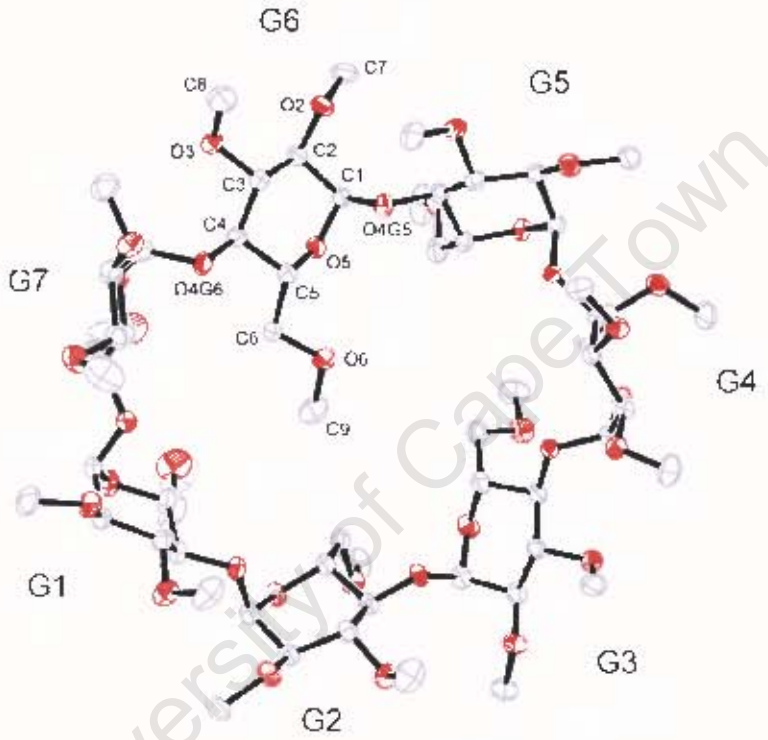

Figure 3.20: Macrocyclic structure and numbering scheme of TRIB with the hydrogen atoms excluded, viewed from the secondary rim.

The glucopyranose residues adopt the $^4C_1$ chair conformation and the macrocycle, except for G6, adopts an elliptically-distorted truncated cone shape. The anomaly, G6, is significantly tilted relative to the other units, with its methoxy group directed towards the centre of the ring. The other C(6)-O(6) bond directed towards the centre of the ring is that of G3, adopting a (+)-*gauche* conformation [ω = +60°], whilst that of G4 is directed away from the ring adopting a (-)-*gauche* conformation [ω = -60°]. The C(6)-O(6) bonds of G1, G2, G5 and G7 are directed vertically, almost perpendicular to the plane of the ring. As seen with most TRIMEB complexes the O(2)-C(7) bonds are directed away from the cavity and the O(3)-C(8) bonds are directed towards the ring. All the O(6)-C(9)

bonds are *trans* [ω = 180°] with respect to the C(5)-C(6) bonds, except in the G4 residue where the dihedral angle is *gauche*. The macrocyclic structure of TRIB is shown in the stereodiagram, figure 3.21, below.

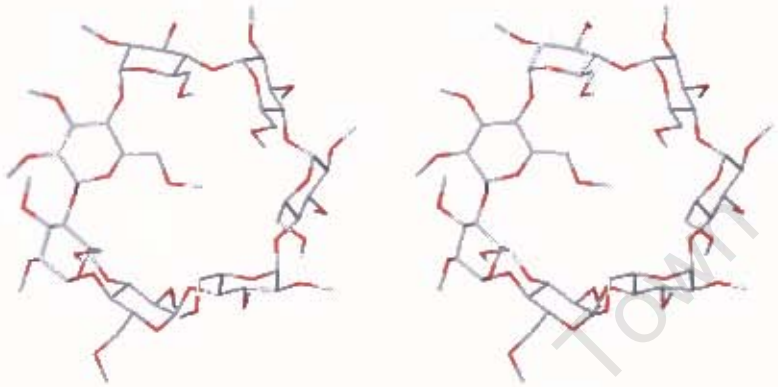

Figure 3.21: Stereodiagram of TRIB viewed down the b-axis.

The geometrical parameters of the O(4) heptagon, calculated from Platon are listed in Table 3.15. This includes the radii, the O(4)···O(4') distances, and the O(4)···O(4')···O(4'') angles, the O(4)···O(4')···O(4'')···O(4''') torsion angles and the deviations of each of the O(4) atoms from the mean O(4) plane (Chapter 1, section 1.2.3).

Table 3.15: Geometrical parameters of the O(4) heptagon for the TRIB structure.

Glucose Unit	Radii (Å)	O(4)···O(4') (Å)	O(4) angle (°)	Torsion angle (°)	Deviation (Å)
G1	5.02	4.47	127	15.2	-0.044(2)
G2	4.81	4.44	136	-24.3	-0.465 (2)
G3	4.85	4.22	111	-2.9	0.339 (2)
G4	5.50	4.34	134	38.8	0.421 (2)
G5	4.59	4.61	132	-38.5	-0.723 (2)
G6	4.77	4.12	118	3.7	0.118 (2)
G7	5.41	4.48	130	3.7	0.355 (2)
Average	4.99	4.38	127	18.2	0.353

Other macrocyclic geometrical features calculated are listed in Table 3.16. These are the intersaccharidic bond angle (φ), which is C(1')–O(4)–C(4), the O(2)···O(3') distance and the tilt angle (τ_1), which is defined as the angle made between the mean O(4) plane and the mean plane through the four pyranose ring atoms, namely O(4'), C(1), C(4) and O(4) of each glucose unit.

Table 3.16: φ, O(2)···O(3') distance and τ_1 for the TRIB structure.

Glucose unit	φ (°)	O(2)···O(3') (Å)	τ_1 (°)
G1	117	3.37	14.2 (1)
G2	117	3.24	26.7 (1)
G3	113	3.26	42.5 (1)
G4	118	3.47	8.4 (1)
G5	117	4.05	37.6 (1)
G6	113	3.46	72.0 (1)
G7	119	3.99	10.6 (1)
Average	116	3.55	30.3 (1)

Average bond lengths and angles are within the standard deviations of those reported for the host in other TRIMEB complexes. However, there are rather large tilt angles which are unusual, particularly that for G6. These large tilt angles are accounted for by the lack of O(2)···O(3') hydrogen bonds and steric strain.[18, 19, 23, 26] The CPK space filling diagrams of the TRIB molecule are depicted in figure 3.22. These clearly show the macrocyclic overall geometry, the vertical alignment of the methoxy groups and how G6 is severely tilted, ultimately blocking the cyclodextrin cavity.

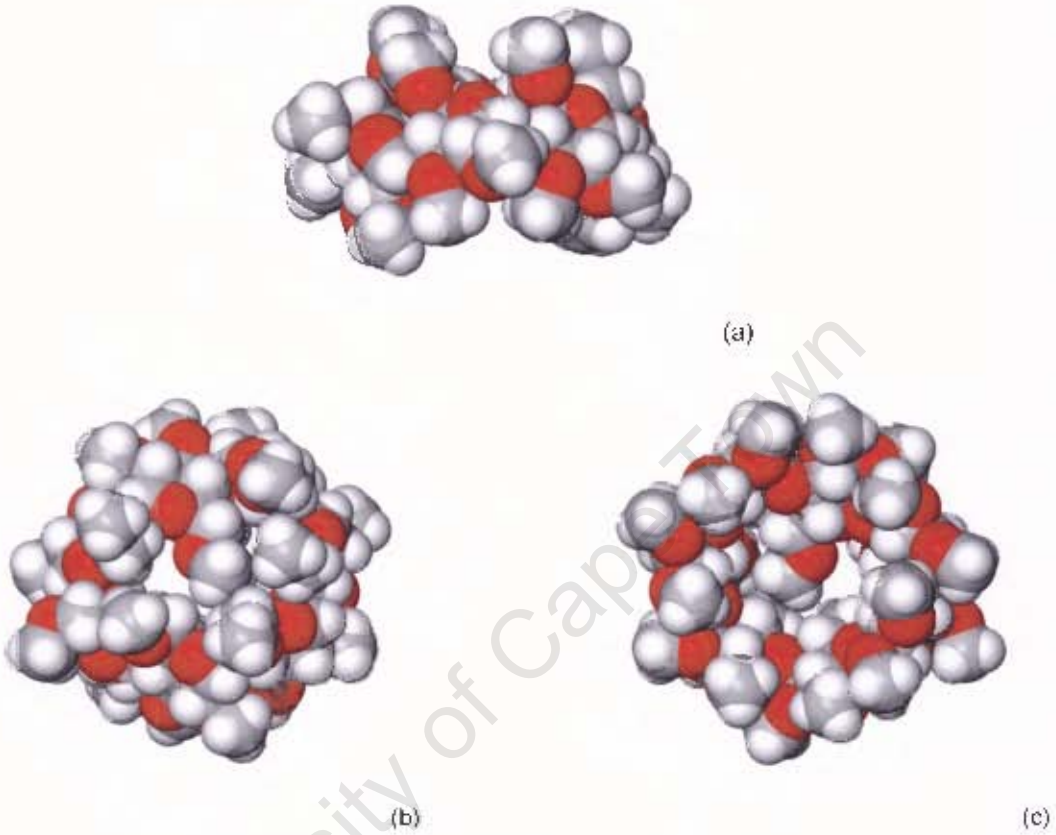

Figure 3.22: Space-filling diagram of the TRIB structure (a) viewed from the side (b) viewed from the primary rim and (c) viewed from the secondary rim.

Crystal Packing

The packing diagrams of the TRIB structure (Figure 3.23) depict projections viewed down the a- and b-axes. The complex units pack in a screw-channel mode in a head-to-tail style with their O(4) planes roughly parallel to the yz-plane. Continuous channels do not exist due to the screw axis.

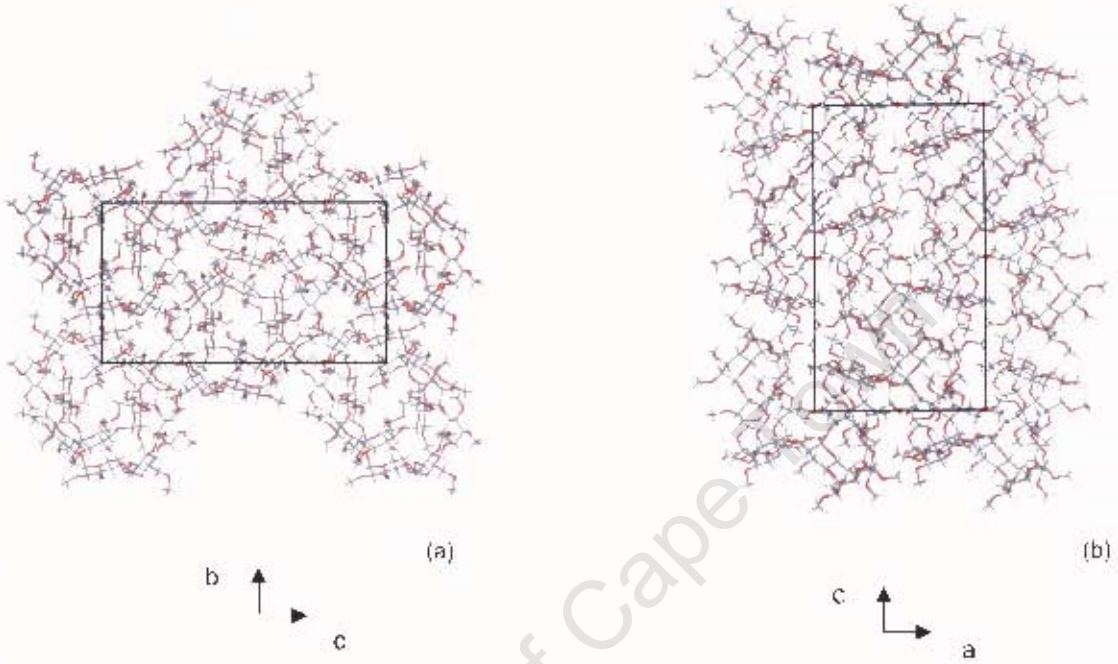

Figure 3.23: Packing Diagram viewed down (a) a-axis and (b) b-axis.

Figures 3.24 and 3.25 show three consecutive TRIB molecules in red and green mode viewed perpendicular to the a-axis. These were selected to view the self-inclusion that occurs in this structure. Two methoxy groups of one TRIB molecule protrude into the cavity of the next TRIB molecule thereby preventing the latter from collapsing. The grossly out of plane glucopyranose unit (G6) is 'sandwiched' between two of the vertical methoxy groups, one each from the two surrounding cyclodextrin molecules, perhaps causing this greatly tilted unit to adopt this conformation. The self-inclusion described above involves successive molecules related by the twofold screw axis parallel to the a-axis.

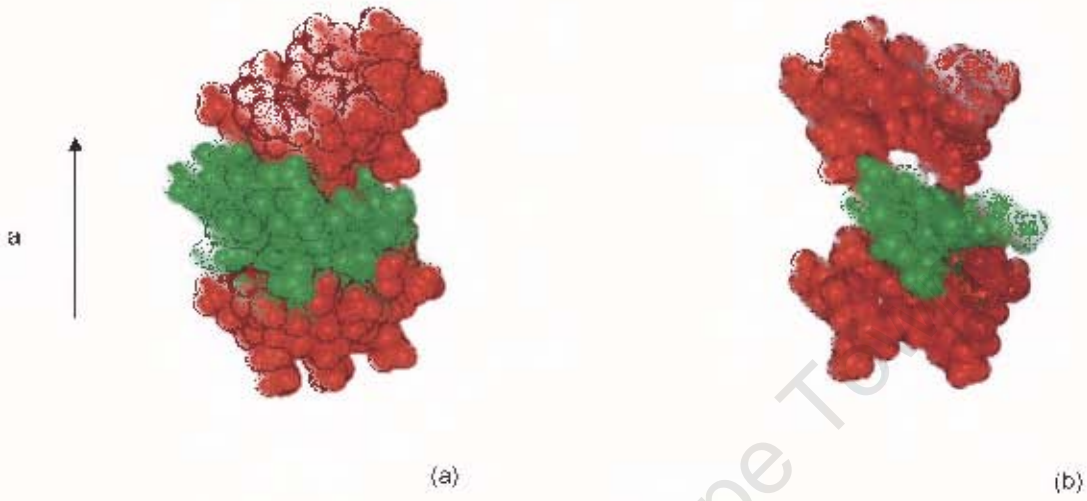

Figure 3.24: TRIB molecules viewed perpendicular to the a-axis with (a) CPK mode and (b) cutaway of the CPK diagram highlighting the self inclusion

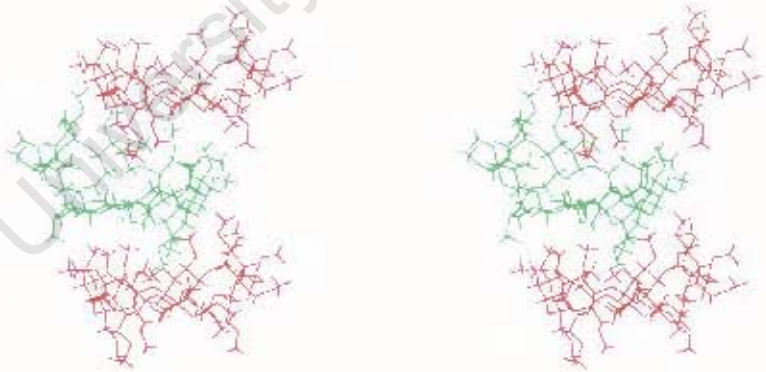

Figure 3.25: Stereoview showing the 'self-inclusion' referred to above.

3.4.6 XRD Powder analysis

Insufficient material prevented the recording of a representative XRPD trace of the new phase. Therefore the program Lazy Pulverix was used to create the XRPD trace using the refined structural data from single crystal X-ray analysis (section 3.4.5). [12] This trace is compared with the XRPD trace of TRIMEB monohydrate (Figure 3.26).

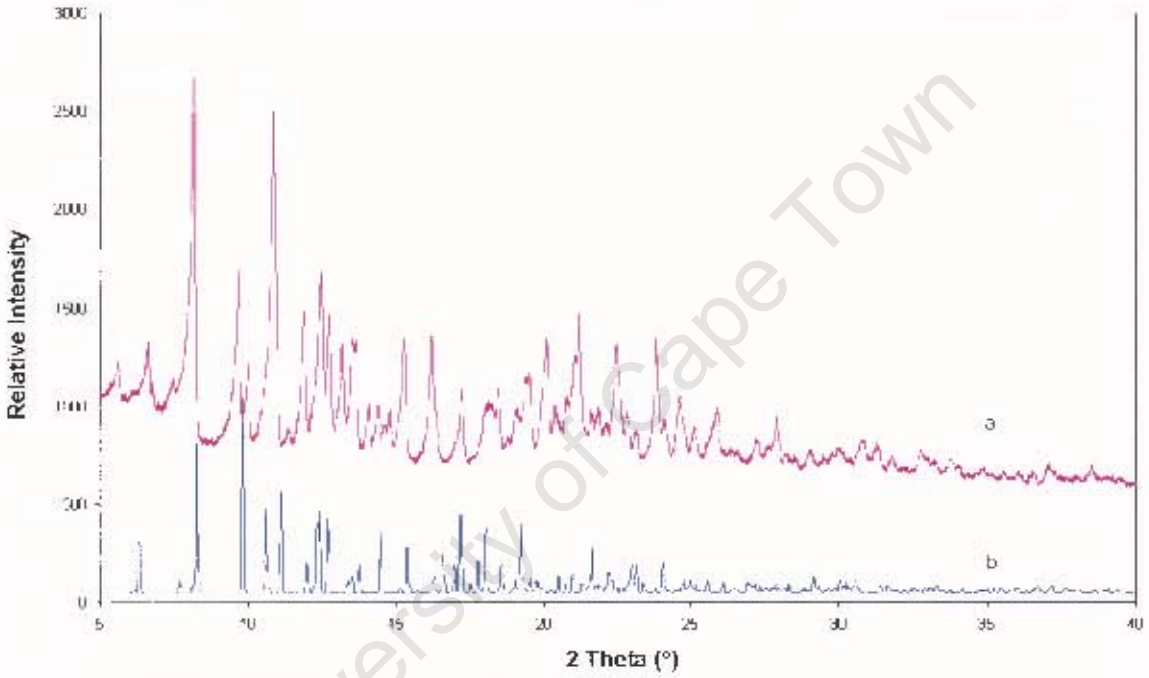

Legend: a: PXRD trace of TRIMEB monohydrate
b: Lazy Pulverix PXRD trace of TRIB

Figure 3.26: XRPD traces for TRIB and TRIMEB monohydrate.

The differing traces indicate that crystallographically these two forms are different, thus proving that a novel crystalline form of permethylated-β-cyclodextrin has been found.

3.5 Discussion

An amorphous form of celecoxib was identified using thermoanalytical, elemental, spectroscopic and crystallographic analyses. This was achieved via the cooling from the melt of celecoxib.[5] Similar results were obtained by Chawla *et al* [2] who obtained the amorphous form of celecoxib by quench cooling. Regrettably, no polymorphs or pseudopolymorphs were obtained, unlike Chawla *et al* who experimentally obtained DMA and DMF pseudopolymorphs via reduced pressure recrystallisation experiments. The above-mentioned solvents were used in recrystallisation experiments and the technique described in the article was followed closely but the author did not succeed in reproducing this work. The thermoanalytical, spectroscopic and crystallographic results obtained for the amorph closely corresponded to those obtained by Chawla *et al* thus verifying that section of their work. An amorphous form is one in which crystallinity and therefore long-range order are absent. Hence the material is generally more energetic, having higher solubility and dissolution rates than that of polymorphic crystalline forms.[27] This makes amorphous forms theoretically advantageous in the pharmaceutical industry but the probability of this metastable state changing to a more stable crystalline state is high, thereby negating its usefulness. However, if the amorphous form is stabilised, pharmaceutical products may be prepared. In this study, celecoxib was stored at room temperature (25 °C) and remained amorphous for more than two months after production.

The nature of a decomposition product of rofecoxib was elucidated using thermoanalytical, elemental, spectroscopic, chromatographic and crystallographic techniques. This cyclized product resulted from the known, possible photo-degradation of rofecoxib. Following strenuous stress trials Mao *et al* [9] discovered that two major side-products formed, one of which results from the base promoted hydrolysis of the lactone moiety followed by oxidation, which yields a dicarboxylate; the other results from photo-cyclization of the *cis*-stilbene moiety which results in a phenanthrene derivative. In this investigation, the latter product was produced.

A new crystalline form of TRIMEB, referred to as TRIB, was discovered and characterised using thermoanalytical methods, elemental analysis and crystallographic techniques. This novel phase was found to be anhydrous and to adopt a non-collapsed

structure due to self-inclusion. Additionally, all the methylglucose residues in TRIB adopt the $^4C_1$ conformation, in contrast to the known monohydrate, in which a single methylglucose residue adopts the $^1C_4$ conformation, thereby imparting an elliptical shape.[21] Another crystalline modification of TRIB was isolated almost simultaneously by Mr. W. Mhlongo (UCT, Supramolecular Group). He discovered a trihydrate in which the host molecule is isostructural with that in TRIB. Both crystal forms were isolated from failed attempts to obtain inclusion complexes. The trihydrate crystallized from a solution of TRIMEB and the antihypertensive drug atenolol (4-[2-hydroxy-3-[(1-methylethyl)amino)propoxy]benzeneacetamide, prepared in 1:1 molar ratio. TRIB crystallized from a solution of TRIMEB and the NSAID bucetin (N-(4-ethoxyphenyl)-3-hydroxybutanamide) (section 3.4.2). These two drug molecules have a close structural likeness and it is surmised that this may be a factor in the crystallization of these TRIMEB polymorphs. The molecular conformation of TRIB and the host in the trihydrate closely resemble one another except for molecular disorder in the trihydrate.[28]

3.6 References

1. Vasu Dev, R; Shashi Rekha, K; Vyas, K; Mohanti, S; Rajender, P; Reddy, G. *Acta Crystallogr.,* **1999**, *C55,* e161.
2. Chawla, G; Gupta, P; Thilagavathi, R; Chakraborti, A.K; Bansal, A.K. *Eur. J. Pharm. Sci.,* **2003**, *20,* 305-317.
3. Hageman, M; He, X; Kararli, T; Mackin, A; Miyake, J; Rohrs, R; Stefanski, J.. PCT Int. Appl. **2001** CODEN: PIXXD2, 47.
4. Leonard, F; Miyake, P. PCT Int. Appl. **2001** CODEN: PIXXD3, 89.
5. Guillory, K.J. *Polymorphism in Pharmaceutical solids,* Marcel Dekker, Inc. **1999,** 183-220.
6. Shashi Rekha, K; Vyas, K; Raju, C.M; Chandrashekar, B; Reddy, G. *Acta Crystallogr.,* **2000**, *C56,* e68.
7. Nicoll-Griffith, D.A; Yergey, J.A; Trimble, L.A; Silva, J.M; Chauret, N; Gauthier, J.V; Leger, S; Roy, P; Therien, M; Prasit, P; Zamboni, R; Young, R.N; Chan, C; Mancini, J; Riendeau, D. *Bioorg. Med. Chem. Lett.,* **2000**, *10*, 2683-2686.
8. Rawat, S; Jain, S.K. *Pharmazie,* **2003**, *58,* 639-641.
9. Mao, B; Abrahim, A; Ge, Z; Ellison, D.K; Hartman, R; Prabhu, S.V; Reamer, R.A; Wyvratt, J. *J. Pharm. Biomed. Anal.,* **2002**, *28*, 1101-1113.
10. Brown, D; Floyd, A; Sainsbury; M. *Organic Spectroscopy,* John Wiley and Sons, UK, **1988.**
11. Sheldrick, G.M. SADABS, Version 2.03, Bruker/Siemens area detector absorption and other corrections, **1999.**
12. Yvon, K; Jeitschko, W; Parthé, E. *J. Appl. Crystallogr.,* **1977**, *10*, 73-74.
13. Clayden, J; Greeves, N; Warren, S; Wothers, P. *Organic Chemistry,* Oxford University Press, UK, **2001.**
14. Neckers, D; Doyle, M. *Organic Chemistry,* John Wiley and Sons, UK, **1977.**
15. Hart, H. *Organic Chemistry,* Houghton Mifflin Company, USA, **1991**.
16. Woolf, E; Fu, I; Matuszewski, B. *J. Chromatogr.,* **1999**, *730,* 221-227.
17. Harata, K; Uekama, K; Imai, T; Hirayama, F; Otagiri, M. *J. Incl. Phenom.,* **1988**, *6,* 443-460.
18. Brown, G.R; Caira, M.R; Nassimbeni, L.R, van Oudstshoorn, B. *J. Incl. Phenom.,* **1996**, *26,* 281-294.
19. Caira, M.R; Griffith, V.J; Nassimbeni, L.R. *J. Incl. Phenom.,* **1995**, *20,* 277-290.

20. Frank, J; Holzwarth, J; Saenger, W. *Langmuir,* **2002**, *18,* 5974-5976.
21. Caira, M.R; Griffith, V.J; Nassimbeni, L.R; van Oudtshoorn, B. *J. Chem. Soc., Perkin Trans. 2,* **1994**, 2071-2072.
22. Okada, M; Kamachi, M; Harada, A. *Macromolecules,* **1999**, *32*, 7202-7207.
23. Loftsson, T; Brewster, M.E. *J. Pharm. Sci.,* **1996**, *85,* 1017-1025.
24. *Cambridge Structural Database and Cambridge Structural Database System,* Version 5.*23*, April **2003**, Cambridge Crystallographic Data Centre, University Chemical Laboratory, Cambridge, England.
25. Sheldrick, G.M. SHELXL-97, *Program for the Refinement of Crystal Structures,* University of Göttingen, Germany, **1997.**
26. Harata, K; Hirayama, F; Arima, H; Uekama, K, Miyaji, T. *J. Chem. Soc., Perkin Trans. 2,* **1992**, 1159-1166.
27. Bernstein, J. *Polymorphism in molecular crystals,* Oxford University Press, **2002.**
28. Caira, M.R; Bourne, S.A; Mhlongo, W.T; Dean, P.M. *Chem. Commun.,* **2004**, DOI:10.1039/B408660K, Article in press.

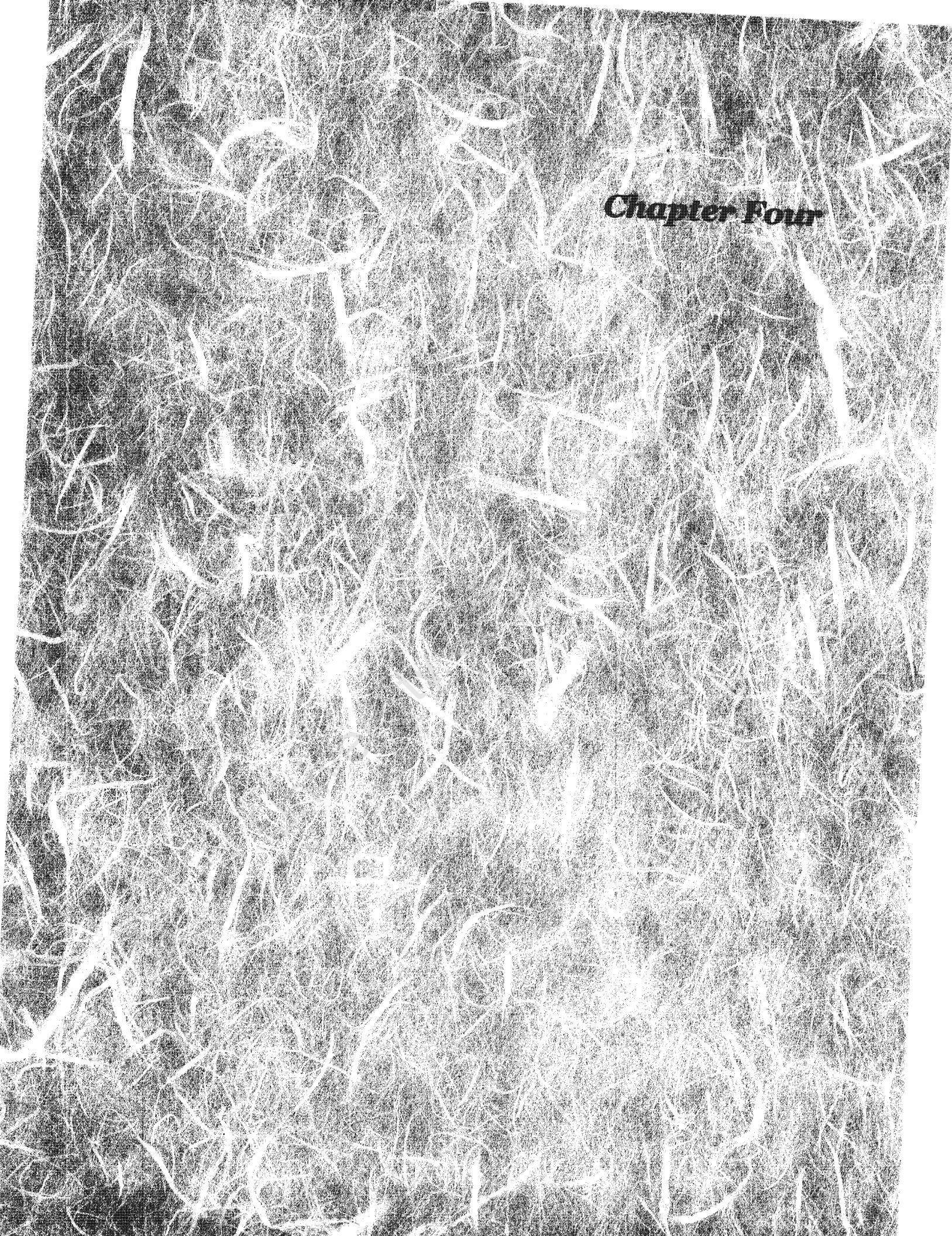
Chapter Four

Chapter Four: Inclusion Complexes between NSAIDs and Cyclodextrins

4.1 Kneaded Complexes

4.1.1 Introduction

Occasionally it is not possible to achieve full crystal structure determination due to the poor quality or small size of the crystals. This hindrance is partially overcome by using another crystallographic technique, namely powder X-ray diffraction (XRPD). A systematic classification of cyclodextrin inclusion complexes was achieved using XRPD, which can then be used as an analysis to test whether a complex may be formed. Caira[1] used the concept of crystal isostructurality and its significance in regards to cyclodextrin complexes to establish that the majority of CD complexes crystallize in distinct three-dimensional arrangements forming several so-called 'isostructural series'. More importantly it was discovered that the XRPD patterns within an isostructural series of complexes are analogous regardless of the differences in the included guest. Therefore by comparing the suspected complex pattern against the reference pattern derived from the isostructural series one may deduce whether the former is a true complex.

4.1.2 Complex Preparation

Possible inclusion complexes were prepared with the guest NSAIDs diflunisal, suprofen and bucetin and the hosts β- and γ-cyclodextrin. Equimolar amounts of drug and cyclodextrin were kneaded together with small amounts of distilled water, with a mortar and pestle for an hour and a half.

4.1.3 XRD Powder analysis

The XRPD technique may be used to identify whether complexation has occurred. Figures 4.1-4.4 show the XRPD patterns of the kneaded materials, the physical mixtures and of the isostructural series traces, which are derived from the Cambridge Structural Database.[2] If the pattern of the kneaded material and that of the physical mixture are considerably different due to dissimilar peaks obtained, the probability that a complex has formed is high. This is due to the fact that the complex generally has a completely

different crystal packing arrangement from the mixture of starting materials used to produce it. The traces for the suspected complexes are also compared with the analogous isostructural series trace. If the pattern for the kneaded sample corresponds to this isostructural trace the possibility that complexation has occurred is practically certain.[1]

Figure 4.1: Diflunisal:β-Cyclodextrin (DIFBCD)

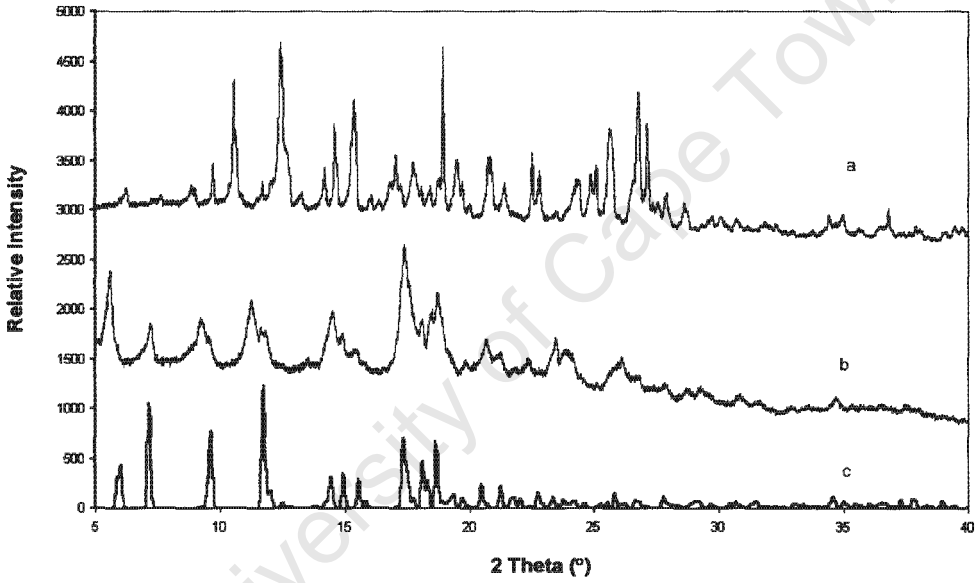

Legend: a: DIFBCD physical mixture (1:1 molar ratio)
b: DIFBCD kneaded sample (1:1 molar ratio)
c: Isostructural pattern 10 (Space group: P1)

Figure 4.2: Diflunisal:γ-Cyclodextrin (DIFGCD)

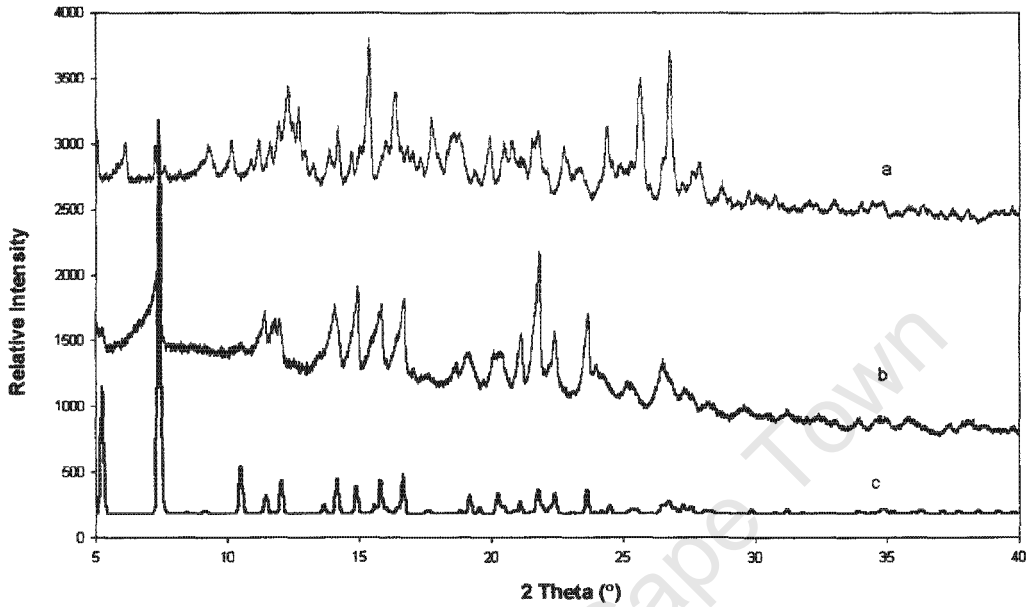

Legend: a: DIFGCD physical mixture (1:1 molar ratio)
b: DIFGCD kneaded sample (1:1 molar ratio)
c: Isostructural pattern 17 (Space group $P42_12$)

Figure 4.3: Suprofen: γ-Cyclodextrin (SUPGCD)

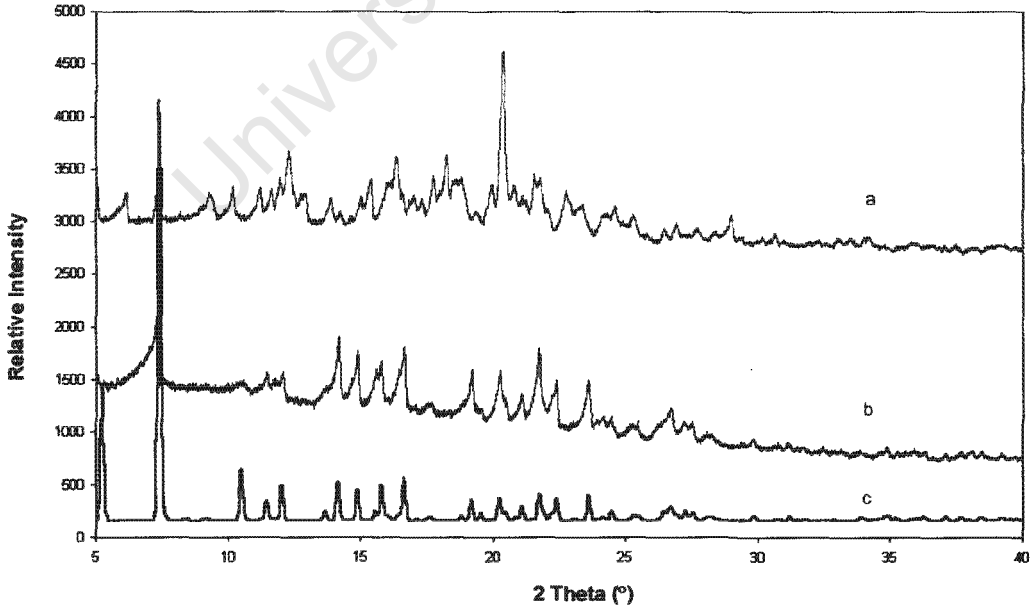

Legend: a: SUPGCD physical mixture (1:1 molar ratio)
b: SUPGCD kneaded sample (1:1 molar ratio)
c: Isostructural pattern 17 (Space group $P42_12$)

Figure 4.4: Bucetin:γ-Cyclodextrin (BUCGCD)

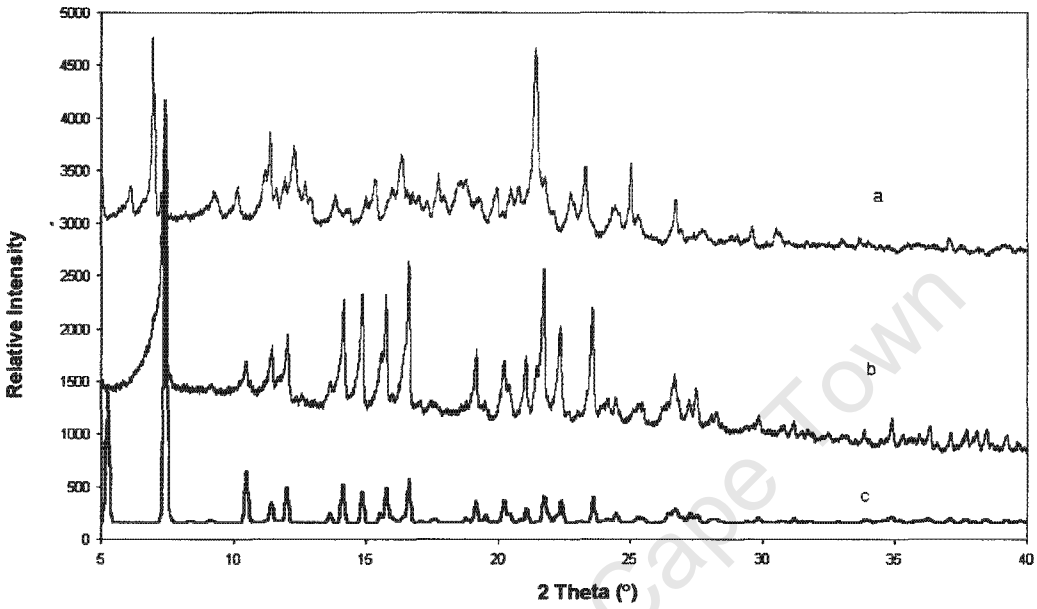

Legend: a: BUCGCD physical mixture (1:1 molar ratio)
b: BUCGCD kneaded sample (1:1 molar ratio)
c: Isostructural pattern 17 (Space group $P42_12$)

All experimental patterns for the kneaded products differ from the patterns for the corresponding physical mixtures and yield convincing matches with reference XRPD patterns. Thus, in all cases, it can be concluded that genuine CD – inclusion complexes with the listed drugs were formed.

As mentioned previously, the term 'isostructurality' in the context of CD inclusion complexes means that two or more complexes have practically identical packing arrays of the host CD molecules, while the different guest molecules occupy common cavities. There are various packing motifs and these are described in Chapter 1 section 1.3.5. Although complexes have been classed according to crystal packing and space groups in the past, this is not a definitive classification used for deciphering complexes using the XRPD technique. The complexes used for a particular isostructural series had to have the following characteristics: (a) near equality of unit cell dimensions, (b) identical space groups and (c) close correspondence of atomic co-ordinates of common CD atoms. Averaging the patterns of the members of that series after conversion of intensities into

absolute values led to seventeen isostructural series.[1] Finding a 'match' between the experimental XRPD trace of a putative complex and a reference XRPD trace for a specific isostructural series, one is able to deduce the space group, the average unit cell dimensions and the packing mode. Listed in Table 4.1 are the crystallographic data used for the computation of the XRPD patterns used in this discussion.

Table 4.1: Crystal data for complexes of β-CD and γ-CD.

Guest	*a* (Å)	*b* (Å)	*c* (Å)	α (°)	β (°)	γ (°)	REFCODE
10: β-CD, P1							
Tridecanoic acid	15.654	15.650	15.937	101.59	101.59	103.59	SOBHUM
7-tetradecanoic acid	15.626	15.623	15.935	101.55	101.56	103.64	SOBJEY
17: γ-CD, $P42_12$							
Methanol	23.808	23.808	23.140	90.0	90.0	90.0	NUNRIX
1-Propanol, crystal I	23.840	23.840	23.227	90.0	90.0	90.0	SIBJAO
1-Propanol, crystal II	23.809	23.809	23.207	90.0	90.0	90.0	SIBJES

The kneaded complex containing diflunisal and β-CD (DIFBCD) corresponds to isostructural series 10. This series is characteristic of channel-packing of a dimeric complex, space group P1. The kneaded complexes with host γ-CD (DIFGCD, SUPGCD and BUCGCD) correspond to isostructural series 17. These crystallize in channel-mode in the tetragonal space group $P42_12$. Most known crystallographically characterised γ-CD complexes contain a disordered guest.

4.2 The inclusion complex β-CD • Suprofen • 20 H_2O

4.2.1 Introduction

Suprofen, α-methyl-4-(2-thienylcarbonyl)benzeneacetic acid (Figure 4.5), a prostaglandin biosynthesis inhibitor, is used for the prevention of pain and inflammation. The reported crystal structure of suprofen belongs to the monoclinic system, space group $P2_1/n$.[3]

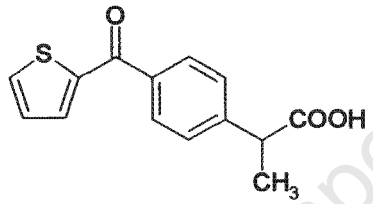

Figure 4.5: Structure of Suprofen.

This arylpropionic acid derivative was discovered in 1975 and was found to be racemic, and to be practically insoluble in water (~5 μg/ml at 25°C). Thus, methods are required to resolve the racemic mixture and in an effort improve the performance of the drug in the human system. Cyclodextrins have been shown to possess both abilities.[1,4] Thus the aim of this study was to prepare a complex using the guest NSAID suprofen and the hosts β-CD and TRIMEB and to successfully crystallise the complex and elucidate the three-dimensional structure. This is described below.

β-Cyclodextrin is a cyclic oligosaccharide consisting of seven glucopyranose units linked by α-(1, 4) bonds (Figure 4.6).[5] Since Schardinger discovered β-cyclodextrin in 1911, the most notable feature of CDs is their ability to form inclusion complexes.[6, 7] Complexation occurs due to various factors, notably the hydrophobic interaction between the apolar guest and the apolar interior of the cavity of the CD.[8] Many complexes exist to date and these crystallize mainly in the space groups $C222_1$, C2, $P2_1$ and P1.[8]

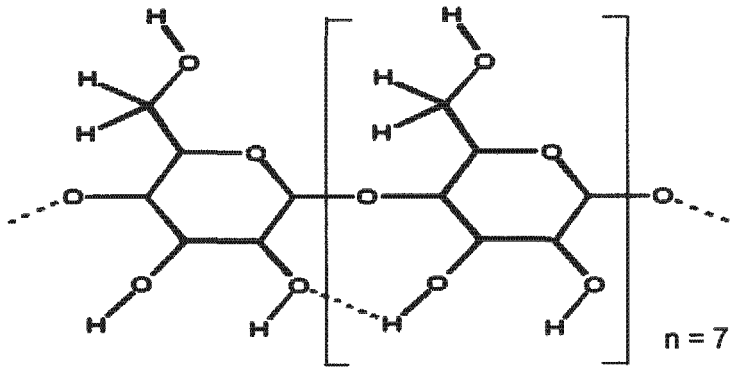

Figure 4.6: Structure of β-cyclodextrin.

4.2.2 Complex Preparation

In a 1:1 molar ratio of racemic drug: CD, a paste was made of the cyclodextrin (0.0505 g, 3.842×10^{-5} mol) and drug (10 mg, 3.842×10^{-5} mol) with a minimum amount of water by kneading for 60 minutes. The paste was then dissolved by adding 5 ml of water and stirred for 30 minutes at 65 °C. The solution was filtered and left at room temperature (25 °C) to evaporate. Single crystals formed after one day. This new form shall be referred to as BCDSUP.

4.2.3 Thermal analysis

DSC and TGA analyses

Since cyclodextrin complexes are prepared in an aqueous milieu raising the probability that a ternary water/CD/drug system is created and given that the cyclodextrin itself is a hydrate, it is imperative that the water content be analysed and this is most adequately done with TGA.[9] Furthermore, confirmation of whether an inclusion complex has formed or not is revealed via DSC. The trace for a physical mixture will exhibit an endotherm at the melting point of the drug, but the endotherm will be absent in the trace for an inclusion complex.[9] Figure 4.7 shows the TGA and DSC traces of the complex and the DSC trace of the pure drug. Endothermic peaks are directed upwards, exothermic peaks downwards. The thermal degradation of the cyclodextrin, which begins around 250 °C, was omitted for clarity.

The water content was calculated from TGA to be 10 water molecules per β-CD molecule. Table 4.2 lists the summary of the observed percentage mass losses over the temperature intervals between 25, 95, 145, 200, 255, 305 and 350 °C.

Table 4.2: The percentage mass losses for BCDSUP.

BCDSUP							
Temperature (°C)	25	95	145	200	255	305	350
Sample mass (%)	100	91.2	86.5	86.4	86.2	85.5	27.6
Δ Mass loss (%) *	-	8.8	4.7	0.1	0.2	0.7	57.9
Average number of water molecules per H:G unit						**10.0**	

* Δ Mass loss (%) = [Sample mass (%) at temperature (n-1)] – [Sample mass (%) at temperature (n)]

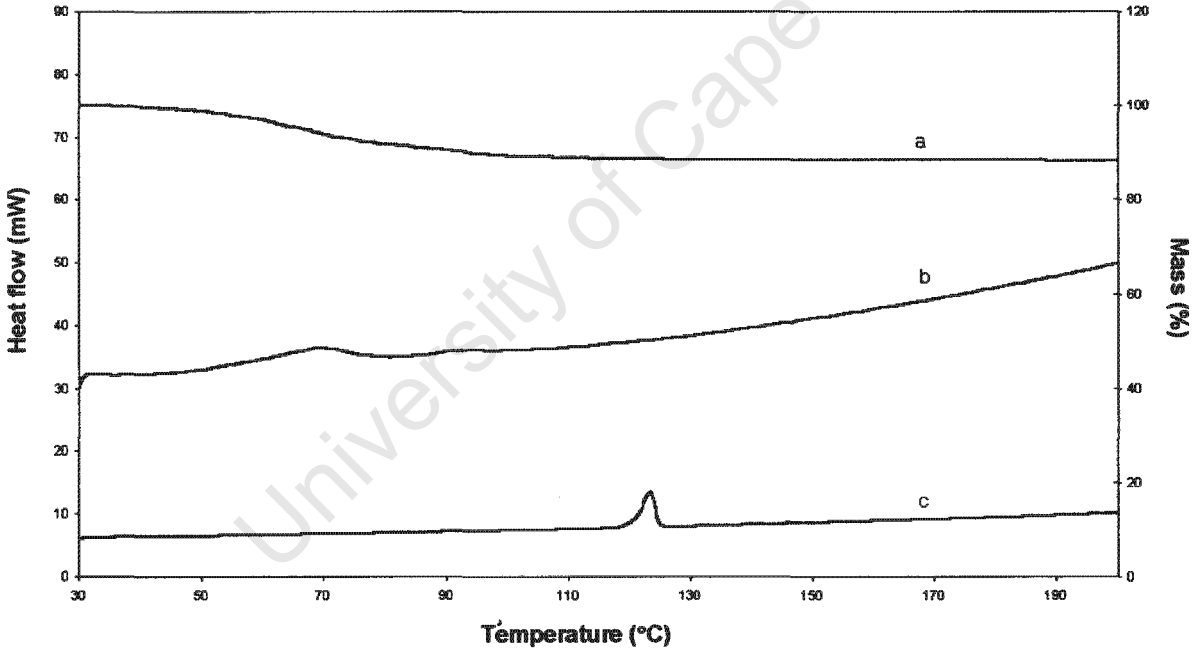

Legend: a: TGA of BCDSUP
b: DSC of BCDSUP
c: DSC of Suprofen

Figure 4.7: TGA and DSC traces for BCDSUP and DSC trace of Suprofen.

Suprofen has a characteristic melting point at an onset temperature of 123.4 °C (ΔH_f = 20.54 J/g) as illustrated by trace (c). Trace (b) illustrates the characteristic water loss of

β-cyclodextrin complexes around 70 °C and is devoid of any endotherm around the melting point of suprofen, indicative of complex formation.

HSM analysis

Visualisation of the thermal differences between BCDSUP and β-CD is depicted in the photo-micrographs in Figure 4.8 below.

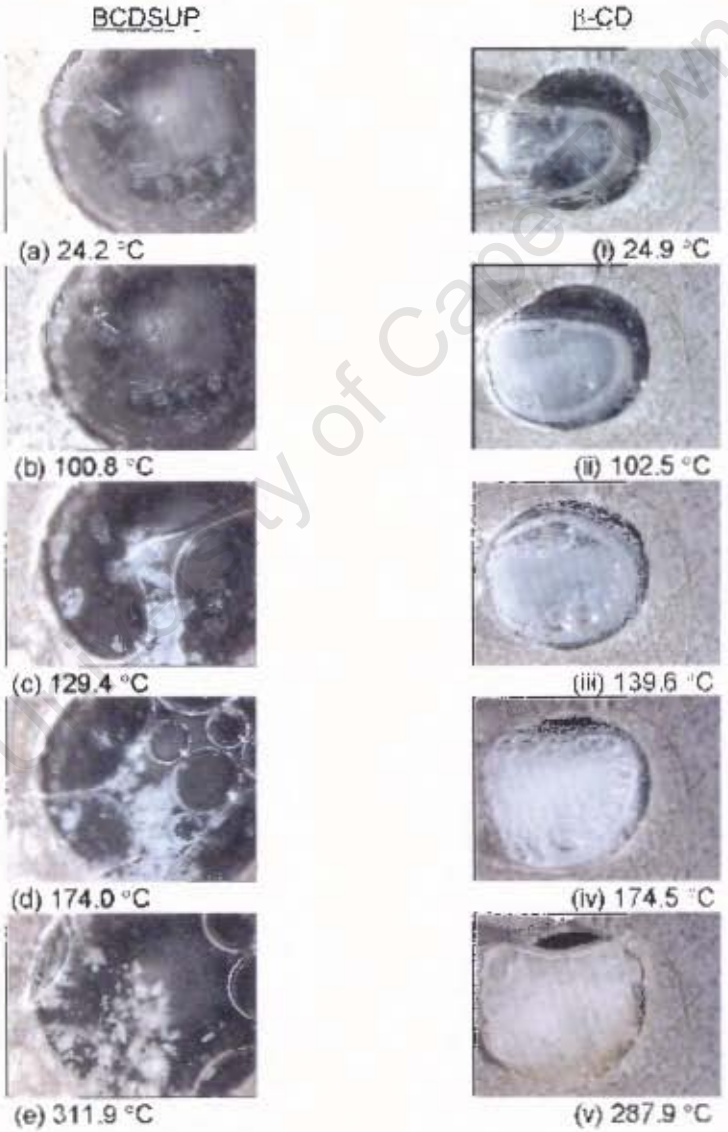

Figure 4.8: HSM photomicrographs of BCDSUP and β-CD.

The morphologies are clearly different and the decomposition behaviours are different. BCDSUP begins decomposing around 310 °C – 312 °C and β-CD decomposes around 286 °C – 288 °C. Both forms exhibit water loss around 100 °C shown by the evolution of bubbles.

4.2.4 Elemental analysis and UV Spectrophotometry

These two techniques were used to determine the host: guest ratio. The water content elucidated by TGA was taken into account when calculating the ratio. Table 4.3 lists the carbon, hydrogen and sulphur elemental analysis results, which confirm the stoichiometry determined by UV spectrophotometry (solvent: methanol, λ_{max}: 285 nm). The host: guest ratio was determined to be 2:1.

Table 4.3: Elemental analysis results for BCDSUP ($(C_{42}H_{70}O_{35})_2 \bullet C_{14}H_{12}O_3S_1 \bullet 20\ H_2O$).*

BCDSUP • 20 H_2O	Calculated (%)	Experimental (%)
C	42.3	41.7
H	6.0	6.4
S	1.2	1.8

* The errors in experimental values are ± 0.5%.

4.2.5 X-Ray Crystallographic Analysis

Data-collection, structure determination and refinement

The data were collected on the Nonius Kappa CCD diffractometer using graphite-monochromated MoKα radiation at 113K. A crystal was selected and mounted on a glass fibre and covered with Paratone N oil to provide a rigid mounting for low-temperature data-collection and to prevent cracking due to loss of water of crystallization.[10] Listed in Table 4.4 are the crystal data and data-collection parameters.

Table 4.4: Crystal data and data-collection parameters for BCDSUP.

Molecular formula	$(C_{42}H_{70}O_{35})_2 \bullet C_{14}H_{12}O_3S_1 \bullet 20\ H_2O$
Formula weight/g mol^{-1}	2890.62
Crystal system	Orthorhombic
Space group	$C222_1$
a / Å	19.0409(1)
b / Å	24.1949(2)
c / Å	32.4707(2)
Z	4
Volume / $Å^3$	14959.01
$Density_{calc}$ / g cm^{-3}	1.2833
μ (MoKα) / mm^{-1}	0.128
F(000)	6160
Crystal size / mm^3	0.10 × 0.15 × 0.20
Index ranges	h: -23, 22 k: -29, 29 l: -39, 38
ϕ scan angle / °	1.0
ω scan angle / °	1.0
Dx / mm	48.0
Total no. of reflections collected	47224
No. of independent reflections	14093
No. of reflections with $I > 2\sigma(I)$	11641
No. of parameters	806
R_{int}	0.0430
S	1.451
R_1 (for 11641 reflections)	0.1103
Reflections omitted	42
wR_2	0.3344
Weighting scheme	a = 0.2000 b = 0.0000
$(\Delta / \sigma)_{mean}$	0.004
$\Delta\rho$ excursions / e. $Å^{-3}$	1.00 and –1.59

The BCDSUP complex crystallizes in the orthorhombic space group $C222_1$ with a single β-CD molecule, half a guest molecule and 10 water molecules comprising the asymmetric unit of the structure. The complex is dimeric, the asymmetric unit being rotated through a diad parallel to the b-axis to produce the other half of the complex. The

structure was solved *ab initio* using the program SHELXD;[11] thereafter SHELX-97[12] was used to refine the structure.

Following refinement of the host atoms in the asymmetric unit using SHELX-97 most of the non-hydrogen atoms were revealed in the difference Fourier maps and thus placed. After further refinement it was found that the primary oxygen atoms O(63) and O(67) were disordered over two positions. All others had full site occupancy. For a given pair, the U_{iso} was allowed to vary and site-occupancy factors [s.o.f.'s] of x and 1-x were assigned, with x variable. The major positions refined to s.o.f.'s of 0.82 and 0.53 for O(6A3) and O(6B7) respectively. All the host atoms except the disordered primary hydroxyl oxygen atoms were refined anisotropically.

Once all the non-hydrogen atoms of the host had been located from subsequent difference electron density maps, all the cyclodextrin hydrogen atoms were placed. These hydrogen atoms were geometrically fixed at idealized positions in a riding model. All the primary hydroxyl hydrogen atoms were assigned a common variable isotropic temperature factor and were placed using the AFIX 147 instruction. The remaining hydrogen atoms of each glucose unit were assigned common variable isotropic temperature factors.

Twenty positions were located for the water molecules and each was assigned a fixed U_{iso} of 0.06 $Å^2$ while the site-occupancy factors were allowed to refine. After further refinement it was found that the oxygen atoms O(1), O(2), O(3), O(4) and O(11) were disordered over two positions; all others had site occupancies varying in the range 0.30-1.0. For a given pair, the U_{iso} was allowed to vary and site-occupancy factors [s.o.f.'s] of x and 1-x were assigned, with x variable. The major positions refined to s.o.f.'s of 0.67, 0.63, 0.82 and 0.55 for O(11A), O(4WA), O(2WA), and O(3WB) respectively. The total number of accounted water molecules per asymmetric unit was 10, supporting the TGA results. The hydrogen atoms of the water molecules were not located.

The subsequent difference Fourier map revealed the positions of the disordered guest atoms. These were assigned and refined with s.o.f.'s fixed at 0.5 since the UV spectrophotometric experiments had indicated that a single suprofen molecule was included per β-CD dimer. The atoms of the phenyl ring were constrained as a rigid

hexagon using the AFIX 66 instruction. This was followed by the placement of the methyl carboxyl group. Thereafter the thiophene ring was placed; this was a challenge due to the diad intersecting this substituent. A single isotropic temperature factor was used for all the non-hydrogen atoms of the guest and this refined to 0.10 $Å^2$. The guest hydrogen atoms were included in geometrically calculated positions and were assigned a common isotropic temperature factor. The site occupancy factors were fixed at 0.5 for the entire guest.

Geometrical Analysis of BCDSUP

The asymmetric unit of the BCDSUP structure contains a single β-CD molecule, half a guest molecule and 10 water molecules. The structure and numbering scheme of the β-CD molecule and water molecules are shown in Figure 4.9. The glucose units are referred to as G1, G2, G3, G4, G5, G6 and G7. The geometrical data for the β-CD molecule are listed in Tables 4.4 and 4.5.

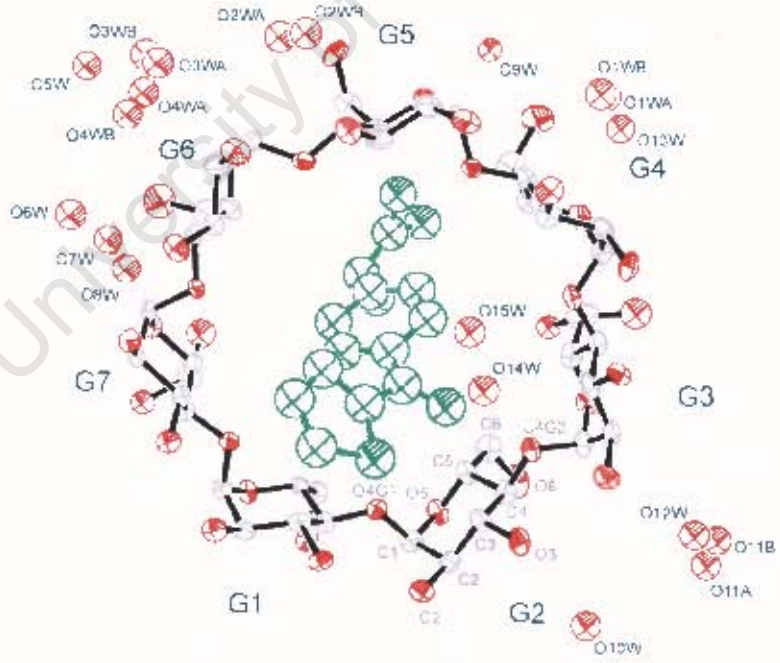

Figure 4.9: Macrocyclic structure and numbering scheme of glucose residues and water oxygen atoms, with the hydrogen atoms excluded. The host is viewed from the secondary face. The guest is green for clarity.

The glucose residues are in the $^4C_1$ chair conformation. The C(6)-O(6) bonds of the G1, G2, G4, G5, G6 residues are directed away from the cavity and are in the (+)-*gauche* conformation to the C(4)-C(5) bonds. The O(6) atoms of the G3 and G7 residues are disordered over two sites. The major position of the O(6) atom of the G3 and G7 residue adopts the (+)-*gauche* conformation while the minor position adopts the (-)-*gauche* conformation. The geometrical parameters of the O(4) heptagon of the BCDSUP structure are listed in Table 4.5. This includes the radii, the O(4)···O(4') distances, and the O(4)···O(4')···O(4") angles, the O(4)···O(4')···O(4")···O(4"") torsion angles and the deviations of each of the O(4) atoms from the mean O(4) plane (Chapter 1, section 1.2.3).

Table 4.5: Geometrical parameters of the O(4) heptagon for the BCDSUP structure.

Glucose Unit	Radii (Å)	O(4)···O(4') (Å)	O(4) angle (°)	Torsion angle (°)	Deviation (Å)
G1	4.97	4.41	126	-0.6	-0.002(3)
G2	5.12	4.34	130	1.2	0.012(3)
G3	5.03	4.41	130	-1.3	-0.015(3)
G4	5.03	4.29	127	1.0	0.010(3)
G5	5.12	4.40	130	-0.9	-0.007(3)
G6	4.99	4.34	128	0.7	0.009(3)
G7	5.01	4.35	130	-0.2	-0.008(3)
Average	5.04	4.36	129	0.8	0.010

Additional macrocyclic geometrical features are listed in Table 4.6. These are the intersaccharidic bond angle (φ), which is C(1')–O(4)–C(4), the O(2)···O(3') distance and the tilt angle (τ_1), which is defined as the angle made between the mean O(4) plane and the mean plane through the four pyranose ring atoms namely O(4'), C(1), C(4) and O(4) of each glucose unit.

Table 4.6: φ, O(2)···O(3') distance and τ for the BCDSUP structure.

Glucose unit	φ (°)	O(2)···O(3') (Å)	τ_1 (°)
G1	117	2.70	4.7
G2	118	2.82	11.6
G3	117	2.83	8.1
G4	117	2.82	11.6
G5	119	2.76	8.6
G6	116	2.83	9.0
G7	119	2.74	7.3
Average	118	2.79	8.7

Generally, the O(4) heptagon has a high degree of planarity and shows a seven-fold symmetry. This is reflected in the O(4)···O(4') distances, and the O(4)···O(4')···O(4'') angles. The tilt angles are all positive; therefore each glucose residue leans toward the centre of the cavity at the primary side. This imparts the characteristic truncated cone shape to the cyclodextrin with the secondary rim being wider than the primary rim. The complex unit forms a dimer, the geometry of which is described below.

Guest geometry and interactions for the BCDSUP structure

The suprofen molecule (Figure 4.10) is held in the β-CD cavity by hydrophobic forces and is inserted in the O(2), O(3) (secondary) side of the cyclodextrin molecule with the methyl carboxyl substituent protruding from the O(6) (primary) side. The (S)-enantiomer of suprofen was preferentially included in the characterised crystal. The thiophene ring protrudes from the O(2), O(3) side. Owing to the bonds of the C=O and C-O groups of the carboxyl substituent being similar it was not possible to distinguish between the two. Thus, analysis of the hydrogen bonding needed to be pursued to identify the difference. Figure 4.11 is a stereoview of the title complex.

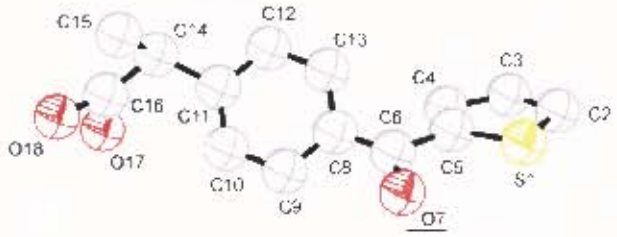

Figure 4.10: Numbering scheme of the guest molecule.

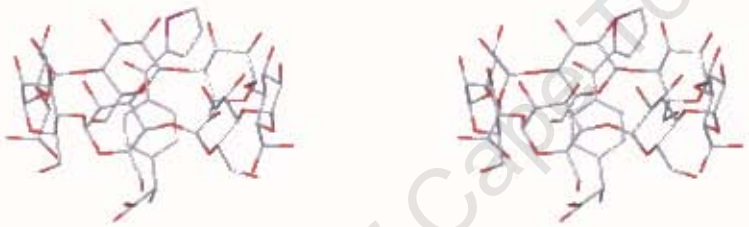

Figure 4.11: Stereo-diagram of the asymmetric unit [excluding waters].

The conformation of the suprofen guest may be defined by three torsion angles. The torsion angles δ_1 [C(5)-C(6)-C(8)-C(9)], δ_2 [C(4)-C(5)-C(6)-C(8)] and δ_3 [C(12)-C(11)-C(14)-C(16)] will be used to describe rotation around the C(6)-C(8), C(5)-C(6) and C(11)-C(14) bonds respectively. The torsion angles of the complexed guest are: δ_1: 148.3(2)°, δ_2: -24.9(4)° and δ_3: 161.3(2)°. The torsion angles of the uncomplexed guest are: δ_1: -144.7(3)°, δ_2: 16.7(2)° and δ_3: -55.9(3)°.[3] The torsion angles of the complexed suprofen have larger 'out-of-plane twists' than those of the uncomplexed suprofen, indicating that for inclusion to occur, suprofen must be rotated and twisted to allow for the guest to enter the host. This necessary conformational change of suprofen is supported by the low average tilt angle value (τ = 8.7°) of the β-CD. The average τ value indicates that β-CD is a rigid molecule and the guest needs to be contorted to fit efficiently into the host cavity.

Figure 4.12 shows the CPK diagrams for a dimer of the BCDSUP structure. The upper half of the dimer shows the position of one component of the disordered guest [with the carbon atoms in green, oxygen atoms in dark red, sulphur atom in orange and hydrogen atoms in light green]. The lower half includes the other component of the disordered guest [with the carbon atoms in blue, oxygen atoms in dark purple, sulphur atom in purple and hydrogen atoms in light blue]. The macrocyclic structure and close contact distances are illustrated clearly in this diagram. Additionally it shows how the disordered guest is nearly completely contained in the dimer, with only the carboxyl moieties protruding from both primary sides.

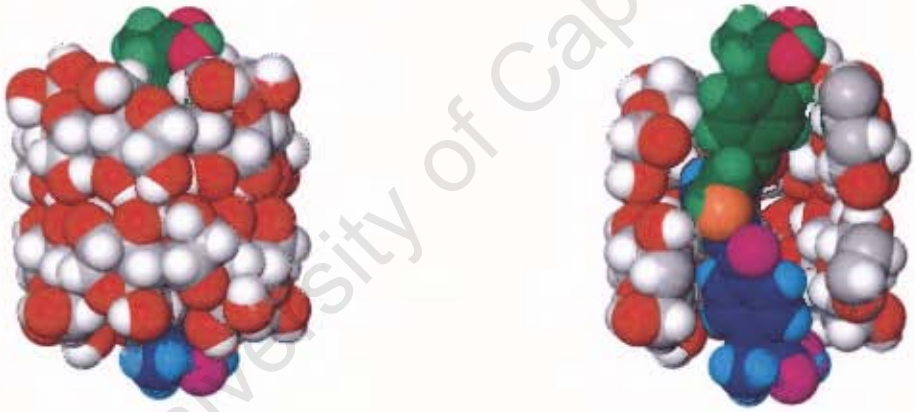

(a) (b)

Figure 4.12: Space-filling diagram of the BCDSUP structure showing the disordered guest in green and blue (a) side view (b) sectioned view of the same orientation.

The two disordered components of the suprofen molecule are related by the C_2-axis which passes through the dimer interface (Figure 4.13).

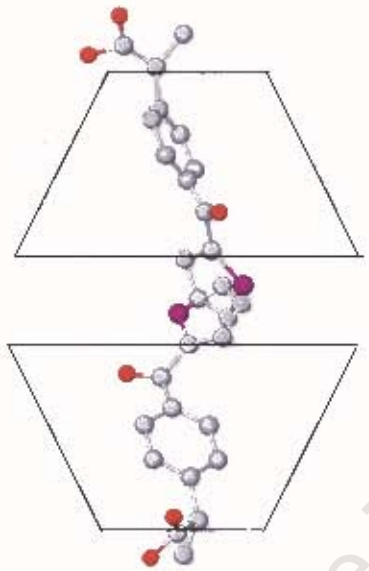

Figure 4.13: A schematic diagram of the guest in the dimer unit, viewed nearly parallel to the b-axis. [excluding the hydrogen atoms].

Hydrogen bonding interactions of the BCDSUP structure.

Host interactions

The host molecules are stabilised by five intramolecular O(2)···O(3') hydrogen bonds on their secondary faces. This differs from other reported β-CD structures which normally have seven intramolecular bonds.[6, 13, 14] Two host molecules form a head-to-head dimer with C_2 symmetry. The dimers are stabilised by six O-H···O hydrogen bonds which involve the O(3) hydroxyl groups. Additional inter-dimer hydrogen bonds occur between cyclodextrin layers, which are referred to as intra-layer interactions. These involve the O(2) and O(6) hydroxyl groups. Table 4.7 lists these lengths.

Table 4.7: Summary of the hydrogen bond distances for the Host and inter-layer interactions.

	Type	Number of H-bonds/dimer	Range (Å)	Mean (Å)
Host interactions	O(2)···O(3)	5	2.74 - 2.83	2.81
	O(3)···O(3)	6	2.75 – 2.88	2.81
Intra-layer interactions	O(2G3)···O(2G6)[i]	2	2.98	2.98
	O(6G1)···O(6G5)[ii]	2	2.78	2.78
	O(6G2)···O(6G6)[iii]	2	2.64	2.64

[i] Related by symmetry operation: 1-x,y,1/2-z

[ii] Related by symmetry operation: -1/2+x,1/2+y,z

[iii] Related by symmetry operation: ½ -x, ½ +y, -z

The conformation of each β-CD molecule is additionally stabilised by four inter- and six intramolecular C-H···O hydrogen bonds. Two of the intramolecular bonds involve the disordered O(6G3) and O(6G7) atoms, implying that disorder in the CD adds to the overall stability of the structure. The hydrogen bonding parameters, based on idealized hydrogen atom positions, are listed in Table 4.8.

Table 4.8: C-H···O hydrogen bonds in the BCDSUP structure.

Type of hydrogen bonds	C-H···O	Distance (Å) C-H	H···O	C···O	Angle (°) C-H···O
Intramolecular	C4G1–H4G1 ..O6G1	1.00	2.54	2.927(6)	103
	C6G2–H6B2 ..O5G3	0.99	2.54	3.386(8)	143
	C4G3–H4G3 ..O6A3	1.00	2.57	2.940(1)	102
	C4G4–H4G4 ..O6G4	1.00	2.46	2.834(8)	102
	C4G5–H4G5 ..O6G5	1.00	2.56	2.951(7)	103
	C4G7–H4G7 ..O6G7	1.00	2.59	2.999(1)	104
Intermolecular	C2G5–H6 ..O3G1[i]	1.00	2.35	3.298(7)	157
	C1G5–H1G5 ..O2G2[i]	1.00	2.54	3.399(6)	144
	C1G7–H1G7 ..O2G4[ii]	1.00	2.57	3.339(7)	134
	C2G7 –H9 ..O3G3[ii]	1.00	2.31	3.302(6)	169

[i] Related by symmetry operation: 1/2+x,-1/2+y,z

[ii] Related by symmetry operation: 1/2+x,1/2+y,z

Guest interactions

The C-O and C=O bonds of the carboxylic acid group were distinguished after identification of a hydrogen bond between one of the O atoms and a neighbouring glucose residue. The hydroxyl substituent was identified to be O(17) of the carboxylic acid group. It is involved in hydrogen bonding with an oxygen atom of the cyclodextrin (O6G2). Additionally there is a weak hydrogen bond between O(7) of the guest and C3G2 of the host and lastly another weak hydrogen bond between O(18) and a neighbouring β-CD molecule. These contacts are listed in Table 4.9. The hydrogen bonding parameters are based on idealized hydrogen atom positions.

Table 4.9: Hydrogen bonding contacts involving the guest.

			Distance (Å)			Angle (°)
Donor (D)	H	Acceptor (A)	D-H	H···A	D···A	D-H···A
O17	–H17	..O6G2*	0.84	2.00	2.613 (2)	129
C3G2	–H3G2	..O7	1.00	2.47	3.324 (2)	143
C1G3	–H1G3	..O18#	1.00	2.57	3.399 (2)	140

* Related by symmetry operation: 1/2+x,1/2-y,-z

Related by symmetry operation: -1/2+x,1/2-y,-z

Water interactions

Thermogravimetric analysis gave a mass loss that corresponded to 20 water molecules per β-CD dimer; all of these were accounted for in the crystallographic analysis. Some of the water molecules were found to be disordered over two positions. Most of the water molecules are situated at the periphery of the cyclodextrin molecule, filling the intermolecular space between complex units. Two water molecules are positioned in the cyclodextrin cavity. Hydrogen bonding distances between the host and water molecules are listed in Table 4.10 and those between water oxygen atoms in Table 4.11. The hydrogen bonding parameters are based on idealized hydrogen atom positions in Table 4.10.

Table 4.10: Hydrogen bonds between the host and water molecules.

			Distance (Å)			Angle (°)
Donor (D)	H	Acceptor (A)	D-H	H···A	D···A	D-H···A
O2G1	–H2G1	..O2WA[i]	0.84	2.42	2.707(8)	101
O6G2	–H6G2	..O9W[ii]	0.84	2.01	2.727(7)	143
O2G3	–H2G3	..O12W	0.84	2.10	2.744(11)	133
O6G4	–H6G4	..O9W	0.84	1.85	2.638(7)	154
O6G6	–H6G6	..O4WA	0.84	2.19	3.029(12)	178
C4G4	–H4G4	..O1WA	1.00	2.53	3.326(12)	136

[i] Related by symmetry operation: -1/2+x,1/2+y,z

[ii] Related by symmetry operation: -1/2+x,1/2-y,-z

Table 4.11: O(water) ··· O(water) contact distances representing possible hydrogen bonds.

Interaction	Distance (Å)	Symmetry operator for the second oxygen atom listed.
O7W ··· O8W	2.80 (2)	x,1-y,-z
O11B ··· O12W	2.57 (2)	x, y, z
O2WB ··· O12W	2.88 (4)	1-x,y,1/2-z
O1WA ··· O6W	2.81 (2)	3/2-x,-1/2+y,1/2-z
O4WA ··· O10W	2.76 (1)	1+x,y,z
O4WA ··· O5W	2.66 (2)	x, y, z
O13W ··· O7W	2.77 (2)	-1/2+x,-1/2+y,z

Crystal packing of the BCDSUP structure

Figure 4.14 is a packing diagram of the BCDSUP structure projected down the c-axis. The diagram illustrates that "endless" channels do not form due to the screw axis symmetry associated with this space group. The two-fold axes parallel to the b-axis relate the two β-CD molecules of a dimer to one another, the disordered guest and relating adjacent dimers. No other inclusion of the guest within neighbouring β-CD dimers occurs.

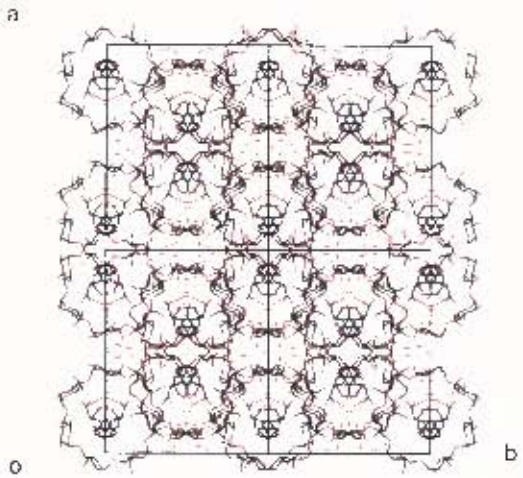

Figure 4.14: Packing diagram of the BCDSUP structure [c-axis projection]. Four unit cells are shown.

Figure 4.15 is a packing diagram of the BCDSUP structure projected down the b-axis. This diagram illustrates the characteristic packing motif for the β-CD dimers. The packing mode is Chessboard (CB). This correlates well with other reported cases of β-CD complexes in the space group C222$_1$, where the packing mode is Chessboard.[8, 14] This structure also corresponds to all other known dimeric β-CD complexes in which β-CD crystallizes in layers.[8] Figure 4.16 shows the stereo-packing diagram of the BCDSUP structure projected down the a-axis.

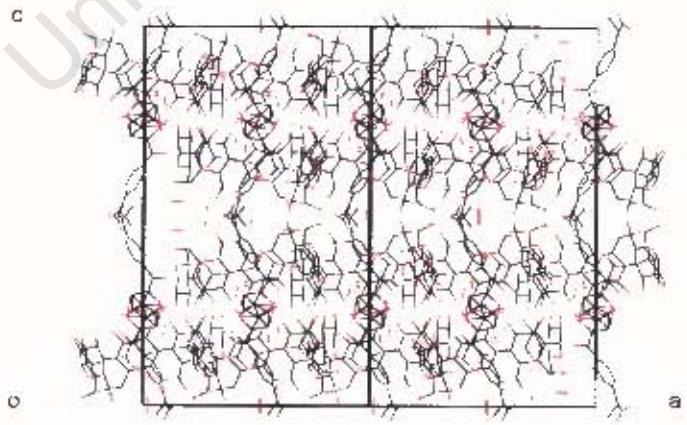

Figure 4.15: Packing diagram of the BCDSUP structure [b-axis projection].

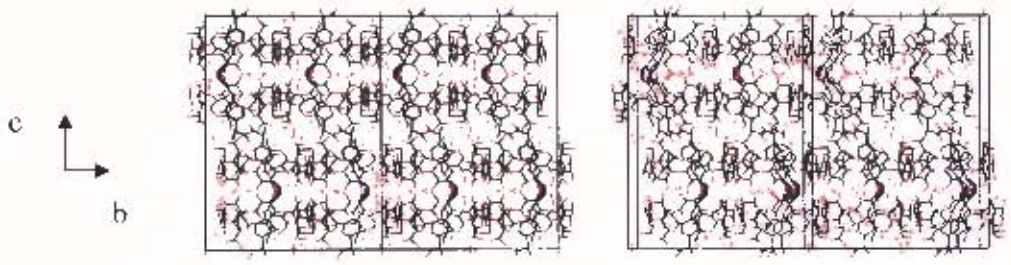

Figure 4.16: Stereo packing diagram of the BCDSUP structure [a-axis projection].

4.2.6 XRD Powder analysis

Figure 4.17 shows the XRPD patterns of the β-CD and suprofen 1:1 physical mixture and the co-precipitate material whose preparation is described in section 4.2.2. Additionally, the computed trace (program Lazy Pulverix[15]) from the refined data of the single crystal structure (section 4.2.5) is also shown. These traces are compared to prove that an inclusion complex has formed and that the bulk material corresponds to the single crystal structure.

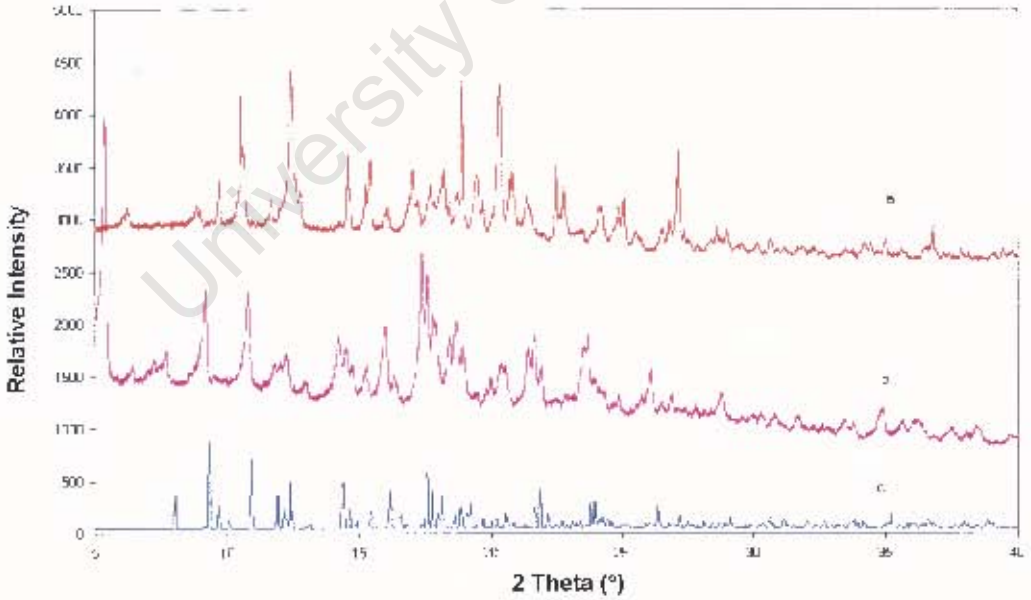

Legend: a: PXRD of BCD and Suprofen physical mixture
b. PXRD of BCDSUP co-precipitate material
c: PXRD of Lazy Pulverix calculated trace

Figure 4.17: XRPD traces for BCDSUP.

The difference between the physical mixture trace and the co-precipitate material trace indicates that a crystalline phase change has occurred. Complexation was proven by the correspondence of the Lazy Pulverix calculated trace and the co-precipitate material trace.

4.3 The inclusion complex TRIMEB • Suprofen

4.3.1 Complex preparation

In a 1:1 molar ratio of drug:CD, a solution was prepared consisting of the cyclodextrin (0.0556 g, 3.842×10^{-5} mol) and racemic drug (10 mg, 3.842×10^{-5} mol) with 1 ml of distilled water. This was stirred in ice for 24 hours, then heated at 70 °C for 30 minutes and finally stirred for a further 30 minutes in ice. The solution was filtered and left at 50 °C in the oven. Single crystals formed after ten days. As shown below, the crystals are those of an inclusion complex between TRIMEB and suprofen. This complex shall be referred to as TRIBSUP.

4.3.2 Thermal analysis

DSC and TGA analysis

Figure 4.18 displays TGA and DSC traces of the complex and the individual drug. Endothermic peaks are directed upwards, exothermic peaks downwards. The thermal degradation of the cyclodextrin, which begins around 250 °C, was omitted for clarity.

The TGA results for the TRIBSUP complex indicated that the complex is anhydrous. In the DSC, a melting endotherm was seen for the complex at onset temperature 154.4 °C (ΔH_f = 12.67 J/g). The melting endotherm corresponding to pure suprofen had an onset temperature of 123.4 °C (ΔH_f = 20.54 J/g). These distinctly different temperatures indicate that a complex has been created. In contrast to the thermal behaviour of β-CD inclusion complexes, TRIMEB complexes exhibit a relatively sharp melting point.

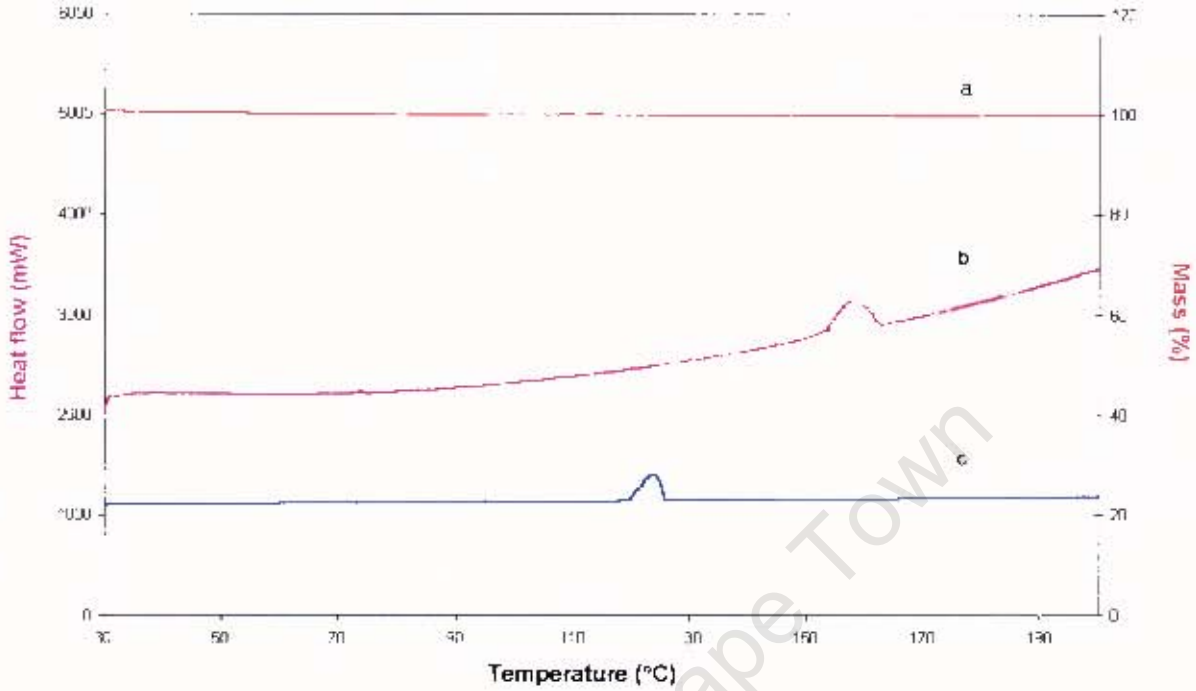

Legend: a: TGA of TRIBSUP
B. DSC of TRIBSUP
C. DSC of Suprofen

Figure 4.18: TGA and DSC curves for TRIBSUP and DSC of Suprofen.

HSM analysis

The photo-micrographs shown in Figure 4.19 indicate that the material examined is not simply uncomplexed TRIMEB. TRIMEB monohydrate shows bubble formation beginning at 124.5 °C indicating water loss and the melt occurs around 157.5 and 160.2 °C (Figure 4.19 (b) – (d)). TRIBSUP shows no bubble formation, indicating that it is anhydrous and the range of melting is between 159.1 and 164.1 °C (Figure 4.19 (iii) – (iv)).

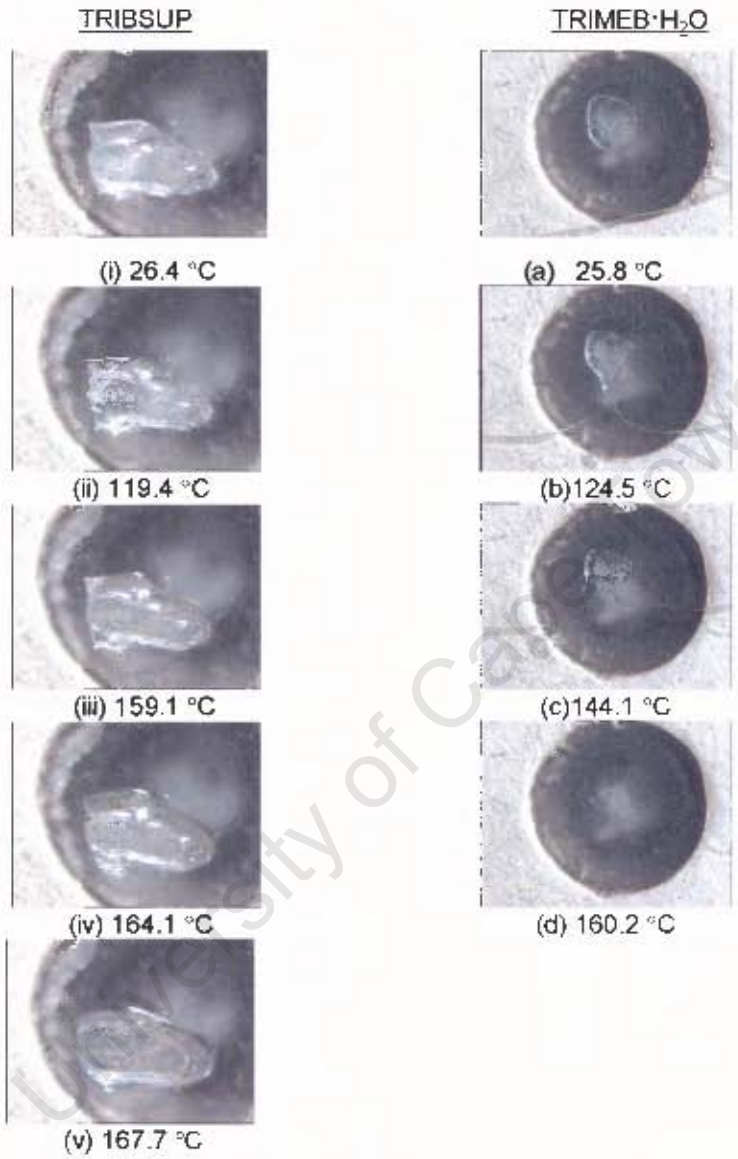

Figure 4.19: HSM photomicrographs for TRIBSUP and TRIMEB.

4.3.3 Elemental analysis and UV Spectrophotometry

UV analysis proved that this is a 1:1 host : guest complex. This was verified by elemental analysis (Table 4.12). The proximity of the experimental values to those calculated proves that this is a 1:1 complex.

Table 4.12: Elemental Analysis results for TRIBSUP ($C_{42}H_{70}O_{35} \bullet C_{14}H_{12}O_3S_1$).*

TRIBSUP	Calculated (%)	Experimental (%)
C	54.2	54.1
H	7.4	7.4
S	1.9	1.6

* The errors in experimental values are ± 0.5%.

4.3.4 X-Ray Crystallographic Analysis

Unit cell determination

The unit cell parameters, crystal system and space group were determined rapidly using the Nonius Kappa CCD diffractometer. A high-quality crystal was selected and mounted using Paratone N oil and used for data-collection. Table 4.13 compares the unit cell parameters of TRIBSUP with those of the TRIMEB • Naproxen inclusion complex.[16] The close correspondence of these data strongly suggests that the two complexes are isostructural.[1] For this reason, isomorphous replacement was the method of choice for solving the structure of TRIBSUP.

Table 4.13: Unit cell parameters for TRIBSUP and the TRIMEB • Naproxen complex.

	TRIBSUP	TRIMEB • Naproxen[16]
Spacegroup	$P2_12_12_1$	$P2_12_12_1$
a	15.389 (1) Å	15.179 (4) Å
b	21.051 (1) Å	21.407 (5) Å
c	27.027 (2) Å	27.67 (1) Å
Volume	8755.4 (1) $Å^3$	8991 (5) $Å^3$
Z	4	4

Data-collection, structure determination and refinement

The data were collected on the Nonius Kappa CCD diffractometer using graphite-monochromated MoKα radiation at 113K. Listed in Table 4.14 are the crystal data and data-collection parameters.

Table 4.14: Crystal data and data-collection for TRIBSUP.

Molecular Formula	$C_{42}H_{70}O_{35} \bullet C_{14}H_{12}O_3S_1$
Formula Weight/g mol^{-1}	1689.88
Crystal System	Orthorhombic
Space group	$P2_12_12_1$
$Density_{calc}$ / g cm^{-3}	1.2818
μ (MoKα) / mm^{-1}	0.12
F(000)	3624
Crystal size / mm^3	0.40 × 0.40 × 0.40
Range scanned θ / °	$2.75 \leq \theta \leq 27.83$
Index ranges	h: -20, 20 k: -27, 27 l: -35, 35
ϕ scan angle / °	1.0
ω scan angle / °	0.8
Dx / mm	45.0
Total no. of reflections collected	80354
No. of independent reflections	20712
No. of reflections with $I > 2\sigma(I)$	15957
No. of parameters	1047
R_{int}	0.0523
S	1.029
R_1 (for 15957 reflections)	0.0609
Reflections omitted	34
wR_2	0.1515
Weighting scheme	a = 0.0637 b = 8.5956
$(\Delta / \sigma)_{mean}$	< 0.001
$\Delta\rho$ excursions / e. $Å^{-3}$	1.79 and –0.64

The structure was solved using published co-ordinates for the non-hydrogen cyclodextrin atoms of the isomorphous TRIMEB • (S)-naproxen complex.[16] Following refinement using SHELX-97[12] most of the non-hydrogen atoms of the drug molecule were revealed in the difference Fourier maps and thus placed.

After further refinement it was found that atoms C(10), C(11), C(12) and C(14) were disordered as were atoms O(17) and O(18). Two alternative positions were found for atoms O(17) and O(18), the oxygen atoms of the carboxylic group of the guest. For a

given pair, a fixed U_{iso} of 0.05Å^2 was assigned and site-occupancy factors [s.o.f.'s] of x and 1-x were assigned. Some of the bonds on these disordered atoms were either abnormally long or too short and thus distance constraints were placed on them. All non-hydrogen atoms [except C11, C12, C14, O17A, O17B, O18A and O18B of the guest] were assigned anisotropic temperature factors and refined.

All the hydrogen atoms [except H18A and H17B] were located from subsequent difference electron density maps and these hydrogen atoms were placed in idealized positions in a riding model and assigned common variable isotropic temperature factors. For H18A and H17B a fixed U_{iso} of 0.05Å^2 was assigned and site-occupancy factors [s.o.f.'s] of x and 1-x were assigned.

At the end of the refinement five significant electron density peaks were unaccounted for with heights of 1.79, 1.03, 0.93, 0.71 and 0.68 e. Å^{-3}, the highest electron density being located at a distance of 1.0 Å from C(14) while the lowest electron density was located at a distance of 0.4 Å from C(11). The possibility that these electron density peaks represented a disordered carbon atom was rejected due to their unfavourable geometric positions relative to those atoms already placed.

Geometrical Analysis of TRIBSUP

The asymmetric unit of TRIBSUP contains a single TRIMEB molecule and its associated guest. The glucose units are referred to as G1, G2, G3, G4, G5, G6 and G7. The structure and numbering scheme of the TRIBSUP structure are shown in Figure 4.20. The geometrical data for the TRIMEB molecule are listed in Tables 4.15 and 4.16.

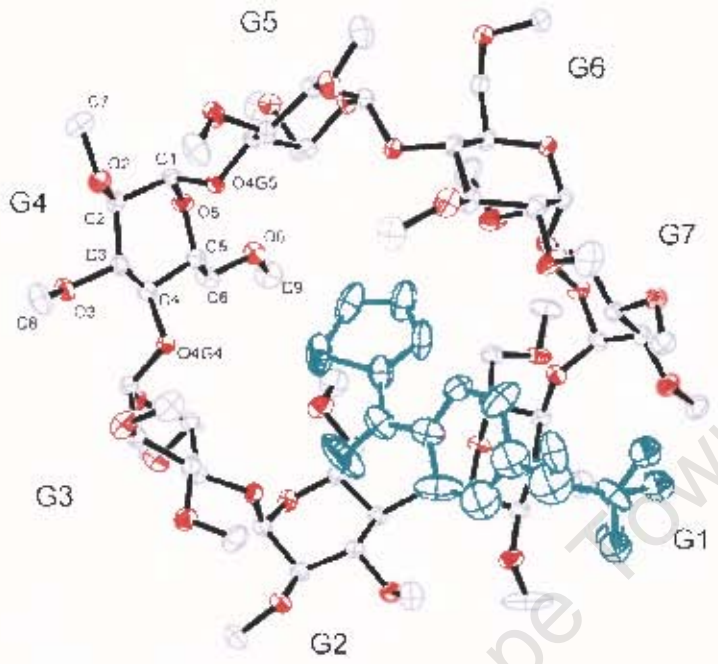

Figure 4.20: Macrocyclic structure and numbering scheme of glucose residues, with the hydrogen atoms excluded. The host is viewed from the secondary face.The guest molecule is green for clarity.

All seven of the methylglucose residues of the TRIMEB molecule are in the $^4C_1$ chair conformation. The macrocycle has adopted the shape of an elliptically-distorted and truncated cone with the C(6)-O(6)-C(9) groups of G1, G2, G4, G5 and G7 almost closing off the O(6) side. No disorder was seen on the TRIMEB molecule. As is normally the case with TRIMEB, the O(2)-C(7) bonds are directed away from the cavity and the O(3)-C(8) bonds are directed towards the cavity.[16] The C(6)-O(6) bonds of residues G1, G3, G5 and G6 are directed away from the cavity in the (-)-*gauche* conformation, while those of G2, G4 and G7 point towards the cavity in the (+)-*gauche* conformation. The O(6)-C(9) bonds of all glucose residues are *trans* to the corresponding C(5)-C(6) bonds except in G6, where it is *gauche*.

The geometrical parameters of the O(4) heptagon of the TRIBSUP structure are listed in Table 4.15. This includes the radii, the O(4)···O(4') distances, and the O(4)···O(4')···O(4'') angles, the O(4)···O(4')···O(4'')···O(4''') torsion angles and the deviations of each of the O(4) atoms from the mean O(4) plane (Chapter 1, section 1.2.3).

Table 4.15: Geometrical parameters of the O(4) heptagon for the TRIBSUP structure.

Glucose Unit	Radii (Å)	O(4)···O(4') (Å)	O(4) angle (°)	Torsion angle (°)	Deviation (Å)
G1	5.00	4.53	127	6.8	0.443(2)
G2	5.00	4.37	129	17.0	0.220 (2)
G3	5.18	4.57	121	-8.9	-0.500 (2)
G4	4.81	4.24	136	-19.3	-0.031 (2)
G5	5.13	4.46	121	25.7	0.586 (2)
G6	4.98	4.39	128	1.5	-0.326 (2)
G7	4.94	4.16	129	-23.3	-0.392 (2)
Average	5.01	4.39	127	14.6	0.357

Table 4.16 lists the intersaccharidic bond angle (φ), C(1') O(4) C(4), the O(2)···O(3') distance and the tilt angle (τ_1), which is defined as the angle made between the mean O(4) plane and the mean plane through the four pyranose ring atoms, namely O(4'), C(1), C(4) and O(4) of each glucose unit.

Table 4.16: φ, O(2)···O(3') distance and τ for the TRIBSUP structure.

Glucose unit	φ (°)	O(2)···O(3') (Å)	τ_1 (°)
G1	116.7 (2)	3.10	27.6
G2	117.2 (2)	3.64	21.6
G3	118.2 (2)	3.65	-7.7
G4	115.2 (2)	3.37	44.8
G5	117.1 (2)	3.78	36.1
G6	117.5 (2)	3.52	-15.8
G7	115.6 (2)	3.23	33.5
Average	116.8	3.47	26.7

Average bond lengths and angles are in agreement with those reported for other hosts in TRIMEB complexes,[16,17,18,19] The data corresponded well with the isostructural TRIMEB-(S)-naproxen complex.[16] The conformation of the TRIMEB molecule is distorted unlike the host molecule which is stabilised due to the presence of intramolecular C-H···O interactions.[16,17,18]

Guest geometry and interactions for the TRIBSUP structure

The suprofen molecule (Figure 4.21) is held in the TRIMEB cavity by hydrophobic forces and is inserted in the O(2), O(3) side of the cyclodextrin molecule with the thiazole ring buried in the cavity near the O(6) side. The (S)-enantiomer of suprofen was preferentially included in the characterised crystal. The carboxylic acid substituent is protruding from the O(2), O(3) side. Figure 4.22 is a stereoview of the title complex. The CPK space filling diagrams of TRIBSUP are depicted in Figure 4.23. These clearly show the macrocyclic overall geometry and the insertion of suprofen within the cyclodextrin cavity.

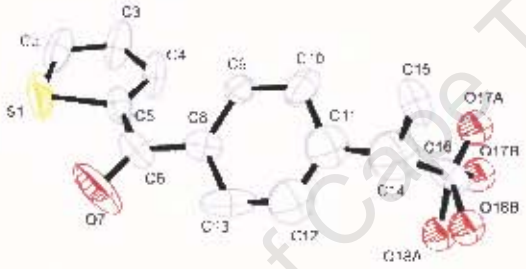

Figure 4.21: Numbering scheme of guest molecule showing disorder around the carboxyl group.

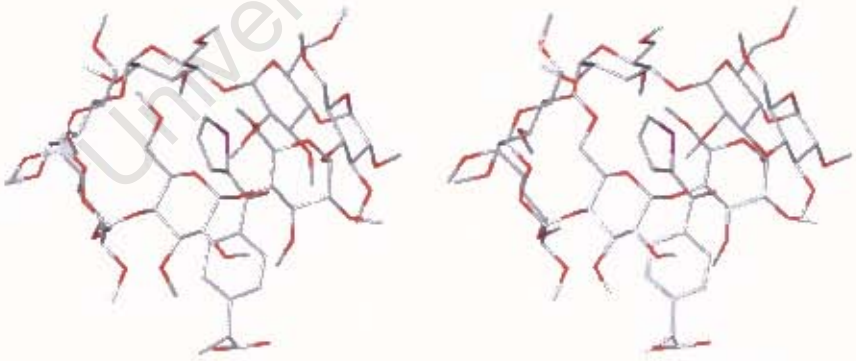

Figure 4.22: Stereodiagram of TRIBSUP.

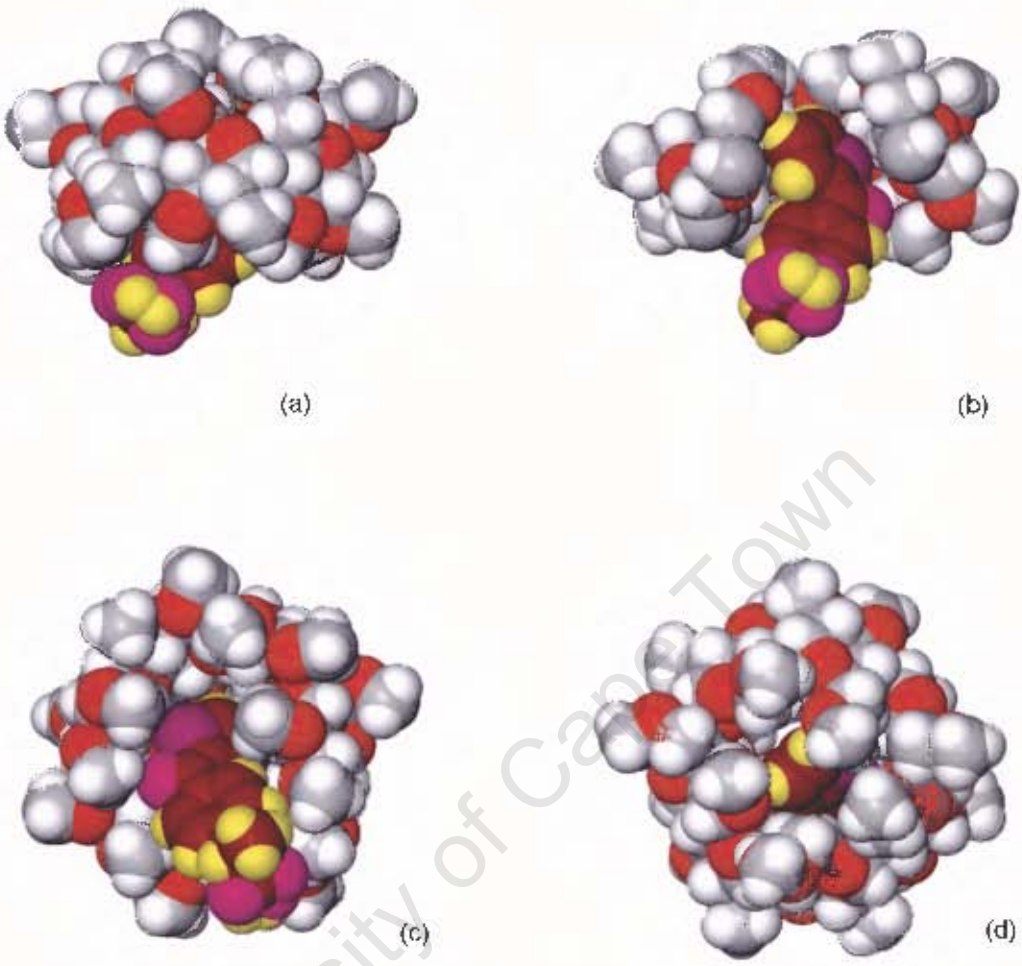

Figure 4.23: Space-filling diagram of the TRIBSUP structure (a) side view (b) sectioned side view (c) viewed from the secondary rim and (d) viewed from the primary rim.

The conformation of the suprofen guest may be defined by three torsion angles. The torsion angles δ_1 [C(5)-C(6)-C(8)-C(9)], δ_2 [C(4)-C(5)-C(6)-C(8)]and δ_3 [C(12)-C(11)-C(14)-C(16)], will be used to describe rotation around the C(6)-C(8), C(5)-C(6) and C(11)-C(14) bonds respectively. The torsion angles of the complexed guest are: δ_1: 27.6(2)°, δ_2: 24.9(3)° and δ_3: 92.3(2)°. In contrast, the torsion angles of the uncomplexed guest are: δ_1: -144.7(3)°, δ_2: 16.7(2)° and δ_3 : -55.9(3)°.[3] The torsion angles of the complexed suprofen have smaller 'out-of-plane twists' than those of the uncomplexed suprofen, indicating that inclusion allows for less rotational freedom around these

specific bonds. This statement is supported with the mean tilt angle value for the host molecule (τ_1 = 26.7°). This value is large indicating that the CD is collapsed thereby allowing the guest less rotational freedom.

Hydrogen bonding interactions of the TRIBSUP structure.

Host interactions

As mentioned previously the distorted conformation of the TRIMEB molecule relative to that of the parent β-cyclodextrin is stabilized due to several intramolecular C-H···O hydrogen bonds. These hydrogen bonds, which are based on idealized hydrogen atom positions, are seen in Table 4.17. The conformation of the TRIMEB molecule in the TRIBSUP complex is stabilized by five C(6)-H···O(5) intramolecular hydrogen bonds. Additionally there is one other intramolecular interaction, namely C(1G5)-H···O(6) stabilizing the tilt angles of G5.

Table 4.17: Intramolecular C-H···O hydrogen bonds in the TRIBSUP structure.

			Distance (Å)		Angle (°)	
C	H	O	C-H	H···O	C···O	C-H···O
C6G1	--H6B1	..O5G7	0.99	2.57	3.217(4)	123
C6G2	--H6A2	..O5G1	0.99	2.41	3.326(4)	153
C6G3	--H6A2	..O5G1	0.99	2.41	3.114(4)	134
C6G5	--H6B5	..O5G4	0.99	2.42	3.134(4)	129
C6G6	--H6B6	..O5G5	0.99	2.43	3.228(4)	137
C1G5	--H1G5	..O6G6	1.00	2.36	3.212(4)	143

Guest interactions

Locating hydrogen bonds identified the hydroxyl group of the carboxylic acid substituent of the guest. O18A and O17B (the disordered component) were identified as the hydroxyl groups of the guest. These two atoms are involved in hydrogen bonding with an oxygen atom of the cyclodextrin. These contacts are listed in Table 4.18. The hydrogen bonding parameters are based on idealized hydrogen atom positions.

Table 4.18: Hydrogen bonding contacts involving the guest.

			Distance (Å)			Angle (°)
Donor (D)	H	Acceptor (A)	D-H	H···A	D···A	D-H···A
O18A --	H18A	.. O3G2^{i}	0.84	1.96	2.651(5)	139
O17B --	H17B	.. O3G2	0.84	1.75	2.588(3)	179

Related by symmetry operation: -1/2+x,1/2-y,1-z

Crystal packing of the TRIBSUP structure

Figures 4.24 (a), (b) are extended packing diagrams showing projections down the a- and b-axes. The stereo-packing diagram of TRIBSUP viewed down the a-axis is shown in Figure 4.25. Complex units pack in a screw-channel mode, in a head-to-tail arrangement. The TRIMEB molecules have their mean O4 plane approximately parallel to the ac-plane. Due to the two-fold screw symmetry, the complexes are laterally shifted with respect to one another, thereby preventing a channel structure but rather forming a cage-like structure. There is no inclusion of the carboxylic acid residue in a neighbouring host molecule.

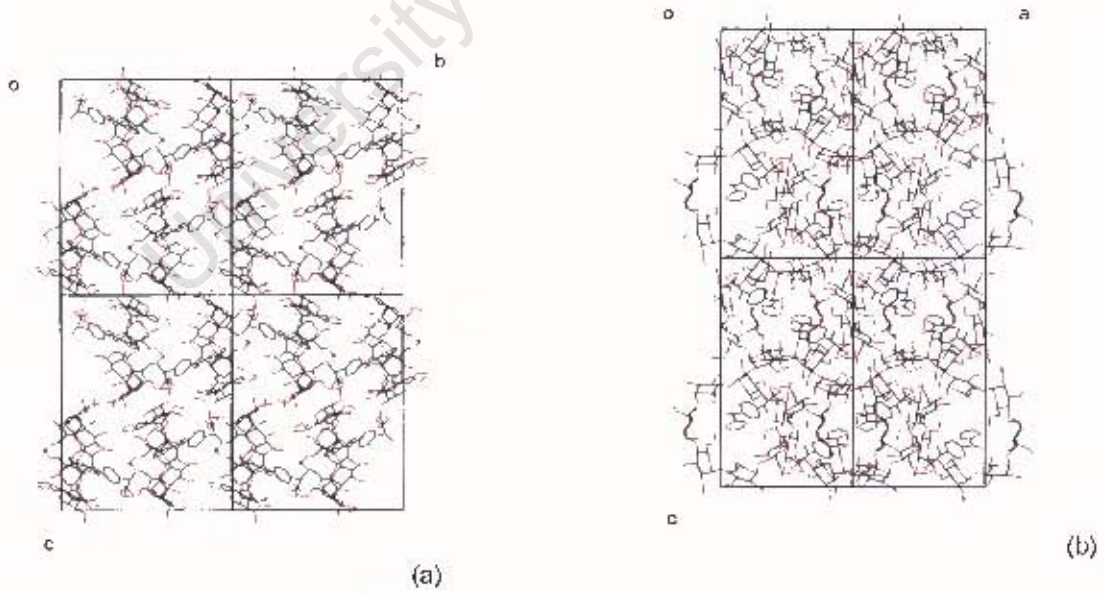

Figure 4.24: Packing diagram viewed down (a) a-axis and (b) b-axis.

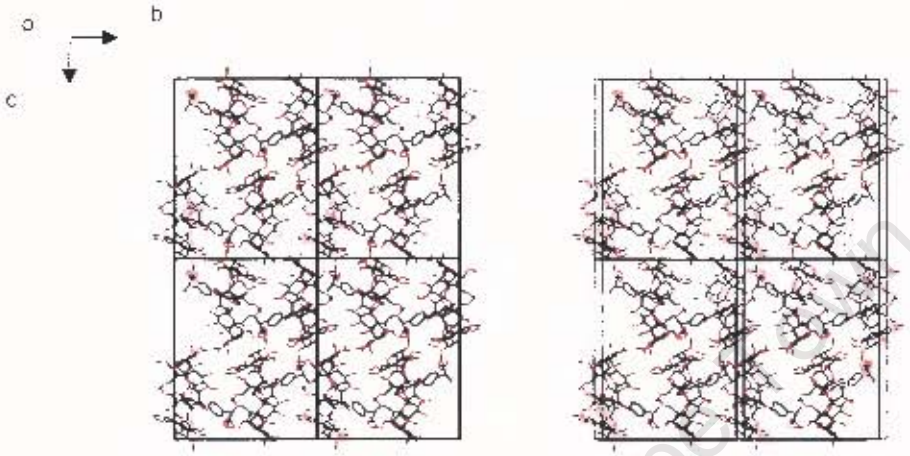

Figure 4.25: Stereo-packing diagram down the a-axis projection showing cage structure.

4.3.5 XRD Powder analysis

The XRPD trace of the physical mixture differs considerably from that of the co-precipitate material, proving that a new crystalline phase has been produced (Figure 4.26). The computer-generated XRPD trace (program Lazy Pulverix [15]) calculated from the refined structural data from single crystal X-ray analysis for the complex (Section 4.3.5) corresponds with that of the co-precipitate material. The angular shift is due to the different temperatures involved (-100 °C and 25 °C respectively).

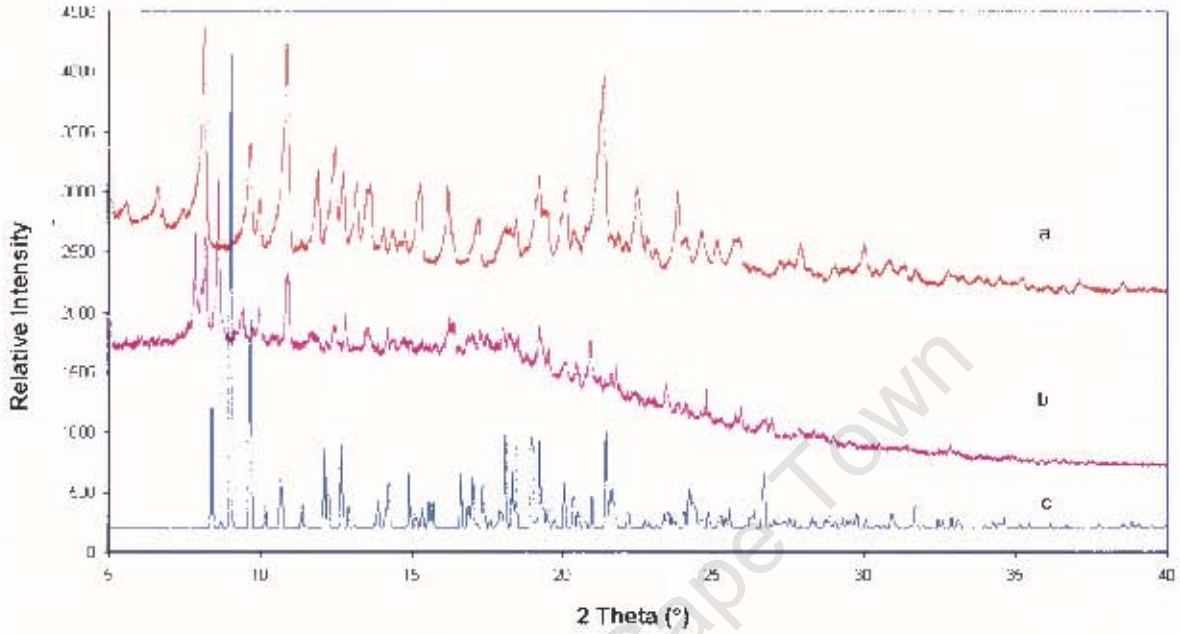

Legend. a. PXRD of TRIMEB and Suprofen physical mixture
b: PXRD of TRIBSUP co-precipitate material
c: PXRD of Lazy Pulverix calculated trace

Figure 4.26: XRPD traces of TRIBSUP.

Only the inclusion complexes involving suprofen and the cyclodextrins β-CD and TRIMEB were obtained and fully characterised in this study.

4.4 Discussion

Several inclusion complexes involving the guest NSAIDs diflunisal, suprofen and bucetin and the hosts β- and γ-cyclodextrin were identified using the XRPD technique. It was suggested earlier that within an isostructural series, the gross features of the patterns are constant regardless of the nature of the included guest.[1] This was proven to be true in this project by comparison of the various XRPD patterns.

A novel inclusion complex between β-CD and suprofen was discovered and characterised using thermoanalytical, elemental analysis and crystallographic techniques. The new dimeric complex was found to have 10 water molecules per β-CD molecule and to crystallize with the host : guest ratio of 2:1. The host adopts the usual conformation seen in other β-CD complexes.[14, 20, 21, 22] The (S)-enantiomer of suprofen was preferentially included in the characterised crystal. The guest is disordered over two orientations due to the C_2-axis. The packing motif was found to be screw channel (SC).

A new inclusion complex between TRIMEB and suprofen was discovered and characterised using thermoanalytical, elemental analysis and crystallographic techniques. The new complex was found to have no water molecules in its crystal structure and the host adopts the usual conformation seen in other TRIMEB complexes.[10, 17, 18, 19] The data corresponded well with the isostructural TRIMEB-(S)-naproxen complex.[6] The (S)-enantiomer of suprofen was preferentially included in the characterised crystal. The O atoms of the -COOH group are disordered over two orientations; this is due to the possibility of free rotation around the C-COOH bond. High electron density peaks were discovered around the disordered carboxyl group and the phenyl ring. The possibility that these electron density peaks represented disordered carbon atoms was rejected due to their unfavourable geometric positions relative to those atoms already placed. These peaks possibly represented minor inclusion of the R-enantiomer. A full study of which enantiomer is preferentially included under different conditions of complex preparation was not carried out because of time constraints. However, this should be the subject of a future study.

4.5 References

1. Caira, M.R. *Rev. Roum. Chim.*, **2001**, 46(4), 371-386.
2. *Cambridge Structural Database and Cambridge Structural Database System*, Version 5.23, April **2003**, Cambridge Crystallographic Data Centre, University Chemical Laboratory, Cambridge, England.
3. Peeters, O; Blaton, N; de Ranter, C. *Bull. Soc. Chim. Belg.*, **1983**, *92*, 191-192.
4. Fanali, S; Aturki, Z. *J. Chromatogr.*, **1995**, *694*, 297-305.
5. Martin Del Valle, E.M. *Process Biochem.*, **2003**, *39*, 1033-1046.
6. Lindner, K; Saenger, W. *Carbohyd. Res.*, **1982**, *99*, 103-115.
7. Liu, L; Guo, Q. *J. Incl. Phenom. Macrocycl. Chem.*, **2002**, *42*, 1-14.
8. Mentzafos, D; Le Bas, G; Mavridis, I.M; Tsoucaris, G. *Acta Crystallogr.*, **1991**, *B47*, 746-757.
9. Giordano, F; Novak, C; Moyano, J.R. *Thermochim. Acta*, **2001**, 380, 123-151.
10. De Vries, E.J. *PhD thesis, Inclusion of Alkylparabens in Cyclodextrins*, University of Cape Town, South Africa, **2003.**
11. Schneider, T; Sheldrick, G. M. *Acta Crystallogr. Section D*, **2002**, *58*, 1772-1779.
12. Sheldrick, G.M. SHELXL-97, *Program for the Refinement of Crystal Structures*, University of Göttingen, Germany, **1997**
13. Caira, M.R; De Vries, E.J; Nassimbeni, L.R; Jacewicz, V. *J. Incl. Phenom. Macrocycl. Chem.*, **2003**, *46*, 37-42.
14. Hamilton, J.A. *Carbohyd. Res.*, **1985**, *142*, 21-37.
15. Yvon, K; Jeitschko, W; Parthé, E. *J. Appl. Crystallogr.*, **1977**, *10*, 73-74.
16. Caira, M.R; Griffith, V.J; Nassimbeni, L.R; van Oudtshoorn, B. *J. Inclusion Phenom. Mol. Recognit. Chem.*, **1995**, *20*, 277-290.
17. Harata, K; Uekama, K; Imai, T; Hirayama, F; Otagiri, M. *J. Incl. Phenom.*, **1988**, *6*, 443-460.
18. Brown, G.R; Caira, M.R; Nassimbeni, L.R, van Oudtshoorn, B. *J. Incl. Phenom.*, **1996**, *26*, 281-294.
19. Harata, K; Hirayama, F; Arima, H; Uekama, K, Miyaji, T. *J. Chem. Soc., Perkin Trans. 2*, **1992**, 1159-1166.
20. Caira, M.R; Dodds, D.R. *J. Incl. Phenom. Macrocycl. Chem.*, **2000**, *38*, 75-84.
21. Caira, M.R; Dodds, D.R. *J. Incl. Phenom. Macrocycl. Chem.*, **1999**, *34*, 19-29.

22. Caira, M.R; Griffith, V.J; Nassimbeni, L.R. *J. Incl. Phenom. Macrocycl. Chem.*, **1998**, *32*, 461-476.

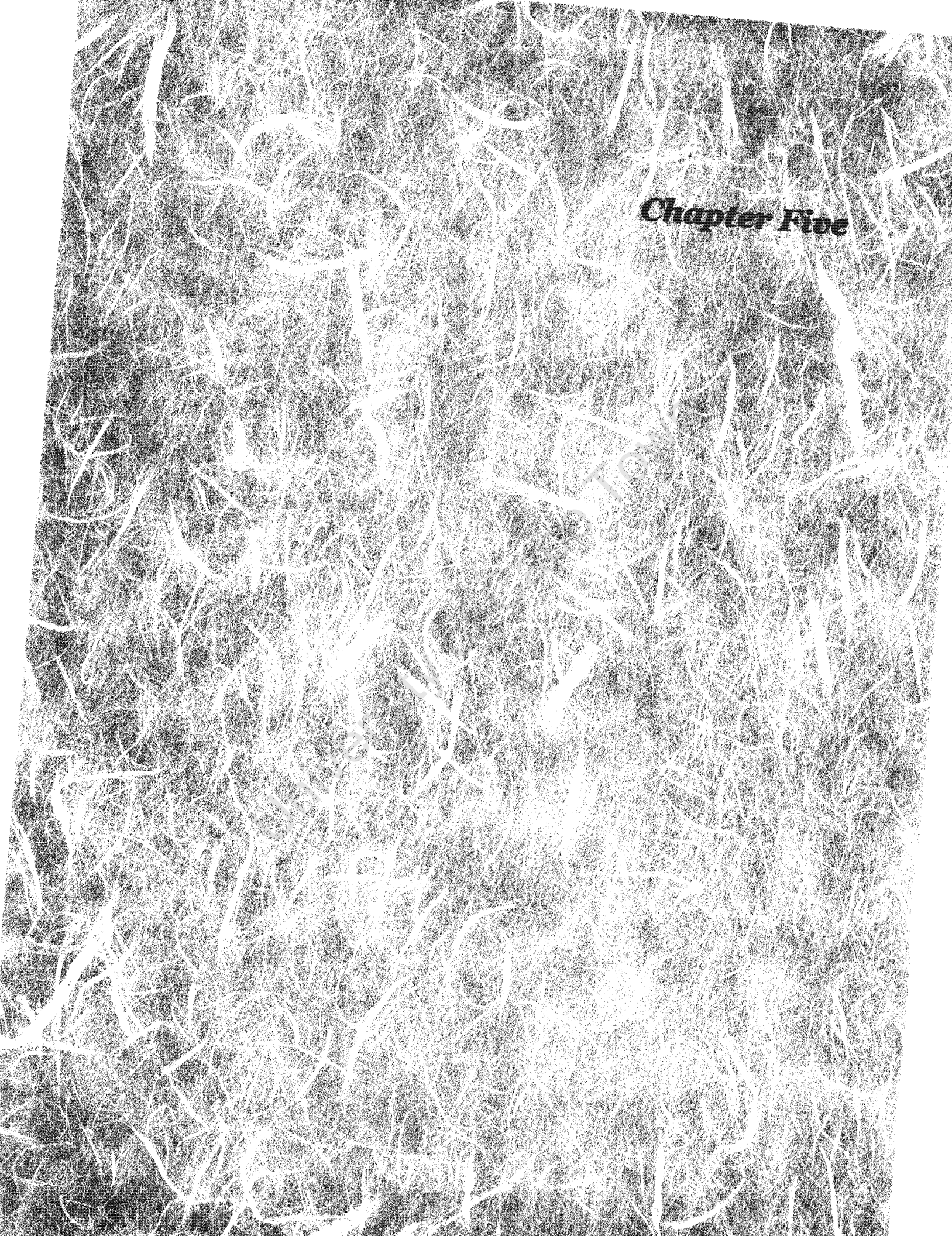
Chapter Five

5.1 Conclusion

In this study seven new cyclodextrin inclusion complexes and three new solid forms, involving two NSAIDs and one permethylated β-CD were prepared. These were characterised using some or all of the following characterisation methods: HSM, TGA, DSC, UV spectrophotometry, elemental analysis, HPLC, NMR spectroscopy, XRPD and single crystal X-ray analysis.

Novel solid-state forms

An amorphous form of celecoxib was identified using thermoanalytical, elemental, spectroscopic and crystallographic analysis. This amorphous form was prepared using the recrystallisation from the melt technique. The elemental analysis results indicated that this new form did not alter chemically from the original crystalline celecoxib, yet the amorphous nature was proven by thermal analysis and XRD powder analysis. This new solid-state form of celecoxib had, however, been identified prior to this study by Chawla *et al.*[1] His group identified three new solid-state forms, two solvates and the amorphous form. The results of the characterisation of the amorphous form in this study corresponded well with his group's results.

A cyclized product resulting from the possible photo-degradation of rofecoxib was elucidated using thermoanalytical, elemental analysis, spectroscopic, chromatographic and crystallographic techniques. This unexpected product was obtained via recrystallisation and co-precipitation methods. The product was proven to be chemically different from rofecoxib via thermal analysis, HPLC, XRPD and elemental analysis. The structure of the product was tentatively assigned by NMR spectroscopy and confirmed by single crystal X-ray analysis. Following an extensive literature search it was discovered that this product had been revealed previously but not characterised to the extent reported in this dissertation.[2, 3, 4, 5]

A new crystalline form of TRIMEB was discovered and characterised using thermoanalytical, elemental analysis and crystallographic techniques. This form was

obtained during a failed co-precipitation experiment involving the monohydrate TRIMEB and the NSAID Bucetin. This phase was proven to be different from that of the monohydrate by thermal analysis, elemental analysis and XRPD. Single crystal X-ray analysis was used in proving that this form is novel in comparison to the monohydrate and in addition to show the geometry and packing of this molecule. This novel form was found to be anhydrous and to adopt a non-collapsed structure, with all residues in the $^4C_1$ conformation. The monohydrate displayed an elliptically shaped collapsed structure, with one methylglucose residue adopting the $^1C_4$ conformation, in order to minimize the hydrophobic cavity in the absence of a hydrophobic guest. [6] The host molecule in this novel form obtained was not collapsed due to a much greater degree of self-inclusion. The structure was found to be free of disorder.

Inclusion complexes

Four inclusion complexes were identified using the XRPD technique. These included Diflunisal•β-Cyclodextrin, Diflunisal•γ-Cyclodextrin, Suprofen•γ-Cyclodextrin and Bucetin•γ-Cyclodextrin. All these complexes resulted from kneading experiments; thus no large single crystals were formed and only XRPD could be used to establish complexation. This was achieved using the isostructural series technique whereby the gross features of the patterns are constant regardless of the nature of the included guest.[7]

A novel inclusion complex involving β-CD and suprofen was discovered and characterised using thermoanalytical, elemental analysis and crystallographic techniques. This complex was prepared using a 1:1 molar ratio of CD to NSAID via kneading and subsequent recrystallisation. Thermal analysis proved that an inclusion complex had been prepared and that it contained 10 water molecules per β-CD molecule. The host: guest ratio was determined to be 2:1 by UV spectrophotometry and elemental analysis. PXRD and single crystal X-ray analysis proved that complexation had occurred. Furthermore, single crystal X-ray analysis elucidated the complex geometry, the hydrogen bonding and the crystal packing. The host adopts the usual conformation seen in other β-CD complexes.[8, 9, 10, 11] The (S)-enantiomer of suprofen was preferentially included in the characterised crystal and was found to be disordered over two orientations to satisfy the crystallographic C_2-symmetry requirement. The packing motif was found to be screw channel (SC).

A new inclusion complex between TRIMEB and suprofen was identified and characterised using thermoanalytical, elemental analysis and crystallographic techniques. The complex was formed via a 1:1 molar ratio co-precipitation experiment. Thermal analysis showed that a complex had been formed and that it was anhydrous. UV spectrophotometry and elemental analysis proved that this is a 1:1 host: guest complex. As in the case of the β-CD inclusion complex with suprofen, XRPD and single crystal X-ray analysis proved that complexation had occurred and likewise single crystal X-ray analysis elucidated the complex geometry, the hydrogen bonding and the crystal packing. The host adopts the usual conformation seen in other TRIMEB complexes[12-15] (the data corresponded well with the isomorphous TRIMEB-(S)-naproxen complex[16]). The (S)-enantiomer of suprofen was preferentially included in the characterised crystal. The O atoms of the -COOH group are disordered over two orientations; this was due to free rotation of this group. Residual high electron density peaks were found surrounding the disordered carboxyl group and the phenyl ring. These peaks most probably represented minor inclusion of the R-enantiomer. The packing motif was found to be screw channel (SC).

Final remarks

In summary, the NSAIDs studied did not yield any 'true' polymorphs; however, these are favourable candidates for inclusion by cyclodextrins. The new phase of permethylated β-cyclodextrin was a serendipitous discovery and shall not be remarked on further. One of the aims of the study was to identify the tendency of NSAIDs to include within CDs. This study used thermal and X-ray diffraction to show how NSAIDs are included within various CDs. The effect of CD complexation of the NSAIDs on their solubility and bioavailability remains a subject for future investigation.

5.2 References

1. Chawla, G; Gupta, P; Thilagavathi, R; Chakraborti, A.K; Bansal, A.K. *Eur. J. Pharm. Sci.*, **2003**, *20*, 305-317.
2. Mao, B; Abrahim, A; Ge, Z; Ellison, D; Hartman, R; Prabhu, S; Reamer, R; Wyvratt, J. *J. Pharm. Biomed. Anal.*, **2002**, *28*, 1101-1113.
3. Reddy, K.V; Babu, J.M; Dubey, P.K; Chandra, S.B; Vyas, K. *J. Pharm. Biomed. Anal.*, **2002**, *29*, 355-360.
4. Woolf, E; Fu, I; Matuszewski, B. *J. Chromatogr. B*, **1999**, *730*, 221-227.
5. Shehata, M.A; Hassan, N.Y; Fayed, A.S; El-Zeany, B.A. *Farmaco*, **2004**, *59*, 139-145.
6. Caira, M.R; Griffith, V.J; Nassimbeni, L.R; van Oudtshoorn, B. *J. Chem. Soc., Perkin Trans. 2*, **1994**, 2071-2072.
7. Caira, M.R. *Rev. Roum. Chim.*, **2001**, 46(4), 371-386.
8. Hamilton, J.A. *Carbohyd. Res.*, **1985**, *142*, 21-37.
9. Caira, M.R; Dodds, D.R. *J. Incl. Phenom. Macrocycl. Chem.*, **2000**, *38*, 75-84.
10. Caira, M.R; Dodds, D.R. *J. Incl. Phenom. Macrocycl. Chem.*, **1999**, *34*, 19-29.
11. Caira, M.R; Griffith, V.J; Nassimbeni, L.R. *J. Incl. Phenom. Macrocycl. Chem.*, **1998**, *32*, 461-476.
12. De Vries, E.J. *PhD thesis, Inclusion of Alkylparabens in Cyclodextrins,* University of Cape Town, South Africa, **2003.**
13. Harata, K; Uekama, K; Imai, T; Hirayama, F; Otagiri, M. *J. Incl. Phenom.*, **1988**, *6*, 443-460.
14. Brown, G.R; Caira, M.R; Nassimbeni, L.R, van Oudstshoorn, B. *J. Incl. Phenom.*, **1996**, *26*, 281-294.
15. Harata, K; Hirayama, F; Arima, H; Uekama, K, Miyaji, T. *J. Chem. Soc., Perkin Trans. 2*, **1992**, 1159-1166.
16. Caira, M.R; Griffith, V.J; Nassimbeni, L.R; van Oudtshoorn, B. *J. Inclusion Phenom. Mol. Recognit. Chem.*, **1995**, *20*, 277-290.
17. Loftsson, T; Brewster, M.E. *J. Pharm. Sci.*, **1996**, *85*, 1017-1025.

Appendix

Appendix

Supplementary information used for the elucidation of each structure can be found on the CD-ROM attached. Five files are included for each solved structure reported in this dissertation, namely:

- Filename.HKL:
  Reflection data
- Filename.RES and Filename.CIF:
  SHELX type co-ordinate file and Crystallographic Information File
- Filename.FCF:
  Structure factor tables
- Filename.LIS:
  Atomic co-ordinates
  Bond lengths
  Bond angles
  Torsion angles
  Displacement parameters
  Geometry between non-bonded atoms
  Intermolecular and inter-atomic contacts

For each structure these five files are grouped into a directory bearing the same name as the filename.

These text files may be opened using WORDPAD in Windows 98 and Windows 2000.